2007

CHIRAL 1, 2-DIAMINO GUESTS IN CHAIN REPLACEMENT PEPTIDOMIMETICS: A NEW HELICAL MOTIF

Marlon D. Jones
University of Kentucky, mdjones310@comcast.net

ABSTRACT OF DISSERTATION

Marlon D. Jones

The Graduate School
University of Kentucky
2006

CHIRAL 1, 2-DIAMINO GUESTS IN CHAIN REPLACEMENT PEPTIDOMIMETICS: A NEW HELICAL MOTIF

ABSTRACT OF DISSERTATION

A dissertation submitted in partial fulfillment of the
requirements for the degree of Doctor of Philosophy
in the College of Arts and Sciences
at the University of Kentucky

By
Marlon D. Jones
Lexington, Kentucky
Director: Dr. Arthur Cammers, Associate Professor of Chemistry
Lexington, Kentucky
2006

ABSTRACT OF DISSERTATION

CHIRAL 1,2–DIAMINO GUESTS IN CHAIN REPLACEMENT PEPTIDOMIMETICS: A NEW HELICAL MOTIF

Peptides are short, sequence and length specific oligomers composed of small amino acid residues. Nature has refined these peptide sequences and their endogenous function through evolution. In addition, peptides have played an important role in medicine, which has lead to further research into developing peptides as lead pharmaceuticals (therapeutic peptides). Unfortunately, therapeutic peptides are inferior as drug candidates due to their low oral bioavailability; immunogenicity and potential to be attacked by peptidases. Fortunately, peptides can be modified by steric constraints, cyclization, and/or replacement of the peptide backbone itself creating a mimic (peptidomimetic) of the original peptide. Peptidomimetics are deliberately designed to have increased protease resistance, reduced immunogenicity and improved bioavailability when compared to the original endogenous peptide.

One such peptide, Magainin is a well-studied, α-helical peptide found in African clawed frogs. This peptide has antibiotic properties (against pathogenic bacteria), which partly arises from the hydrophilic portion of the peptide having basic amino acid side chains periodically disposed on one side of the α–helix. This property of magainin causes its attraction to negatively charged bacteria cell

membranes. Unfortunately, as in the case of other antibiotics, pathogenic bacteria have developed effective countermeasures against magainin. We designed a peptidomimetic based on magainin and implemented a plan to determine what type of molecules could be assembled for a magainin mimic. We successfully utilized molecular modeling (Monte Carlo conformational search), as well as results from previous experiments to elucidate what type of molecules, as well as how many molecules would be necessary to create a novel helical-like magainin peptidomimetic. It was discovered that C_2 symmetric diamines would be best at generating the helical-like motif and the amino acid lysine to generate the basic side chain. The next step was the successful connection of two C_2 symmetric molecules via a urea linkage and then one more connection to a lysine (α–amino group) residue, creating a short sequence of oligoureas (trimers). Finally, attempts to connect the oligoureas trimers were attempted using a solid-phase synthesis approach to generate a functional magainin mimic.

KEYWORDS: Peptidomimetics, Antibiotics, Magainin, Helices, Solid Phase Synthesis

___Marlon D. Jones___

__September 30, 2006___

CHIRAL 1, 2–DIAMINO GUESTS IN CHAIN REPLACEMENT PEPTIDOMIMETICS: A NEW HELICAL MOTIF

By

Marlon D. Jones

_____Dr. Arthur Cammers_____
(Director of Dissertation)

____Dr. Robert B. Grossman_
(Director of Graduate Studies)

RULES FOR THE USE OF DISSERTATIONS

Unpublished dissertations submitted for the Doctor's degree and deposited in the University of Kentucky Library are as a rule open for inspection, but are to be used only with due regard to the rights of the authors. Bibliographical references may be noted, but quotations or summaries of parts may be published only with the permission of the author, and with the usual scholarly acknowledgments.

Extensive copying or publication of the dissertation in whole or in part requires also the consent of the Dean of the Graduate School of the University of Kentucky.

A library that borrows this dissertation for use by its patrons is expected to secure the signature of each user.

DISSERTATION

Marlon D. Jones

The Graduate School
University of Kentucky
2006

CHIRAL 1, 2–DIAMINO GUESTS IN CHAIN REPLACEMENT PEPTIDOMIMETICS: A NEW HELICAL MOTIF

DISSERTATION

A dissertation submitted in partial fulfillment of the
requirements for the degree of Doctor of Philosophy
in the College of Arts and Sciences
at the University of Kentucky

By

Marlon D. Jones

Lexington, Kentucky

Director: Dr. Arthur Cammers, Associate Professor of Chemistry

Lexington, Kentucky

2006

ACKNOWLEDGMENTS

The following dissertation, while an individual work, benefited from the insights and direction of several people. First, I would like to thank my Advisor, Dr. Arthur Cammers. I would also like to thank Dr. David W. Emerson (UNLV) for giving me my start in Organic Chemistry, as an undergrad and Dr. Joseph P. Konopelski (UCSC) for his timely and instructive comments during my summer internship at Univ. of California, Santa Cruz, in 1994.

Next, I wish to thank the complete Dissertation Committee, and outside reader, respectively: Dr. Folami L. Ladipo, Dr. Boyd E. Haley, Dr. Mark S. Meier and Dr. Marcos Oliveira. Each individual provided insights that guided and challenged my thinking, as well as, just being helpful and giving timely advice when I really needed it.

Thanks go to current and former students in the Cammers research groups. They have provided support and assistance that allowed me to achieve my goals as a chemist. Special thanks go to Dr. Venkatraj Muthusamy for his assistance in the Cammers group lab and for the timely conversations when I needed someone to talk to. I would also like to thank Raghu Chamala and Razi Husseini for their assistance with coordination the informal group meetings between the Cammers and Grossman groups. Those group meeting have really helped me become a more knowledgeable organic chemist. Also, I would like to thank Dr. Robert B. Grossman and Dr. Peter A. Crooks for giving me an opportunity, as well as a wealth of experience that will last a lifetime.

In addition, I received equally important assistance, as well as advice from family and friends. Both are necessary to keep one focused on the real goal, no matter what the situation(s) may be.

TABLE OF CONTENTS

List of Figures

List of Equations

List of Charts

List of Schemes

List of Files

Marlon D. Jones.PhD.dissertation.pdf

Adobe Acrobat portable document file

Chapter 1

Rational Peptidomimetic Design

1.1 Overview of Dissertation

This dissertation is divided into four chapters. In chapter one, *"Rational Peptidomimic Design"*, the use of peptidomimetics as therapeutic agents will be discussed, as well as the application of molecular modeling to develop the profile(s) of a peptidomimetic of interest. Based on a naturally occurring antibiotic peptide and using the results generated from molecular modeling, we developed a plan to create these compounds through solution and solid-phase synthesis. Chapter 2, entitled *"A Brief Review on Cationic Peptide Antibiotics"*, discusses the history and diversity of antibiotic peptides, as well as their different modes of action against pathogenic bacteria with special interest directed towards the helical antibiotic peptide, Magainin. Chapter 3, *"Experimental Section"*, will discuss the experimental program needed for the manufacture of target compounds, as well as eventual assembly via fragment condensation. The fourth and final chapter "*Conclusions*" summarizes the results obtained from this dissertation work.

1.2 Introduction to Peptidomimetics

Peptides play an important role in medicine, physiology and pharmacology. Many naturally occurring peptides function as hormones, growth factors[1,2], antibiotics and are implicated in diseases, such as Alzheimers.[3,4] Nature has refined naturally occurring peptide sequences and their endogenous function through evolution. This has led to significant interest in exploiting peptides as lead pharmaceutical compounds, mainly in the areas of antibiotics[5], cancer[2], immune system[6] and cardiovascular diseases.[7] Unfortunately, peptides themselves are inferior as drug candidates due to several factors including: their low oral bioavailability; immunogenicity and potential to be attacked by peptidases.[5] However, peptides can be modified by using steric constraints, cyclization, and/or replacement of the peptide backbone itself or possibly a small part of the backbone to stabilize the bioactive conformation and fine tune bioavailability.

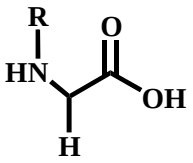

Figure 1.1. Peptoids. Peptoids are composed of N–substituited glycines.

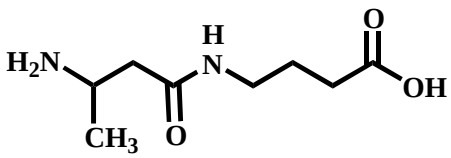

Figure 1.2. γ–Peptides. This structure is a generalized representation of a class of compounds known as γ–peptides.

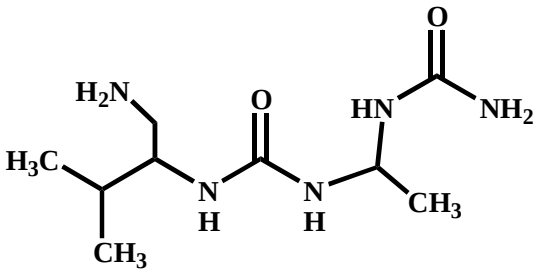

Figure 1.3. N,N'– linked oligoureas. This structure is a generalized representation of a N,N'–linked oligourea.

These novel compounds that have new/maintained biological and/or chemical function are referred to as peptidomimetics.[5] Peptidomimetics are deliberately designed to have increased protease resistance, reduced immunogenicity and improved bioavailability when compared with the natural peptides. In addition to this, a peptidomimetic may fold to create well-defined secondary structural elements such as helices, turns and small sheet-like structures allowing for biological or chemical activity. The term foldamer broadly encompasses these molecules and are not just limited to peptidomimetics.[8] In general, a foldamer is any oligomeric molecule consisting of some regularly repeating motif that adopts a constrained conformation in solution (with a loss of chain entropy). Foldamers are divided into two major classes: biotic (natural and closely related backbones) and abiotic (non-natural synthetic backbones) depending on their chemical composition.[8] Among these, peptidomimetic foldamers and single-stranded abiotic foldamers are the best developed. Peptidomimetic foldamers, including peptoids[9] **(Figure 1.1)**, and γ–peptides[10] **(Figure 1.2)**, *N*,*N*–linked oligoureas[11]

(Figure 1.3), are created from a design that involves systematic structural variations of parent chain molecules which are known to adopt predominant conformations. Single-stranded abiotic foldamers including oligo(*m*-phenylene ethynylene)[13] **(Figure 1.4)** and aedamers[12] **(Figure 1.5)** arise from a design that involves novel, abiotic backbones which fold into conformationally ordered states. Foldamers have applications such as temperature sensors[14] and molecular recognition[14] elements in non–biological and biological systems.

In addition to this, molecular folding is influenced by solvent interactions and conformation, which arise from non-covalent interactions between non–adjacent monomer units. Therefore, the development of synthetic foldamers provides scientists with an excellent opportunity to explore various relationships between structures, molecular shapes, and functions.

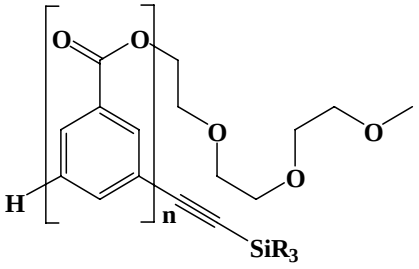

Figure 1.4. An oligo(m–phenylene ethynylene) foldamer.

1.3 Design of Foldamers

Although, the ideas for foldameric design come from concepts derived from biophysics and polymer science, it would be best to design a foldamer and predict/utilize its properties by studying previously known foldamers.

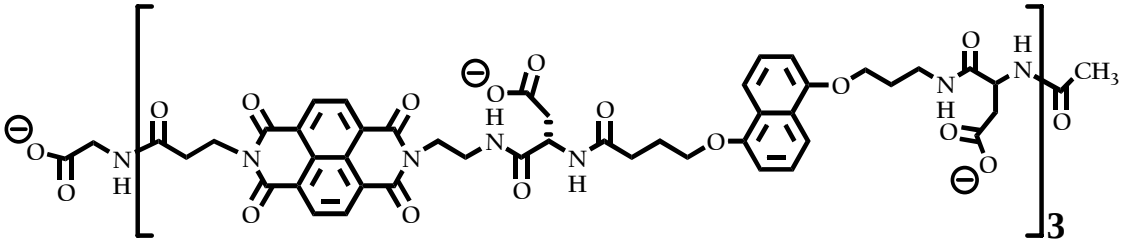

Figure 1.5. An aedamer. Another foldameric motif.

To understand a foldamer's properties we must take into consideration the mechanism(s) of folding, as well as identifying the kinetic and thermodynamic

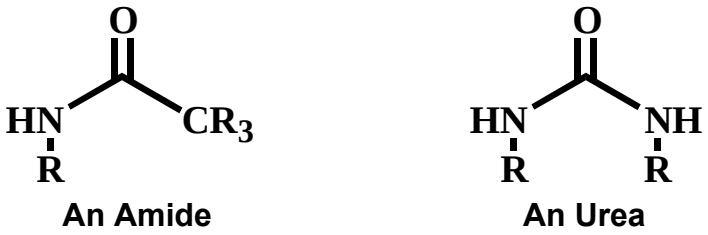

Figure 1.6. Amides and Ureas. Ureas are more stable and more conformationally flexible than an amide due to the donation of electrons from both nitrogens into the C–O antibonding orbital.

properties responsible for folding to occur.[15] The path to creating successful and useful foldamers involves several factors, including: preparation of the parent monomers (that the foldamer is comprised of) in a stereochemically pure form; identification of novel backbones that have suitable folding propensities; carrying out tests on the newly created foldamer for interesting biological/chemical function(s) and probably one of the most important factors is the efficient production of the foldamer itself. Of course, repetition will occur until the desired outcome is obtained. The types of secondary structures most crucial for foldamer development are those that display "long-range order", such as helices and sheets. One important aspect of this "long range order" is cooperativity, which will improve the integrity of the active sites in the folded states. Cooperativity suggests that the next unit of global conformation forms faster due to the presence of the preceding unit. This is important, because a cooperative structure will tend to have the most important groups in the correct location for most of the time, since the entire structure is more stable than the sum of its parts. Earlier it was mentioned that before one can think about the molecular tasks a foldamer might perform, it must be designed with a predictable outcome (shape), in mind. We can apply this principle to our own molecules, using a C_2 symmetric molecule as a guide. A C_2 symmetric molecule, in principle, should be able to translate its local symmetry into a global 'helical' shape. **(Helices, in general, have C_2 as the only symmetry point group operation)**. However, a

few issues must be considered to make the design remotely feasible. When designing a peptidomimetic, one has to consider the multiple interactions and behaviors of the constituent monomer units.[16] Here, the more important internal peptidomimic interactions will be broken down to describe the different aspects that have to be considered. The first and probably most important aspect of a peptidomimetic and its behavior will arise from the backbone. In our case, the peptidomimetic's backbone will be composed mainly of ureas and amides (**Fig 1.6).** Typically, a stable peptidomimetic molecule is defined by the rigidity of the constituent monomer units[16], with conformational preferences given by the bonds that link the monomer units together. A peptide mimic that is mainly composed of oligoureas may have advantages over natural peptides.

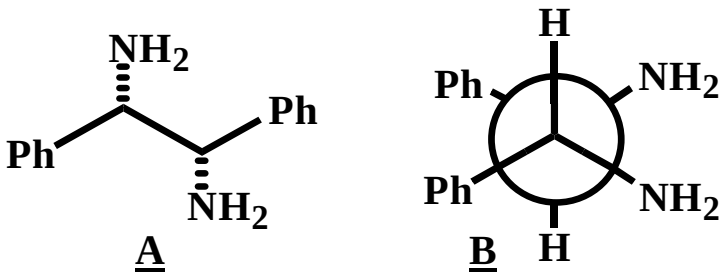

Figure 1.7. *S,S*–1,2-diphenyl–1,2–diphenyl–1,2–diamine (A) and its lowest energy conformer **(B)**.

Some of these advantages include the following: oligoureas do not differ greatly from naturally occurring peptides in structure and this may allow the peptidomimetic to fold in a similar manner to the native peptides; oligoureas should not be susceptible to degradation, because ureases, enzymes that degrade urea bonds, are not as developed as peptidases. In addition to this, the backbone will allow stabilization of the secondary structure, via hydrogen bonding between the carbonyl oxygen and the hydrogen attached to the nitrogen. Also, secondary structures are stabilized by factors such as π–stacking, hydrophobic-hydrophilic interactions.[17] In our case, having aromatic rings present in our molecules will allow π–stacking to occur. Secondary structure will show the conformation(s) of a given foldamer, defined in terms of four dihedral angles. In general, the most common secondary structures of a natural peptide foldamer

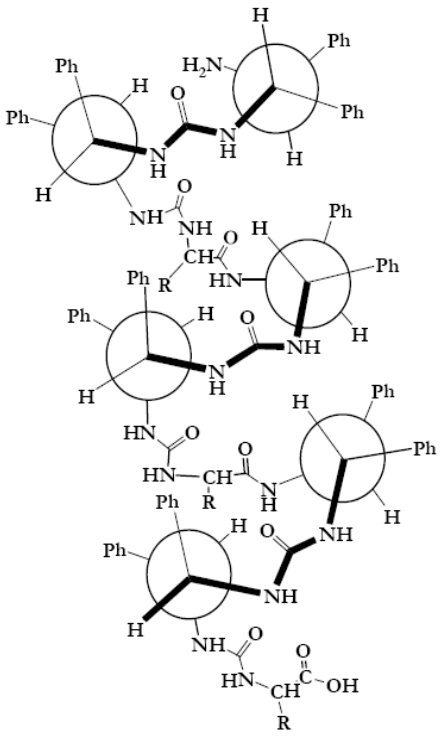

Figure 1.8. An oligourea foldamer

include α–helices, β–sheets, turns, and random coil. The α–helix, discovered by Pauling and Corey,[18] is one of the most common secondary structural motifs, which contains residues that wrap themselves around a central axis in a regular pattern. α–Helices are stabilized by internal hydrogen bonds where the carbonyl bonds and amide/urea NH bonds lie parallel to helical axis with the carbonyls pointing downward towards the carboxyl terminus with amino groups pointing upward towards the amino terminus. In our case, the linkage of several C_2 symmetric monomer units (**Figure 1.8 -** in their lowest energy conformer, in tandem with natural occurring amino acids) should be sufficient in producing a helical–like motif. Also, the main helix will be affected by any side chains, more specifically the geometry on the side chains, as well as, any functional groups that are present on those monomers. These side chains may enhance formation of secondary structures and allow the peptidomimetic to carry out interesting functions. One possible example of this is having a peptidomimetic imbued with side chains, possessing a positive charge, which allows interaction with negatively charged bacterial membranes to occur. Although these types of aspects are to be taken under consideration, one can not be sure of the outcome of the design. After all, nature does not follow the rules of man, so there's a chance that the foldamers will not follow these rules as well, no matter how well they are planned.

1.4 Conformational Aspects of Design

1.4.1 Monte Carlo simulations

Molecular modeling is used to predict conformation in molecules of interest, whether those molecules are natural or designed. Unfortunately,

because of the way molecular modeling programs locate energy minima, the resulting structure from a conformational search may not be the lowest minimum energy conformer for the molecule (This will be explained shortly). For molecular

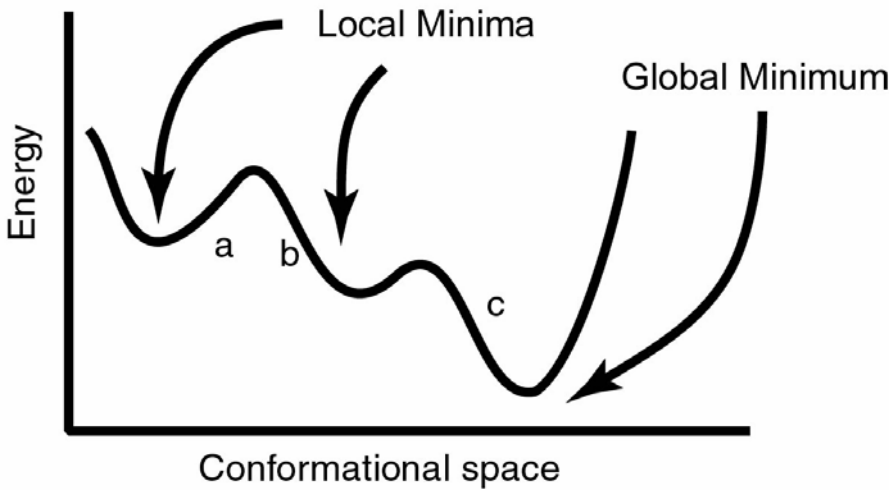

Figure 1.9. Monte Carlo conformational searching.

modeling programs, the lowest possible energy conformation produced by the minimization process can be called the global minimum. In **Figure 1.9,** the global minimum shown is the deepest energy well. Also, local minima, (the smaller energy wells) are also important for conformation. In order to explore molecular conformations, we use Monte Carlo methods.[19] Monte Carlo (MC) methods refer to any simulation of an arbitrary system which uses a computer algorithm explicitly dependent on a series of (pseudo) random numbers. The name, which derives from the famous Monaco city, emphasizes the importance of randomness, or chance (just like gambling), in the method. MC methodology is particularly important in stochastic analyses, where systems that have a large number of degrees of freedom and quantities of interest, such as thermal averages, cannot be computed exactly. The majority of minimization programs calculate energy derivatives at a particular conformation. Next, conformational variables are adjusted (based on the energy derivatives), allowing for rapid determination of minima. Using this method, the local minima are discovered if starting from points **a** or **b** in conformational space or from the global minimum if point **c** is the starting point **(see Figure 1.9)**. Modeling software users defeat the

tendency to achieve local minima by intelligently choosing the starting points. (This is the main reason why we started with a helical-like motif having all carbonyls pointed in the same direction). Monte Carlo calculations simulate heat energy to explore the conformations of a molecule. The process works by applying a random change to a set of rotatable bonds, such as rotational increments between 0 and 360°, or via atom displacement.[19] If no high-energy steric interactions are discovered, then a minimization calculation is run. The energy from this minimization calculation is compared to the energy of the lowest minima structure. If a minimum structure is found then this structure is adjusted and becomes the new starting point. If not, the Metropolis algorithm comes into play and provides a prescription for choosing which moves in conformational space to accept or reject.[20] This algorithm works by randomly "strolling" through the conformational space of interest. This process is designed in such a way, that the points on the random "stroll" are distributed according to the required probability distribution. At each point on this "stroll", a random movement from the current position in conformational space is selected. This trial move is then either accepted or rejected according to a simple probability given by the Boltzmann distribution **(Figure 1.10).**[21] If the move is accepted then the

$$N = Ag\, e^{-\Delta E/kT}$$

Equation 1.1

Equation 1.1 Boltzmann distribution equation. In the Boltzmann distribution equation, **A** is a constant, **g** is degeneracy (the number of states with identical energy) and **k** is equal to 1.38×10^{-23} J/K, (Boltzmann's constant).

algorithm moves to the new position picked in conformational space; otherwise it remains where it is. Next, another trial step is then chosen, either from the new accepted position or from the old position. If the first move is rejected the process is repeated. In this way it should be possible for the exploration of all conformational space.

1.4.2 AMBER

The AMBER[22] torsional parameterization set, employed with Macromodel (Version 8.0), was used to find the low energy conformers of the tetramers. Amber, consisting of a set of molecular mechanics force fields, is widely used for the computerized simulation of biomolecules. Amber, in a similar manner to the majority of molecular mechanics force fields, is quite dependent on variables which are experimentally determined. Molecular stability is conferred to the molecule when optimal bond angles, dihedral angles and bond lengths are reached. In addition to this, van der Waal forces are also employed as well.

1.4.3 Solvent Effects

Solvent effects play a tremendous role upon the relative energy of many materials in solution. The Macromodel program uses the Generalized Born/Surface Approximation **(GB/SA)** model to describe solvent effects.[23] For the analysis of the tetramers, a $CHCl_3$ parameter set was used. Solvent associated free energy, $\mathbf{G_{sol}}$, is the sum of three independent terms[23] **(Equation 1.2)** which are: a solvent-solute polarization term, $\mathbf{G_{pol}}$, a solvent-solvent cavity term, $\mathbf{G_{cav}}$

$$G_{sol} = G_{cav} + G_{vdW} + G_{pol}$$

Equation 1.2

Equation 1.2. This equation relates the free energy of a solvent, $\mathbf{G_{sol}}$. $\mathbf{G_{sol}}$ is related to 3 specific parameters which are $\mathbf{G_{cav}}$, $\mathbf{G_{vdW}}$ and $\mathbf{G_{pol}}$.

and a solute-solvent cavity term, $\mathbf{G_{vdW}}$, For saturated hydrocarbons, G_{sol} is linearly related[24,25] to the surface area which must be solvent accessible (SA). The terms G_{vdW} and G_{cav} can be calculated by determination of solvation parameter and the surface area for each atom. The other parameter modifies the system's electrostatic attractions. The generalized Born equation, described by Still, is used to relate the dielectric constant of the solvent to a contraction of both the attractive/ repulsive forces of two or more charges.[23]

1.4.4 Computational Foldamer Design

Computation is a common point of departure for molecular design, especially in studying foldamer motifs. The actual ideas for this project originated from a different project in the Cammers' lab, which through molecular modeling and CD studies of short oligoureas sequences derived from the molecule *trans*–1,2–cyclohexyldiamine **(Fig 1.10),** showed that the minimal energy conformation of the compound *trans*–1,2–cyclohexyldiamine **(Fig. 1.11)** (Amber*/Macromodel 8.0) suggested that the molecule may be helical in solution.[26] This also gave us an indication that the local symmetry of the monomer (C_2) could be translated into global symmetry, forming a motif with residues placed periodically. Therefore, we expected a similar trend to occur in our compounds, even with the natural amino acid residues present. Performing Monte Carlo conformational searches on the two tetramer structures, **Figs**. **1.12a–d (right-handed motif) and 1.12e–f (left-handed motif)** with the force field, Amber/Macromodel 8.0, resulted in an energetic preference for a right-handed helical-like motif, containing *S,S*– 1,2–diphenyl–1,2–diaminoethane units and a left handed motif composed containing 2 symmetric molecules with units of the *R,R*–1,2–diphenyl–1,2–diaminoethane. The CH_3Cl continuum dielectric field[27] gave a more helical–like motif, but otherwise the results were similar to the calculations using the water solvent continuum. These computations were initiated from helical–like conformations, consisting of 12 monomer units, with all the urea carbonyls pointed in the same direction. Within a window of 25 kJ/mol (1000 max iterations for each cycle), 48 possible lowest energy structures were found.

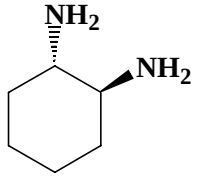

Figure 1.10. *trans*–1,2–diaminocylohexane

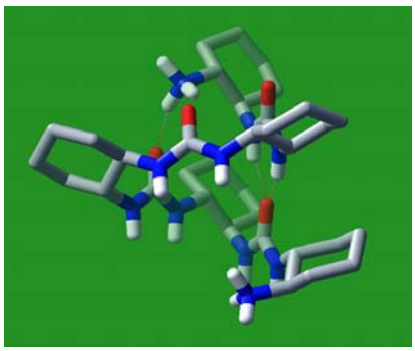

Figure 1.11. Oligoureas.

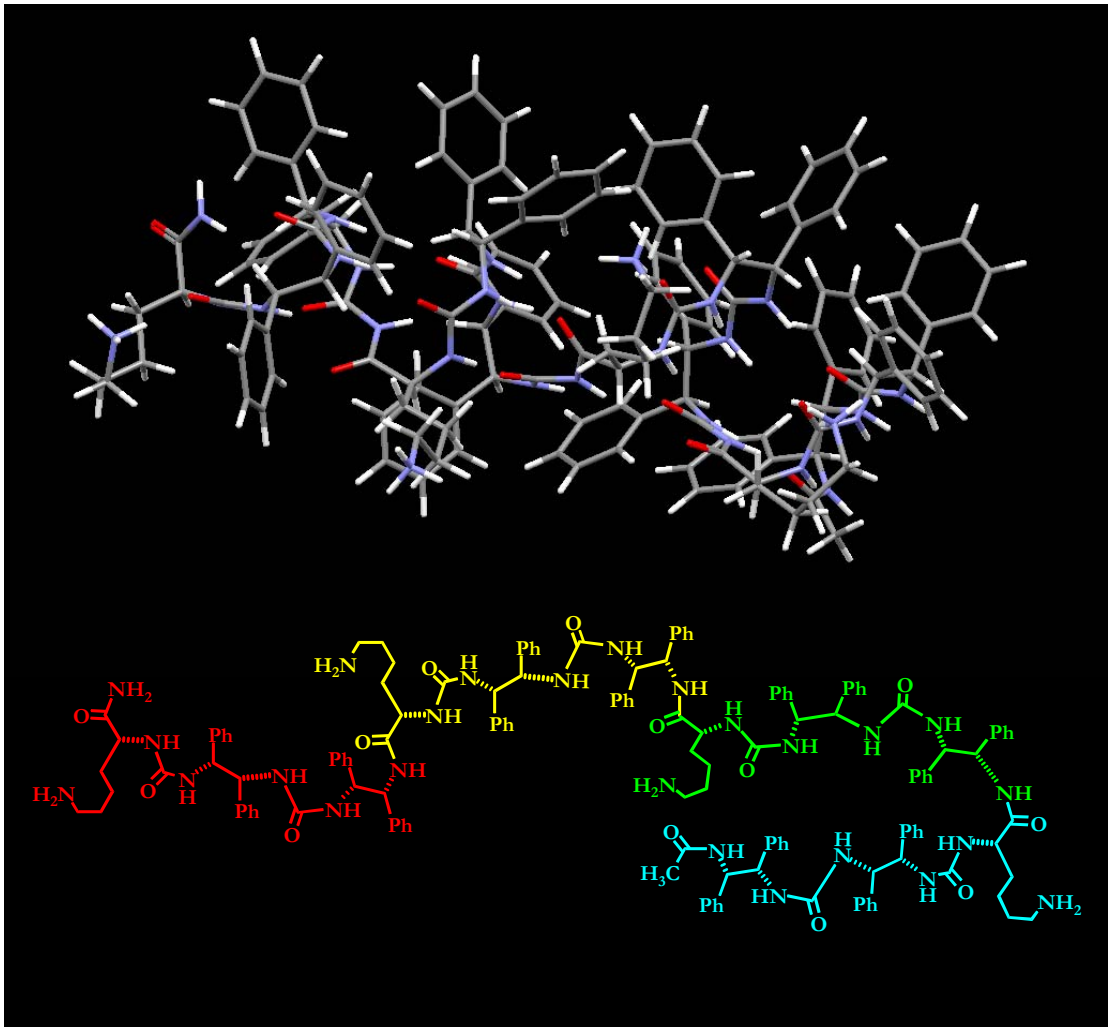

Figure 1.12a. *S*,*S*–tetramer **(Rt. handed motif)**.

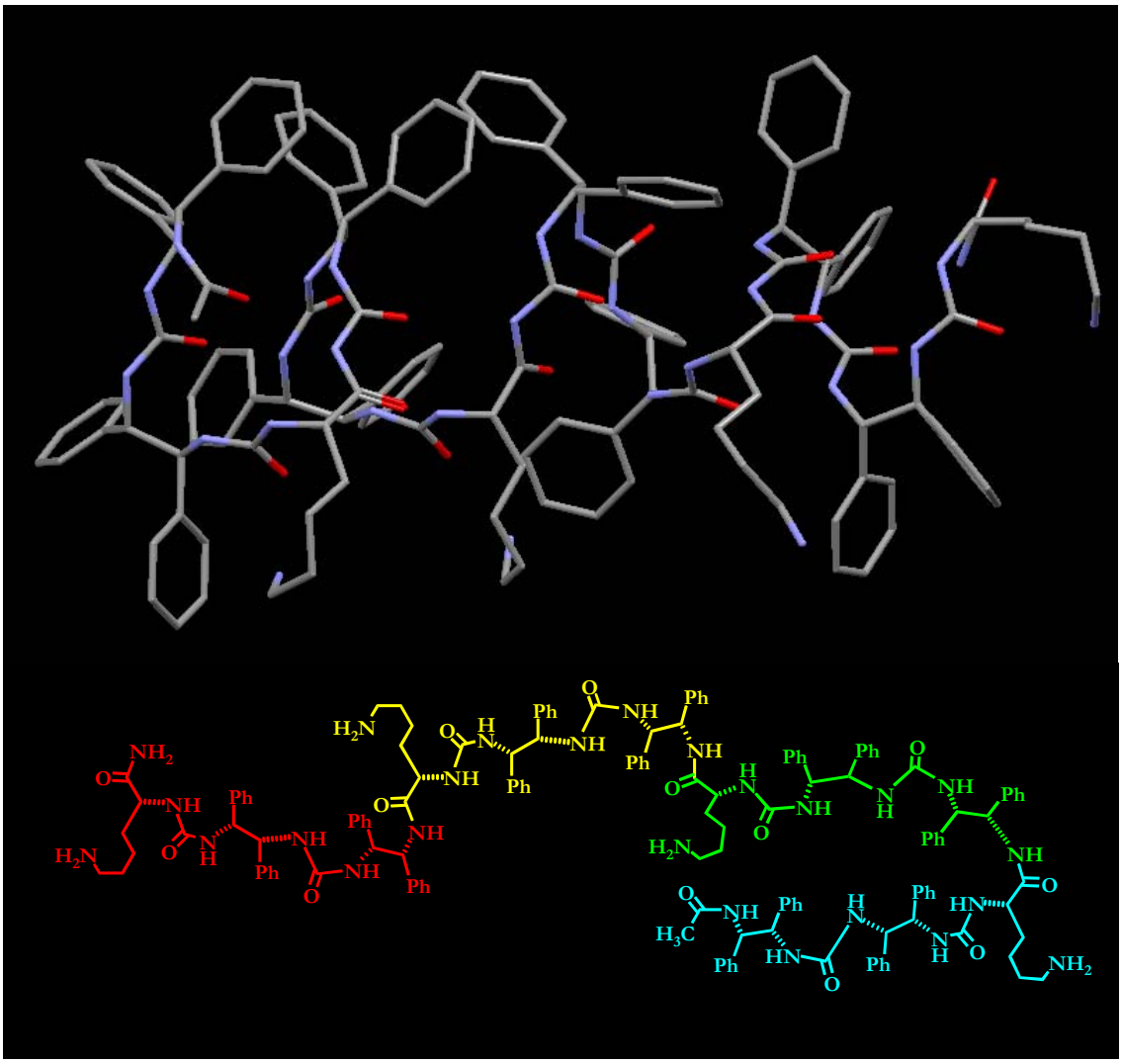

Figure 1.12b. *S,S*–tetramer **(Rt. handed motif)**. Phenyl groups are on the exterior of the motif.

(Hydrogen atoms removed for clarity)

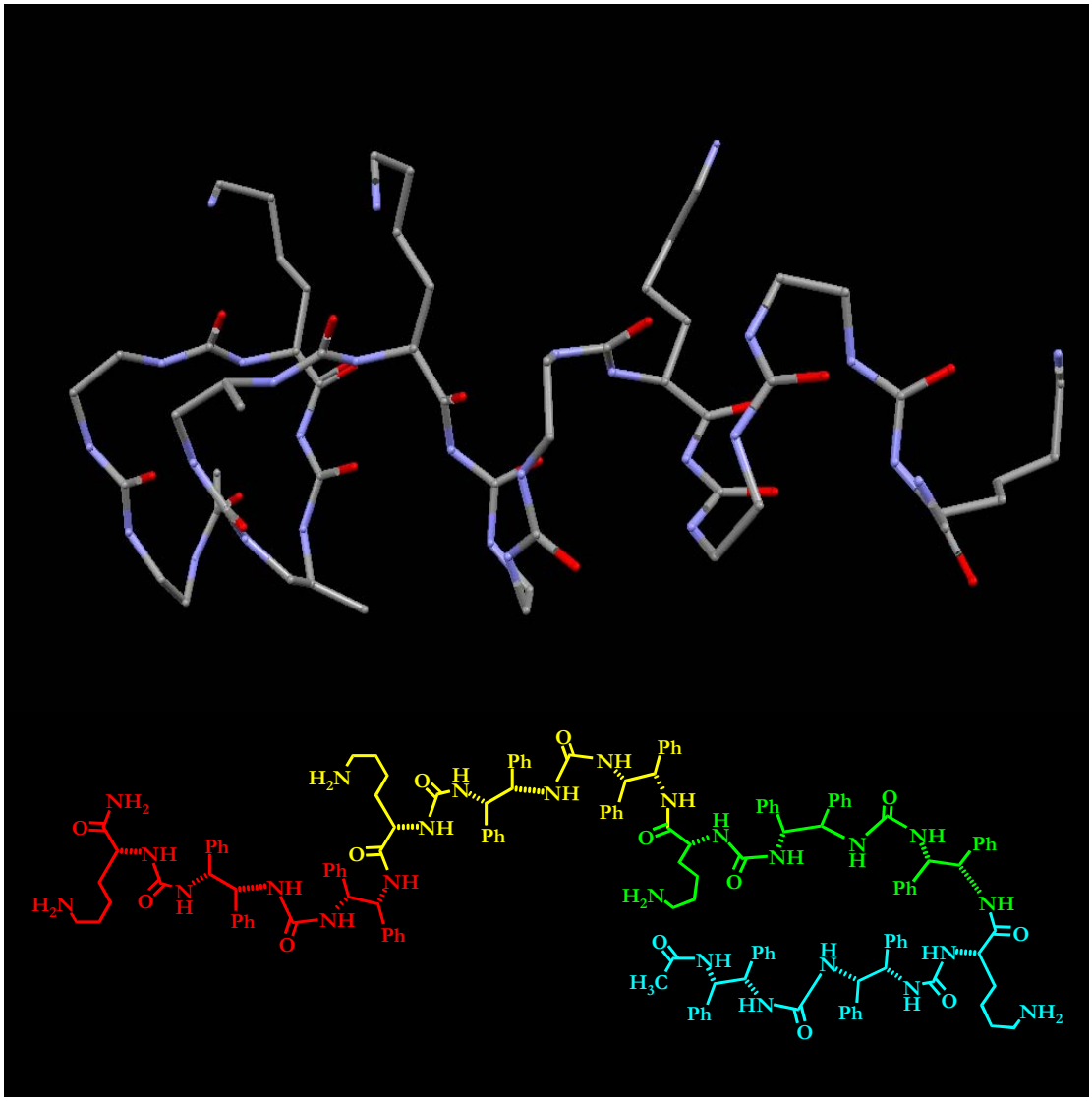

Figure 1.12c. *S,S*–tetramer. **(Rt. handed motif)** Most carbonyl units are orientated towards one direction.

(Phenyl rings and hydrogen atoms removed for clarity)

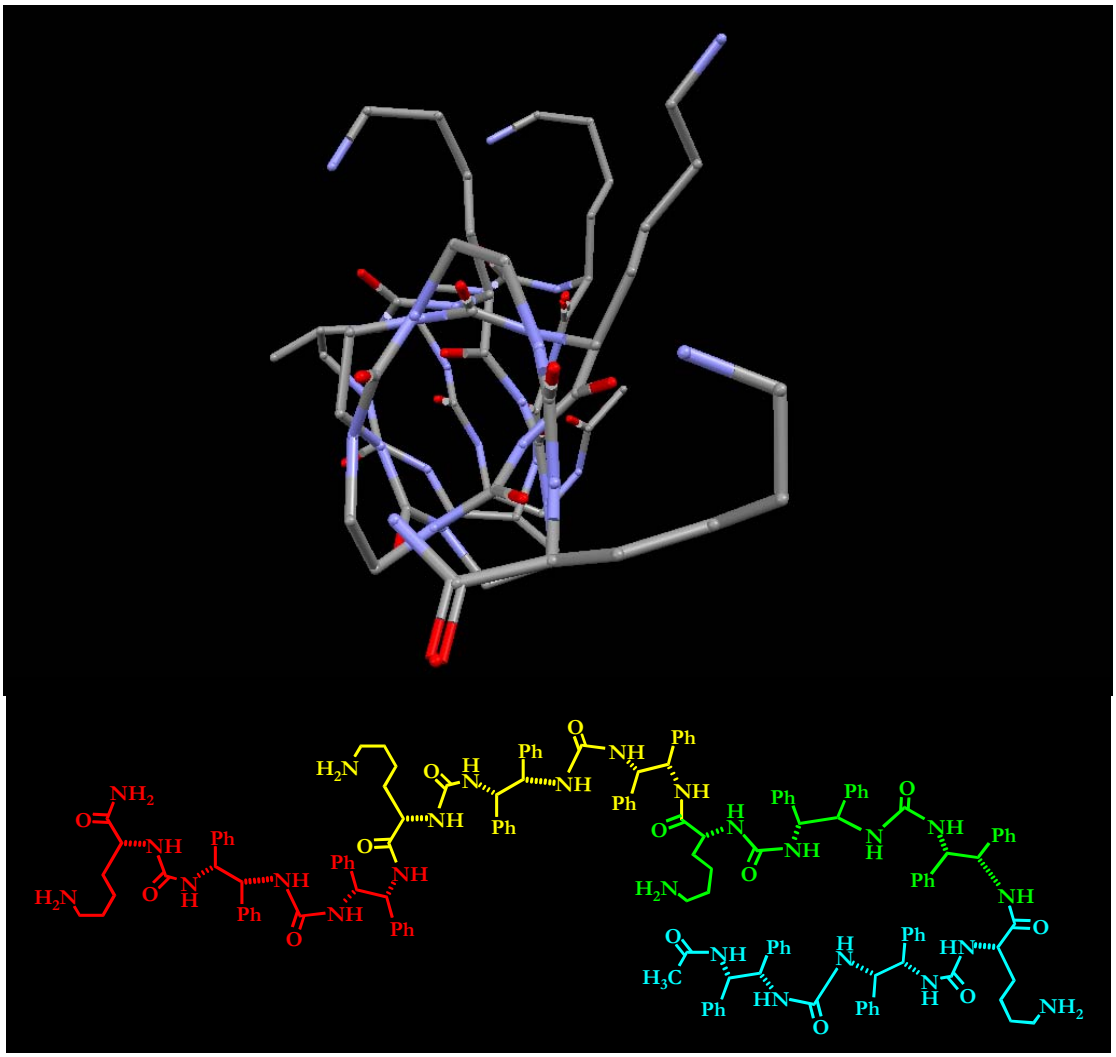

Figure 1.12d. *S*,*S*–tetramer. **(Rt. handed motif)** Polar units are located in the interior of the helical motif.
(Phenyl rings and hydrogen atoms removed for clarity).

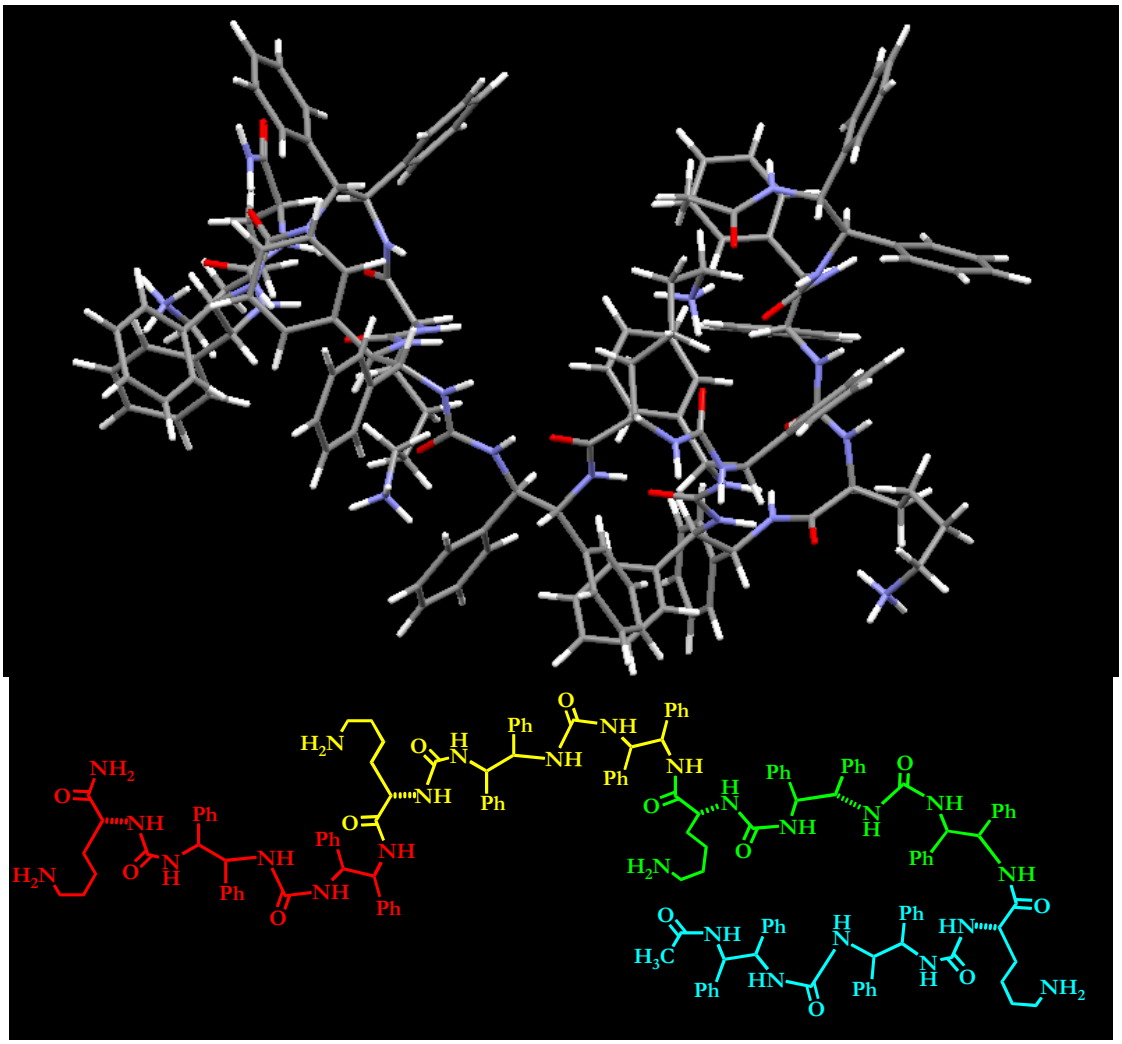

Figure 1.12e. *R,R*–tetramer. **(Lt. handed motif)**. Upon comparison with the *S,S*–tetramer, the *R,R*–tetramer looks disordered.

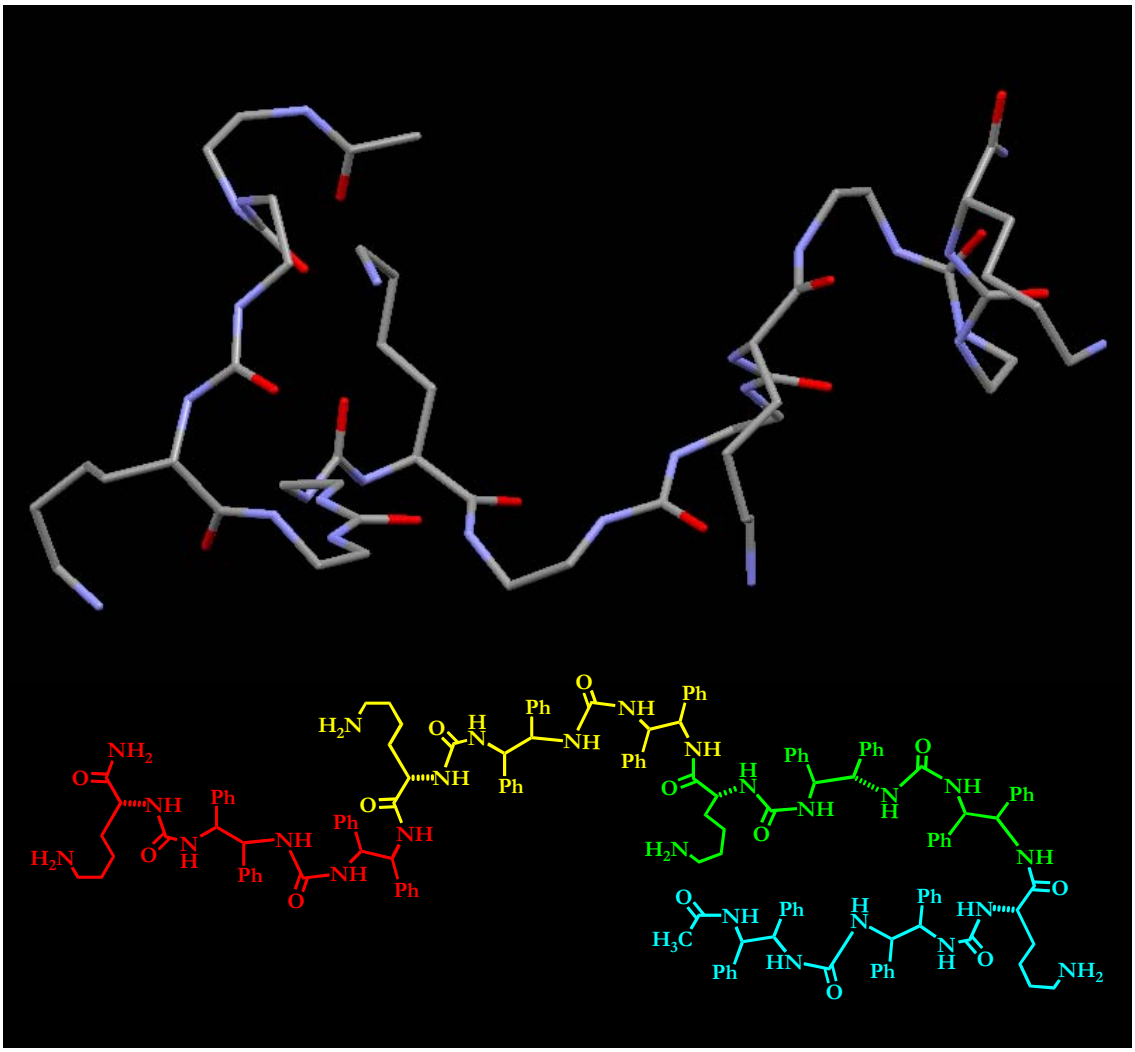

Figure 1.12f, *R*,*R*–tetramer. **(Lt. handed motif).** Carbonyl units are orientated in many directions.

(Phenyl rings and hydrogen atoms removed for clarity).

.

As evident from **Figures 1.12 a–d**, the helical-like motif comprised of units from *S*,*S*–1,2–dipheyl–1,2–diamine is more ordered. Also, this motif has the carbonyls pointing generally in the same direction, which allows for hydrogen bonding which leads to structure stabilization and positioning of the amino acid side chains preferentially on one side. However, the motif comprised of units from *R,R*–1,2–diphenyl–1,2–diamine, **Figures 1.12 e–f** shows that the motif is not ordered, does not have the lysine side chains positioned preferentially on one side of the molecule and its carbonyl groups are not orientated towards the same direction.

1.5 Solid Phase Organic Synthesis

1.5.1 Introduction

Isolation of peptides from natural sources and solution phase synthesis of some types of polymers is often a tedious, time-consuming operation which often fails, leading to disastrous results. However, one way to make peptides is to clone the appropriate peptide from a gene in a suitable host. Still, this may be problematic due to the cost of the operation, isolation from the media used to grow the peptide and length of time. Plus, if one desired analogs of these same peptides, this would not be a good way to make them. Furthermore, peptides can not be readily isolated via expression. For other types of polymers, large scale reactions must be carried out in order to have abundant quantity of material to be used in subsequent steps. Fortunately, solid phase organic synthesis (SPOS) has provided a way to access these molecules of interest. In addition, various derivatives of these molecules can be made, leading to some intriguing and fascinating results. However, SPOS still has its problems and limitations. For example, in the realm of peptide synthesis, if one wanted to synthesize a peptide comprised of 25 different amino acids, some questions would have to be addressed first. How long would it take to make such a peptide? Would there be a point of diminishing returns? How could the peptide be purified? Are there any issues of solubility that needed to be addressed? Another problem could be epimerization at the activated C–terminus of an amino acid. Despite these problems there have been many successful solid phase syntheses, including the

enzyme, reverse transcriptase, which is responsible for replication in the human immunodeficiency virus.

1.5.2 Principles of Solid Phase Synthesis

The methodology behind SPOS, first developed by Bruce Merrifield[28] in the 1960's to synthesize peptides, was not fully appreciated by chemists at first, but slowly began to be accepted as a good way to synthesize oligomeric compounds, such as peptides. Today, SPOS is a major tool in the synthetic chemists' armory for the generation of purified organic molecules of all types.[29] The principle of SPOS is simple and straightforward. SPOS consists of the tethering of a substrate to an insoluble polymer matrix (mainly either composed of polystyrene or PEG) solid support. A growing chain whether it be a peptide, nucleotide or any other foldamer molecule is attached to this stable solid support by a linker, which keeps the molecule of interest attached to the solid support

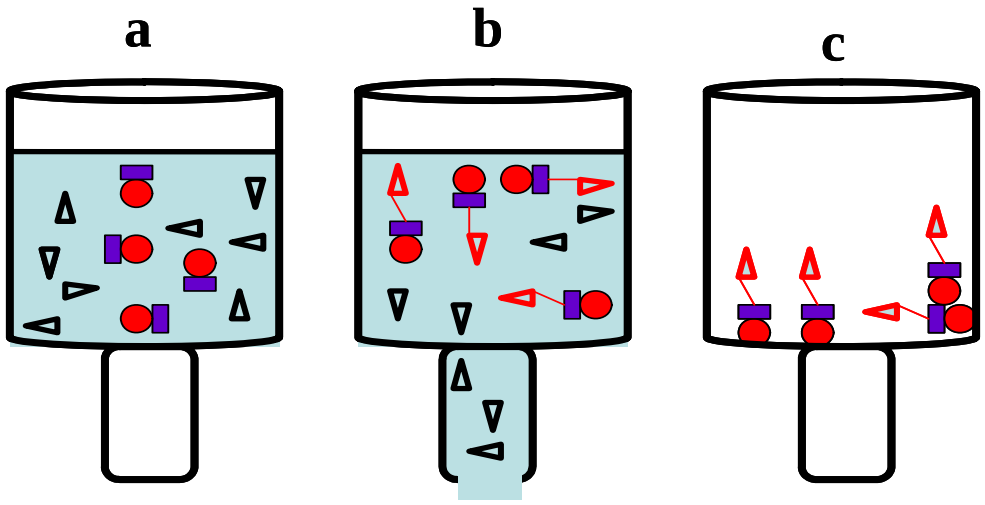

Figure 1.13. General Principle of Solid Phase Synthesis.
a). Shows reaction vessel containing solvent, reagent and resin.
b). Attachment to resin and eventual removal of excess reagents.
c). Reaction vessel containing only resin with attached substrate.

throughout all of the synthetic steps. Each reaction can be driven to completion, in theory by using an excess of reagents. Excess reaction materials and solvents are simply washed away by simple filtration. Finally, after assembly is complete, the desired product is removed from the solid support through different methods depending on the type of linker used. There are definite advantages to solid

phase synthesis over conventional (solution phase) synthesis. These advantages include: shortened time periods, especially if an automated process is used, ease of purification, not being labor intensive and by keeping the beads from being filtered away in each reaction step, physical loss of material is not encountered. Since soluble reagents can be easily removed by filtration, large excesses of reagents can be used, encouraging high efficiency in the various chemical steps. Of course, where there are advantages, there are disadvantages as well. These disadvantages include: the efficiency of coupling reactions; being able to accurately monitor the reaction by conventional techniques such as TLC (However, the reactions can be monitored by NMR, FTIR); production of insoluble material and accumulation of the growing peptide chain, which could block or slow down the progress of a reaction. The coupling reactions must be efficient, simple to carry out and produce the product in good yield. Despite these difficulties solid phase synthesis has become one of the premier ways of synthesizing molecules of biological and structural importance.

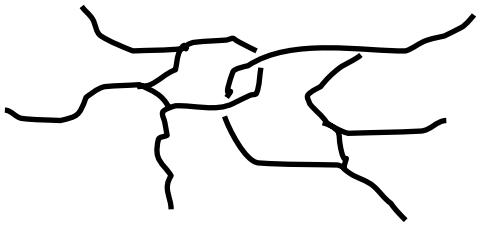

Figure 1.14. Cross-linked polystyrene

1.5.3 Choosing a Solid Support

One of the most important aspects of SPOS is having and utilizing the correct solid support for the ultimate attachment of material (via a linker). Solid supports, as stated earlier, are composed of cross-linked polystyrene (and derivatives) or PEG (and derivatives). Cross-linking imparts mechanical stability, improved structural integrity and enhancement of the resin's swelling properties.[30] If the support is not cross-linked, the polymeric chains will fall-apart under thermodynamic conditions. In general, there are some requirements needed for an ideal solid support. These requirements include: having enough reactive sites where the

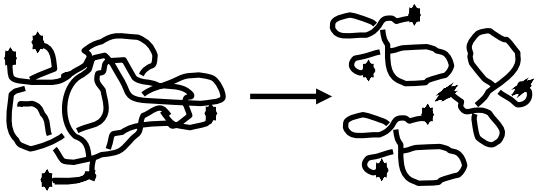

Figure 1.15. Non-cross linked polystyrene. May fall apart if certain conditions are met.

polymer chain can be attached and later removed; allowing for unhindered contact between the growing polymer chain and the reagents; being separable from the liquid phase at any part of the synthesis; being physically stable to reaction conditions and finally the support must minimize the interactions between bound polymer chains. Other things that must also be taken into consideration are the swelling properties of the solid support. If the polymer does not swell sufficiently, the substrates and solvents cannot permeate through the solid support. One last important factor is the size of the solid phase operation itself. Of course, as the size of the resin increases, more material can be loaded on it. However, one must take into consideration that there is a relationship between the size of the resin and how efficient material can diffuse through the polymer matrix **(Fig. 1.16)**.

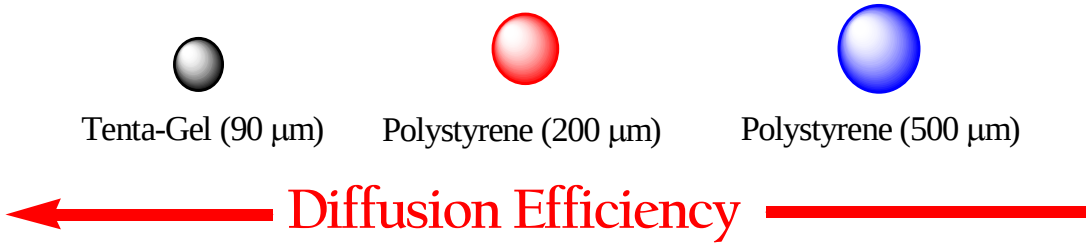

Figure 1.16. Solid Phase Resins. This figure shows a few of the different sizes of solid phase resins and well as their diffusion efficiency.

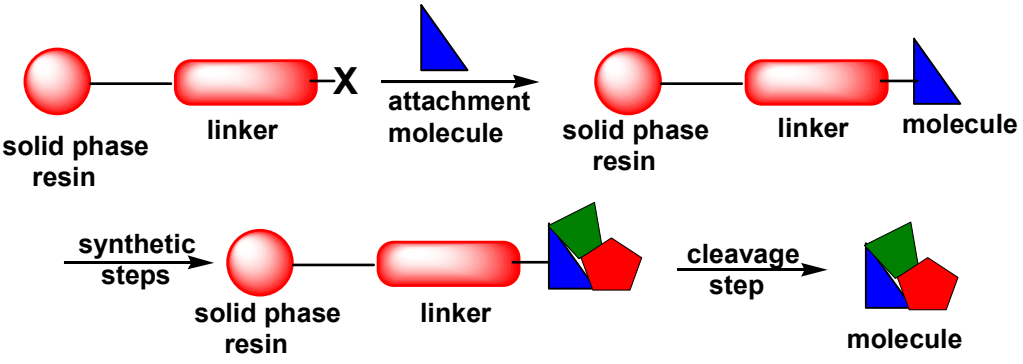

Figure 1.17. Process on use of a linker. The linker is a conduit for attachment of the molecule to the solid support.

1.5.4 Choosing a Linker Molecule

After choosing the correct solid support, one must connect the potential substrate to this support. The best way to accomplish this is by using a “linker” molecule. A linker is a molecule that covalently connects the growing polymeric chain to the solid support providing a means for chemical attachment and cleavage[31] **(Fig 1.17)**. Linker stability has a direct impact on the types of chemical reactions that can be employed on the solid phase. Solid phase linkers are quite diversified, ranging from linkers that break apart from the target substrate via nucleophilic reactions[32] to linkers that decompose on exposure to light.[33]

1.5.5 Fragment condensation

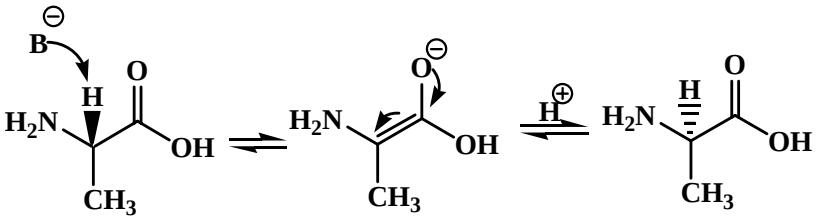

Figure 1.18. Amino acid Racemiztion. This figure shows how an amino acid can racemize under basic conditions.

There are two types of methods for synthesizing foldamers, whether by a solid-phase approach or solution synthesis. One method involves stepwise elongation, in which the monomers are connected step-by-step in turn. The other approach is the fragment condensation method, in which fragments (composed of several units) are coupled to each other. There are a few problems encountered while utilizing a step-by-step approach to the SPOS synthesis of foldamers. Some of these problems include: obtaining a lower overall yield by having the material go through many different reactions, especially protection and deprotection steps; the length of time involved for doing a multitude of reactions and the high likelihood that racemization may occur if a peptide or any monomer that has a possibility of becoming racemized **(Figure 1.18)**. Fragment condensation[34] is better than stepwise elongation, especially for the synthesis of sophisticated and/or lengthy foldamers. Fragment condensation strategies enhance the overall yield and purity of a foldamer by reducing the number of coupling and deprotection steps required during the course of the synthesis, relative to the

sequential strategy. In addition, the time involved in the synthesis would be lower and if one has peptides, the chances of having racemization occur would be lower. In addition to this, as oligoureas get longer it becomes more difficult to chemically differentiate an oligomer with ***n*** residues from an oligomer with **(*n+1*)** residues.

1.6 Conclusion

Peptides, short sequences of amino acids have various roles in our body and are implicated in certain disease process. Peptides can also be used as novel drug candidates to treat diseases such as arteriosclerosis, Alzheimer's disease and others. Unfortunately, therapeutic peptides have problems associated with their use, such as degradation, immunogenicity and absorption. Fortunately, peptide mimics can be made by modification of the backbone structure, as well as the inclusion of non-amino acid segments. These modifications must allow the newly created peptidomimetic to adopt a similar folding motif (foldamer) to the native peptide, giving the mimic similar abilities to the native peptide. Molecular modeling provides a good template to predict conformations in molecules of interest. Molecular modeling programs attempt to find the lowest possible energy for a structure. Unfortunately, the lowest energy conformer that is found may be a localized molecule and not the absolute lowest energy molecule possible. One of the methods molecular modeling programs use for searching conformational space is by use of Monte Carlo calculations. These Monte Carlo calculations attempt to simulate heat energy, by applying random change to rotatable bonds. Conformations are accepted or rejected by this process according to simple probability. Solution phase reaction of small peptides is tedious, time consuming and often lead to deleterious results. Fortunately, solid phase synthetic techniques eliminate some of the problems associated with solution phase chemistry. Solid Phase Organic Synthesis (SPOS) principles are rather simple, involving attachment of a substrate to a solid support; using an excess of reagents to drive reactions to their completion and then finally removal of the desired molecule from the solid support. There are two approaches to doing reactions on the solid support. One way, is by fragment

condensation, while the other approach is simply a linear step by step synthesis. The fragment condensation approach is preferred, allowing for fewer coupling steps, in comparison to the linear approach. This results in higher yields, shortened synthetic time and minimization of racemization. Also, the impurities produced in the linear synthesis will have oligomers with ***n*** and (***n+1*)** residues. However, the oligomer product generated from fragment condensation will have oligomers with **m**, **n** and **(m+n)** residues. Therefore, oligomers generated from the fragment condensation approach should be easier to purify when compared to the oligomers generated by a linear step by step method.

Chapter 2
Brief Review on Cationic Peptide Antibiotics

2.1 Introduction to Brief Review of Cationic Antibiotic Peptides

In chapter 1, it was discussed how peptides could be used as drugs, including their use as antibiotics. There are some common features in cationic antibiotic peptides, herein referred to as CAPs, which can be simulated in peptidomimetics. But first, a brief review on the different types of CAPs, some proposed mechanisms of action and a few bacteria defense mechanisms against CAPs is necessary to understand why the parameters mentioned in chapter one would be useful in the peptidomimetic.

The antibiotic era began more than 70 years ago resulting from the discovery that a Penicillin mold inhibited the growth bacteria on bread. From this discovery, led to one of the greatest advances in medicine and with the use of antibiotic therapy many, many lives have been saved. Unfortunately, misuse of antibiotics has contributed to the production of resistant bacteria. Fortunately, it has been found that organisms, than span every kingdom and phylum, produce cationic peptides which possess antibiotic activity.[35]

These peptides may have been progenitors of the first immune system and are quite diverse. CAPs have selective activity against both Gram-positive and Gram-negative bacteria and other pathogenic organisms. The vast majority of CAPs destroy bacteria by pore formation and/or by destruction of bacterial membranes.[36,37] CAPs share several items in common, despite their diversity. Some of these items include: being composed less than 100 amino acid residues[38]; having an overall positive charge between +2 and +7 and possessing amphipathicity (this means that one face of the peptide is cationic, the other side hydrophobic).[35] The peptide's nature and the nature of target bacterial cells help to control the actions of all CAPs. Several scientists believe that CAPs work by the following process(es). First, an electrostatic attraction between the peptide (which is positively changed) and the cell membrane of the bacteria (negatively charged) occurs. When contact with the cell membrane is made, pores are created or the permeability of the cell membrane increases. Both pore creation

and increased permeability leads to loss of integrity of the bacterial membrane and eventual leakage of intracellular contents, causing the death of the bacterial cell. However, the exact mode(s) of action is (are) not known. Various models to explain these phenomena have been hypothesized to explain the mechanism of CAPs. These models include: The Barrel-stave model, Carpet model, Toroidal Pore model and Aggregate model.[39-41] Because of their different mechanisms of action, diversity and variability, CAPs are currently being considered as an attractive replacement and supplement as well, to the current armory of antibiotics.

2.2 Cationic Antibiotic Peptides and their Biological Activity

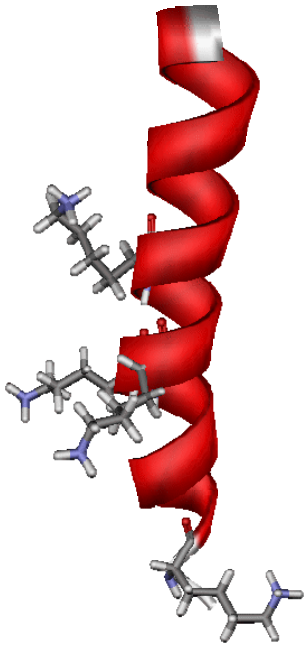

Figure 2.1. Magainin. The antibiotic peptide found in the African clawed frog. Lysine residues (shown) are responsible for peptide attraction to biological membranes.

Bacteria, both gram-positive and gram-negative, possess a negatively charged cell membrane in common. Interestingly; some CAPs display broad spectrum activity against only Gram negative bacteria. Others CAPs attack only on Gram positive bacteria. The reason why CAPs display this versatility is due to the cell membrane differences between both gram-negative/gram-positive bacteria **(Figure 2.6 and Figure 2.7)**. Fortunately, red blood cells (Erythrocytes) tend to be relatively resistant to CAPs, due to the very small negative potential on erythrocyte cell membranes. Some CAPs found in venoms, such as Melittin (bee venom)[42], Mastoparan (wasp venom)[43,44] and Cobatoxin (scorpion venom)[45] can attack and destroy red blood cells.

2.3 Cationic Antibiotic Peptides and their Diversity

CAPs have been discovered in all types of plants and animals (more than 800, at this time). Due to the molecular diversity of CAPs, the best way to categorize them is to place the CAPs in four distinctive groups by their secondary structure commonalities (van't Hof method).[46]

2.3.1 α–Helical Cationic Antibiotic Peptides

G-I-G-K-F-L-H-S-A-K-K-F-G-K-A-F-V-G-E-I-M-N-S
Chart 2.1. Magainin Amino Acid Sequence

Peptides which have a structure are the largest class of cationic antibiotic peptides. α–helical peptides are found in all types of organisms and have been the most studied class of CAPs at this time. In general, these CAPs stay disordered until contact with lipid surfaces occurs. Upon contact with these lipid surfaces, these peptides will fold into a α–helical motif. The most famous α–helical peptide and also the most studied is Magainin **(Figure 2.1)**, a 23 residue peptide **(Chart 2.1)** from *Xenopus laevis,* the African clawed frog. Other members include Cecropin A, which is found in wasps and the interesting Melittin **(Figure 2.2)**, the major constituent of bee venom that causes destruction of red blood cells. α–helical cationic antibiotic peptides depend on several factors which define their activities. These factors include: degree of helicity, Hydrophobicity, cationic charge and amphipathicity. Let's discuss these parameters in some detail. **Helicity:** Helicity is an important factor for antibiotic activity because it allows the creation of both a cationic and hydrophobic face, which is necessary for initial attraction to membranes and eventual membrane insertion itself.

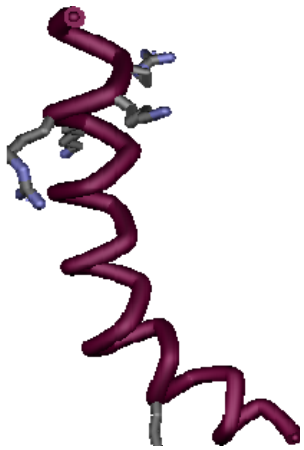

Figure 2.2. Melittin. The major peptide constituent of bee venom. The basic side chains are mainly on one side of this peptide, causing Melittin to have hemolytic activity.

However, some α–helical CAPs such as Magainin lose their antibiotic activity when certain D–amino acids are present in the peptide. These D–amino acids prevent Magainin folding into a helical motif. **Amphipathicity:** Amphipathicity is simply the measurement of the distances between both the hydrophilic and hydrophobic sides of a peptide. Amphipathicity is measured by the hydrophobic moment, which calculates the likelihood that a peptide residue will be located between hydrophobic and hydrophilic regions.[47] **Hydrophobicity:** Hydrophobicity measures the strength of peptide attraction for cell membranes and does not depend on the charge, as well as amphipathicity of a particular peptide. **Polar angles:** Polar angles are the angles that lie between the hydrophilic and hydrophobic peptide faces. These angles are one major controlling factor that modulates the way CAPs attach to membranes. CAPs that are highly hydrophobic, containing small polar (hydrophilic) angles tend to create pores through the cell membrane. **Charge**: CAPs are positively charged (between +2 to +9) due to the basic amino acid side chains (lysine and arginine). Peptides containing net positive charges (in this range) attach themselves to the target bacterial membrane (which is neg. charged). However, if the net positive charge is too high, peptide activity decreases due to the charge repulsion that occurs at the site of attachment.

2.3.2 Linear Cationic Antibiotic Peptides with Unusual Composition

H-Ile-Leu-Pro-Trp-Lys-Trp-Pro-Trp-Trp-Pro-Arg-Arg-NH_2

Chart 2.2. Indolicidin Sequence

Linear CAPs are peptides that have over-abundance in one or more amino acids. One example of this is Indolicidin. A 13 residue, tryptophan containing peptide, **(Chart 2.2)** and **(Figure 2.3)**.[48] Initially, it was thought that Indolicidin adopted a helical conformation[49], similar to other peptides, but CD studies show that Indolicidin adopts a different conformation instead. This conformation consists of a turn, which is believed to enhance Indolicidin's membrane activity.[50] Indolicidin is also believed to work by targeting nucleic acids blocking replication of the

bacteria.[51] Other members in this family of peptides include histatin[52], attacin[53] and tritrpticin.[54]

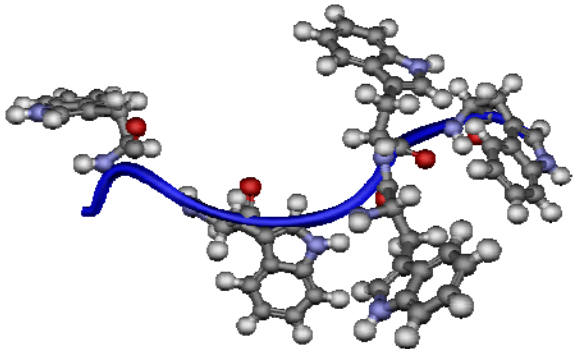

Figure 2.3. Indolicidin. An unusual antibiotic peptide containing the amino tryptophan (residues shown).

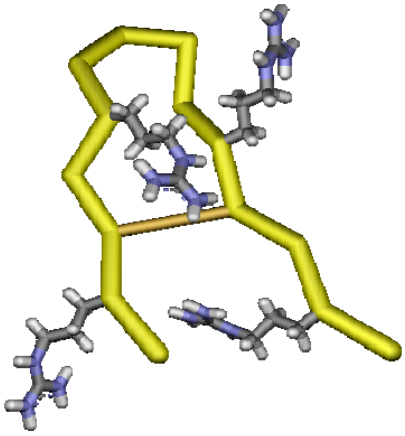

Figure 2.4. Bactenecin. A looped antibiotic peptide, highly rich in proline. Basic side chains are responsible for activity.

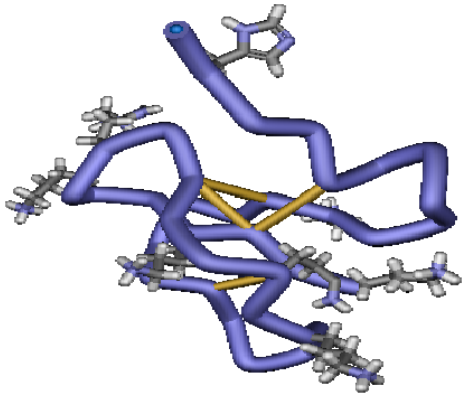

Figure 2.5. Defensin. A complex antibiotic peptide found in mammals, such as humans and rabbits. Side chains responsible for peptide activity are shown.

2.3.3 Looped Peptides

Bactenecin **(Figure 2.4)**, from bovine neutrophils[55], is the smallest natural CAP being only 12 amino acids long. Bactenecin also contains two cysteine residues capable of forming a disulfide bond. This disulfide bond allows Bactenecin to have a loop in its structure. Upon removal of the disulfide bond, this peptide possesses no activity against bacteria.[56] So, this disulfide bond is responsible for

maintaining the peptides structural integrity. Other members in this family of peptides include brevinin-1[57], brevinin-2[57] and thanatin.[58]

2.3.4 β–sheet Peptides containing Intramolecular Disulfide Bonds

Unlike other peptides, β–sheet peptides are simply cyclic peptides which are held together by a few disulfide bonds. One example of these types of peptides are the Defensins **(Figure 2.5)**, which are the principal constituents of cytoplasmic granules of mammalian neutrophils and certain macrophages. Defensins are one of the most studied β–sheet antibiotic peptides. Also, some studies show for activity to occur for these CAPs, the disulfide bonds must be present. Other members in this family include Tachyplesin and Gomesin.[59]

2.4 Cationic Antibiotic Peptide Specificity for Certain Cells

One of the unique properties of most CAPs is their specificity to destroy bacteria, while remaining relatively non-toxic to eukaryotic cells. The reason for this is due to differences that are present in bacterial and mammalian cell membranes.[60,61]

One difference between the two types of cells is the presence of lipopolysaccharides (LPS) in Gram-negative bacteria and teichoic acids in gram-positive bacteria. LPS plays an important role in bacterial toxicity by causing sepsis in humans. Lipopolysaccharides are located on the outermost surface on these bacteria (gram-negative) **(Figure 2.6).** For Gram-positive bacteria **(Figure 2.7)**, acidic polysaccharides (teichoic acids) are also found on the outermost surface of the bacteria. Having either LPS or teichoic acids on the bacteria surface gives bacteria a net negative charge. In addition to this, the phospholipids that are present in bacterial cell membranes are also negatively charged, thus increasing the net negative charge for the bacteria. On the other hand, the typical mammalian cell is mainly composed of zwitterionic phospholipids, therefore the typical mammalian cell is not as negatively charged upon comparison with bacteria.

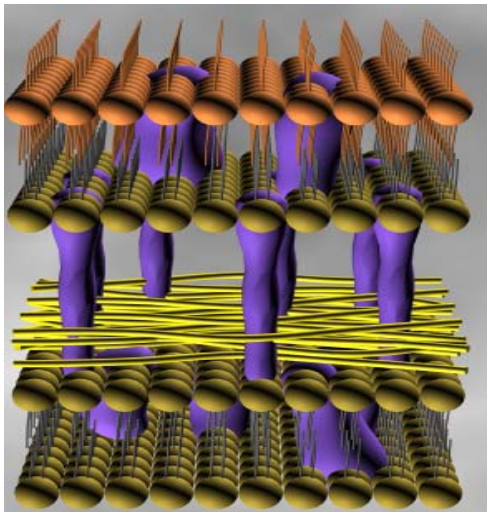

Figure 2.6. Gram negative bacteria cell wall. The LPS (orange) provides the virulence factor for this bacteria, as well as the negative charge needed for antibiotic peptide activity.

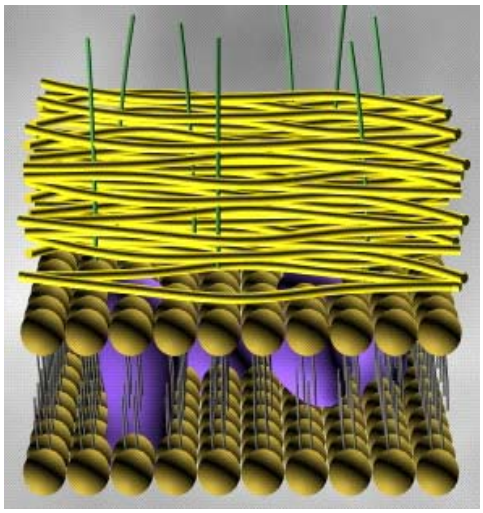

Figure 2.7. Gram positive bacteria cell wall. Teichoic acid (green) is provides the negative charge which is needed for antibiotic peptide activity.

2.5 How do Cationic Antibiotic Peptides Work?

The various effects of cationic antibiotic peptides (CAPs) eventually results in disruption of cellular structure and/or function. Also, CAPs adopt similar themes in activity, regardless of size, source, composition or conformation. The activity of these peptides begin by initial attraction to the target via biochemical or biophysical affinities, (i.e. negatively charged bacteria membranes) or by self-promoted uptake. After the initial attraction has taken place, the peptide makes contact with the bacterial membrane where conformational changes begin to occur. A great example of this is Magainin. As stated earlier, Magainin exists, in aqueous solution, as a random coil and folds into a helical motif upon interaction with bacterial membranes. One great aspect about conformational change is that it only occurs after the peptide interacts with appropriate target. This is important because it allows the peptide not to be active against a “friendly” cell. Next, peptides begin to accumulate in the cytoplasm and also on the bacterial membrane. After the appropriate amount of peptide has interacted with the membrane, peptides insert and eventually destroy the bacterial membrane, leading to leakage of cellular contents and cell death. In addition to this, after

entering the interior of the cell, CAPs seek out and disable specific intracellular components, making them non-effective. Several models have been theorized to explain how CAPs work. Due to the different compositions and the environment of bacteria membranes, a CAP can work by different modes of action, sometimes simultaneously or in tandem. The following four models have been presented to explain the mechanism of cationic antibiotic peptides.

2.5.1 The Barrel-stave Model

In the barrel-stave model **(Figure 2.8)** CAPs line up in a ring-like manner forming a pore (This would be the top of a barrel). The “stave” refers to transmembrane spokes within the barrel, where the spokes consists of individual peptides or peptide complexes. After additional peptides are attracted to the membrane, an increase in the overall pore size occurs. This eventually causes cell death by leakage of intracellular components out these newly created pores.

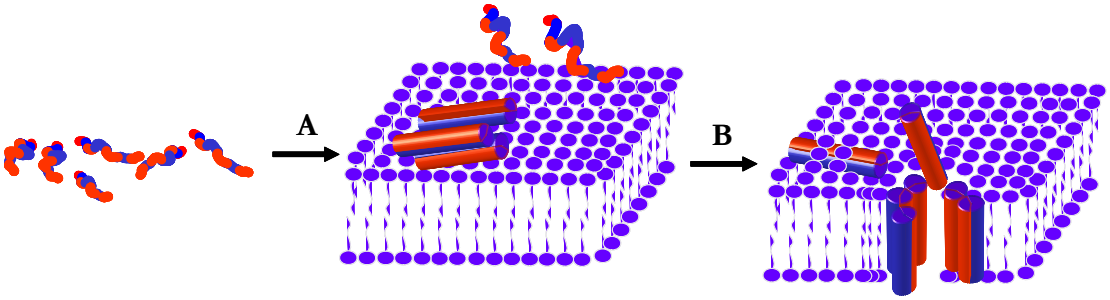

Figure 2.8. Illustration of the Barrel Stave Model. Antibiotic peptides are attracted to and coordinate themselves to the surface of the bacteria. **(A)** Peptides insert themselves into membrane as staves **(B)** allowing for leakage of cytoplasmic material.

Scientists believe that CAPs position themselves in such a way that their hydrophobic side chains interact with the lipid environment of the bacterial membrane, while the polar side chains are aligned inward forming transmembrane pores. This process is driven mainly by hydrophobic interactions with the bacterial membrane. However, if the peptide has a high net positive charge (from basic side chains) it is unlikely that bacterial destruction will occur by this mechanism due to repulsion arising from electrostatic interactions.

2.5.2 The Carpet Model

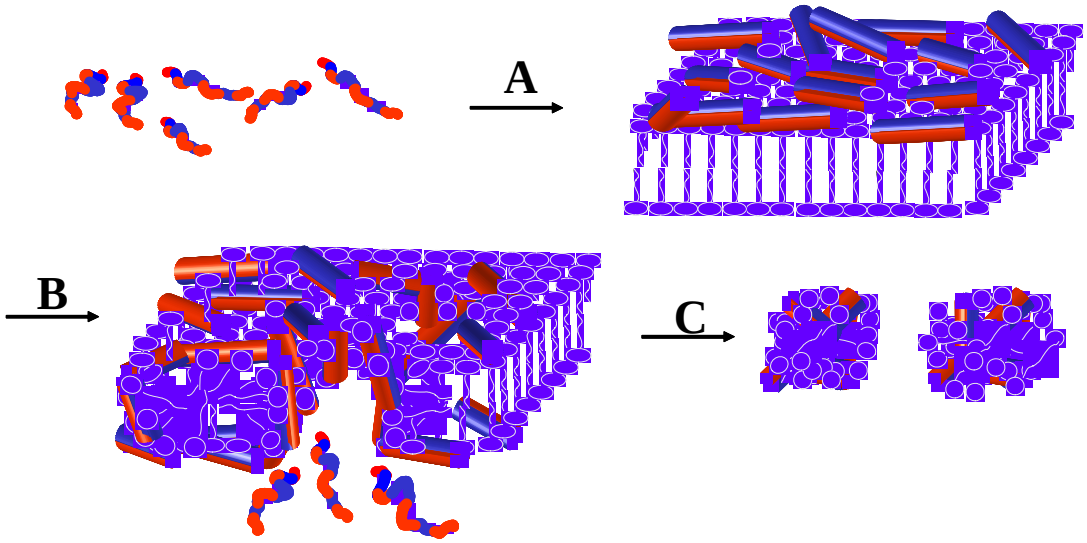

Figure 2.9. Illustration of the Carpet Model. Antibiotic peptides are attracted to and coordinate themselves to the bacterial surface **(A)**. Peptides randomly insert themselves into the membrane **(B)**. When a threshold concentration of peptides is reached, the bacterial membrane disintegrates, leading to bacterial death **(C)**.

In the beginning, it was assumed that all CAPs kill bacteria by the creation of membrane pores through the barrel-stave model process. However, the interaction of Magainin and other CAPs, with membranes did not work by the 'barrel-stave' model. Therefore a different model called the carpet model **(Fig. 2.9)** was described and proposed[40]. According to this model, CAPs are initially attracted to the bacterial membrane by an electrostatic attraction. Next, the peptides aggregate on the surface and eventually coat the bacterial membrane until the surface is completely covered with peptides. Unlike the barrel-stave model, peptides do not penetrate the membrane. Instead peptides remain in contact with the membrane leading to membrane disruption, leakage of cytoplasmic contents and finally, total membrane destruction, itself. The peptides that work via the carpet model have a high net positive charge and do not bind strongly to bacterial membranes. Therefore, peptides that utilize the carpet model to destroy bacteria have the following propensities: A high net positive charge as well as the ability to not bind strongly to cell membranes.

2.5.3 The Toroidal Pore Model

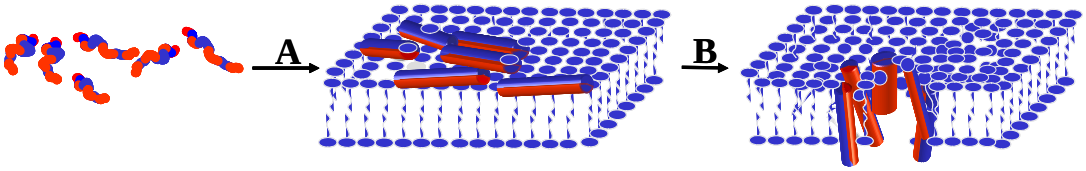

Figure 2.10. Illustration of the Toroidal Pore Model. Antibiotic peptides are attracted to and coordinate themselves to the bacterial surface **(A)**. Peptides randomly insert and integrate themselves into membrane opening a pore in the bacteria, which allows intracellular contents to leak out, resulting in cell death **(B)**.

The Toroidal Pore model **(Figure 2.10)** initially begins quite similar to the previously mentioned carpet model, but midway in the process, the cationic antibiotic peptides form a toroidal pore. These toroidal pores allow leakage of small cytoplasmic molecules prior to complete destruction of the bacterial membrane. Unlike barrel-stave pores, toroidal pores consist of peptides intercalated with the cell membrane. Experiments with Magainin[63] and Melittin[64] show the toroidal pore model is the principle model by which CAPs attack bacteria cell membranes. The toroidal pore mechanism suggests that α–helical CAPs initially lie parallel to the bacterial cell membrane. In the next step, the hydrophobic portion of peptide inserts itself and displaces the polar portion(s) of the membrane. This process leads to peptide insertion into the membrane.[65] When enough CAPs have inserted themselves into the membrane, strain and membrane thinning begins to take place. The ultimate result of this membrane thinning is the destabilization and eventual membrane destruction.[66] Finally, the CAPs, now in the cytoplasm, begin to attack intracellular targets rendering those targets useless.[67]

2.5.4 The Aggregate Model

It has been noted that some CAPs have bactericidal activity without significantly destroying or altering the bacterial membrane. The models which were previously mentioned are unable to explain why certain peptides are able to destroy bacteria by shutting down DNA synthesis; protein inhibition or receptor interactions. Due to these interesting findings another model named the Aggregate Channel was proposed.[41] This model suggests that CAPs cluster together in a more or less random fashion on the surface of the bacterial

membrane, capturing small negatively charged ions or water molecules. This leads to electrostatic repulsion between the positively charged amino acid side chains. Peptides cluster together and migrate throughout the bacterial membrane without causing major damage to it. The result of this is membrane local destabilization and peptide migration into the cytoplasm. It is assumed that the CAPs (now in the cytoplasm) attack specific intracellular targets and turn off cellular functions. Cationic antibiotic peptides can work by any mode of action. However, some CAPs may work by just one or perhaps many different mechanisms. This depends on the target bacterial cell of interest and of the CAP itself. The good news is that the end result of any of the aforementioned processes, the disruption of bacterial membranes, eventually leads to destruction of the target bacterial cell.

2.6 Cationic Antibiotic Peptides and Bacterial Resistance

Bacteria are tough little organisms that can survive in diverse places ranging from the cold of the ocean depths to desert hot springs. Therefore, it is realistic to expect that some bacteria would be resistant to CAPs. There are two types of resistance bacteria can have and it is not understood at the molecular level why some bacteria have immunity towards CAPs. One reason for this could be that some bacterial membranes may not contain enough negative charge or repel the peptide itself, due to a mutation. Also, outer cell membrane structural modifications (Gram-negative bacteria) have also been theorized to help bacteria become resistant to CAPS.[68]

2.6.1 Passive Resistance - Membrane Energetics

Some antibiotic peptides work by using the transmembrane potential of bacterial membranes as a driving force. Therefore, transmembrane potential can be regulated blocking the efficacy of CAPs. For example, one class of defensins (type-I) exert comparable antibiotic activities against bacteria that is either metabolically active or in a resting state.[69] However, a different class of defensins (type-II) exerts antibiotic potency against only metabolically active bacteria. This shows that certain bacteria which have low transmembrane potential, will have significant resistant against cationic antibiotic peptides.

2.6.2 Shielding by Electrostatic Interactions

A lot of pathogenic bacteria rely on encapsulation to prevent phagocytosis from immune system cells or just to adhere themselves to a preferred location. Capsule production is also an important, particularly among bacteria that infect the bloodstream, gastrointestinal and respiratory tracts. The glycocalyx (capsulation material) of many pathogenic bacteria is composed both carbohydrates and phosphates. Since the glycocalyx is negatively charged, CAPs are attracted to it and upon contact with this anionic material, CAPs become incapable of reaching the membrane, rendering them ineffective.[70]

2.6.3 Region Specific Resistance

Some pathogenic bacteria are able to resist CAPs, due to preferences for certain anatomical or physiological regions. One example of this is *Pseudomonas aeruginosa,* a class of bacteria responsible for urinary tract infections. These bacteria preferentially colonize tissues, such as the bladder and stomach which have abnormal ionic strength and/or abnormal osmotic pressure. The environment of these colonized tissues helps to prevent attack from antibiotic peptides.[71]

2.7 Inducible Resistance

Many pathogenic bacteria have evolved to produce successful counter defenses intended to block the effectiveness of cationic antibiotic peptides, which must be defeated for the pathogenic bacteria to survive and multiply. Some of these countermeasures range from permanent modification of the bacteria membrane and well as activation of toxic factors.

2.7.1 Defense via Peptidases

Probably one of the easiest ways bacteria defend themselves against cationic antibiotic peptides is through the secretion of peptidases that attack and destroy CAPs. One example of this occurs in the *Salmonella* species of bacteria. *Salmonella* has the ability to produce outer membrane endopeptidases, for example, which are able to attack and degrade CAPs.[72]

2.7.2 Structural Modifications to the Outer Membrane

As stated earlier, cationic antibiotic peptides (CAPs) initially target and interact with bacterial components, such as LPS, outside the cellular membrane. Evolution has provided bacteria with feedback systems that are utilized to prevent its destruction by CAPs. These feedback systems are rapidly induced in response to exposure to cationic antibiotic peptides. For example, CAPs can influence gene activation in *Salmonella* bacteria. This gene influences changes in the transmembrane gradient of the bacteria, which blocks CAPs from working.[33,74] Also, Gram-negative bacteria have the ability to modify its lipid A and LPS components leading to increased resistance to CAPs.[68,75]

2.7.3 Cytoplasmic Membrane Modifications

Another type of modification pathogenic bacteria can use to block CAPs activity is by changing their cytoplasmic membrane composition. One example, comes from the species, *Pseudomonas fluorescens* (colonizes both soil and plant surfaces). If there aren't enough phosphate sources available, this species has the ability to lose their negative cell potential, by modification with ornithine derived lipids, which are positively charged, leading to a decline of CAP activity towards this bacteria.[76]

2.7.4 Attacking Intracellular Components

Besides attacking extracellular components, CAPs also have the ability to attack intracellular targets. Bacteria have also devised mechanisms to prevent this from occurring. One species of *E. coli*, shows that mutation in one gene (named *gyrB*), led to significant decline of the bacteria being destroyed by the antibiotic peptide microcin B17, which is thought to block DNA replication (DNA gyrase). Specifically, E. coli's mutation causes an arginine residue to replace the normal tryptophan residue found in the polypeptide produced by the *gyrB* gene. This change leads to the reduced activity of microcin B17. Due to these recent findings, researchers are now aware that cationic antibiotic peptides can exert other actions, such is targeting internal components that goes beyond just simple interactions with the bacterial cell membrane.[77]

2.8 Conclusion

Widespread use/abuse of antibiotics, such as penicillin, erythromycin and others has led to a situation where pathogenic bacteria are becoming resistant to antibiotics. Organisms from divine phyla have evolved antibiotic mechanisms that generally involve the production of cationic antibiotic peptides with varying antibiotic activity. CAPs are found in various organisms and may be the first progenitor to an early immune system. Cationic antibiotic peptides (CAPs) are quite diverse, ranging from α–helices to constrained sheets, but all share certain commonalities such as a moderately high positive charge, less than 100 residues and amphipathicity. CAPs have high activity against bacteria in addition to possessing low activity towards mammalian cells. The mechanism(s) of action used by CAPs is (are) not known, but several models such as the Carpet, Barrel-Stave and Toroidal have been hypothesized to explain peptide activity. Unfortunately, bacteria possess resistance to these peptides through different methodologies. Some of these methods are simple such as hiding in a specific location in the host to complex such as gene modification to provide resistance.

2.9 Notes

Notes: Figures 2.1 - 2.5 were created by obtaining the peptide sequence from various sources, then drawing and minimization with Macromodel and finally resolution with the drawing program, Pov-ray.

Figure 2.10 was created by modification of Figure 2.9

Chapter 3

General Syntheses of Compounds

3.1 Synthesis of (*S*,*S*) and (*R*,*R*)–1,2–Diphenyl–1,2–Ethylenediamine

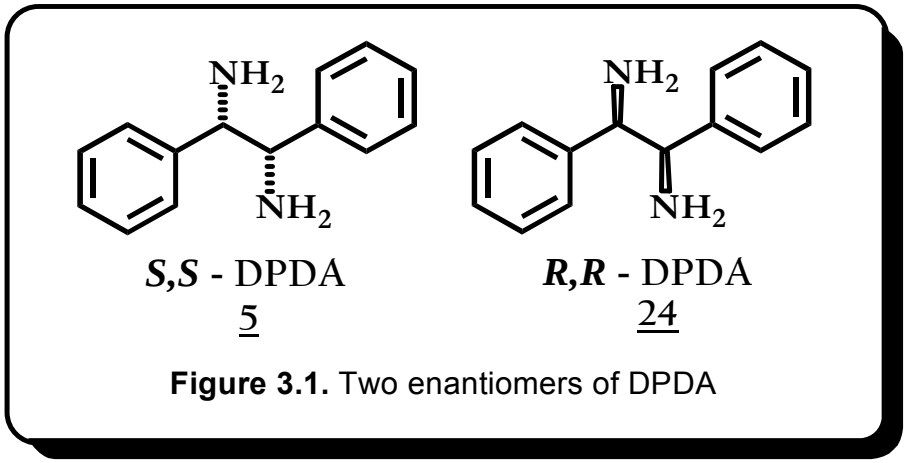

Figure 3.1. Two enantiomers of DPDA

The compounds (*S*,*S*) and (*R*,*R*)–1,2–diphenyl–1,2–ethylenediamine (DPDA) and its derivatives have been used as chiral controllers and chiral catalysts in many asymmetric reactions[78-81] **(Figure 3.1).** There are various approaches one can use to synthesize either enantiomer of DPDA. Some of these synthetic routes to the both diamine enantiomers include: manipulation of the chiral diol from styrene using Sharpless asymmetric dihydroxylation protocols[82] **(Scheme 3.1);** the titanium mediated coupling of two simple imines derived from benzaldehyde[81],

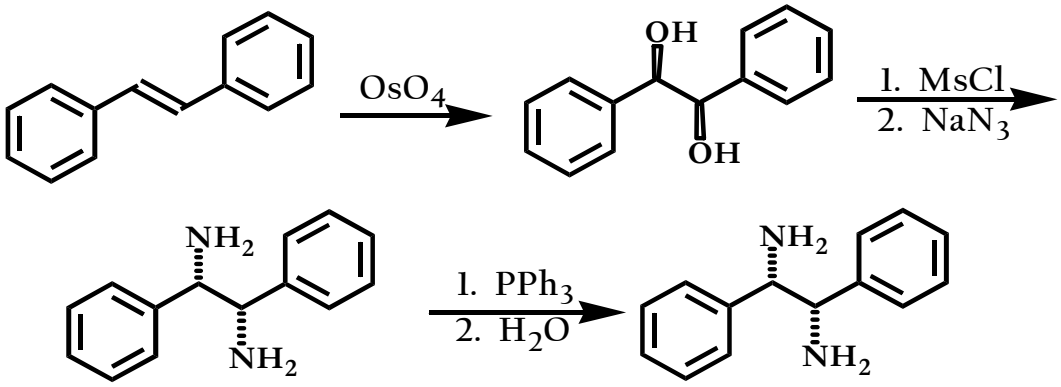

Scheme 3.1. Sharpless approach to enantiomerically pure DPDA.

then resolution leading to both enantiomers of DPDA **(Scheme 3.2)** and a protocol by Mistryukov, where a hydrobenzamide was converted to a *d,l* -DPDA precursor by an electrocyclic ring closure[83] **(Scheme 3.3)**.

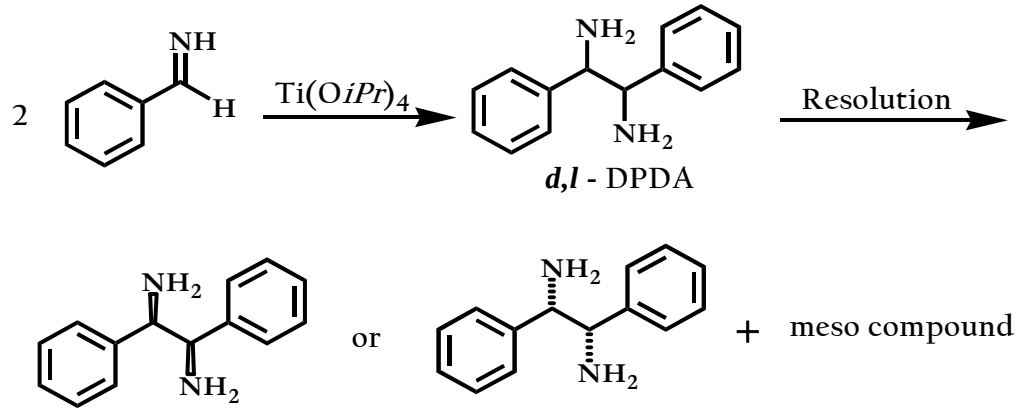

Scheme 3.2. Titanium mediated coupling.

One of the problems with the Sharpless approach to DPDA (which is actually a known procedure) is the use of toxic OsO_4 on a scale needed to obtain a large amount of product and the extra steps needed to convert the chiral diol to the diamine itself. Although the titanium method works fairly well, on a small to moderate scale, it produces the meso product (15 %) which first has to be removed before resolution can take place. Mistryukov's approach, albeit novel, has some drawbacks associated with it, such as: the use of mercury salts and the use of a pressure bomb to make the appropriate intermediates.

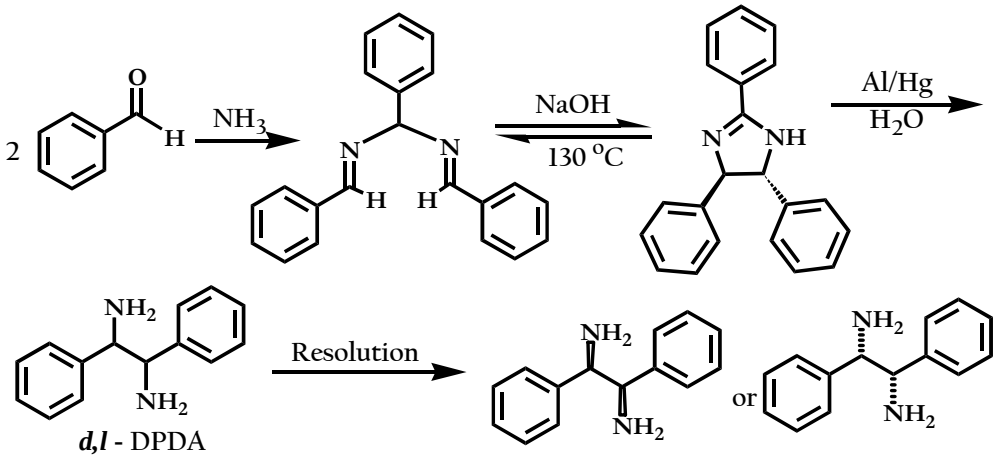

Scheme 3.3. An electrocyclic ring closure.

The preferred approach, the one we used, involved synthesis of the racemic diamine (*d*,*l* isomers only), then resolution by the appropriate tartaric acid, into pure enantiomers.[84] The materials used in this synthesis are extremely cheap and easy to obtain, which is an advantage. The synthesis begins by the reaction of a mixture of cyclohexanone, benzil, ammonium acetate refluxing in acetic acid.

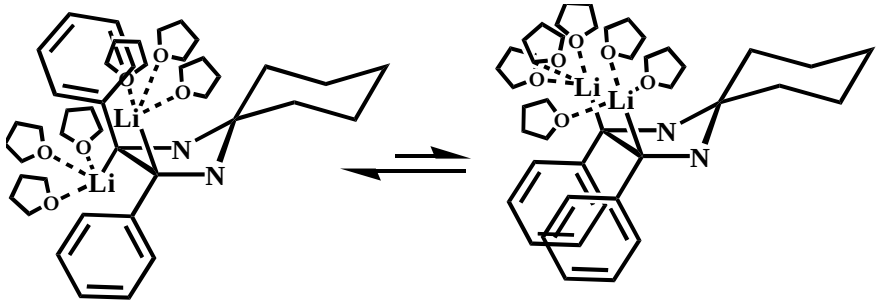

Figure. 3.2. Dianion formed from Lithium Reduction.

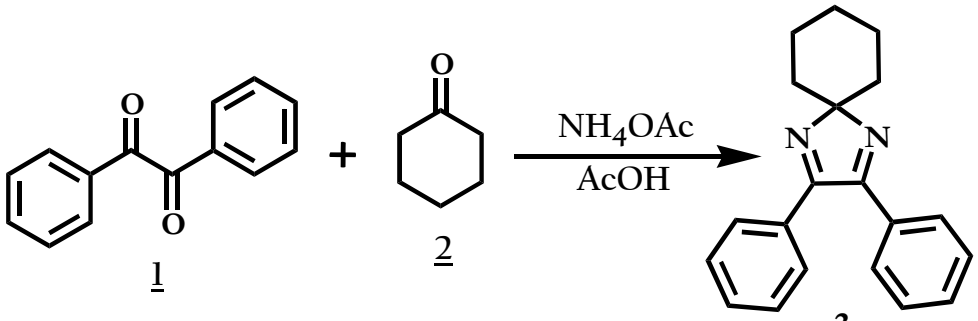

Scheme 3.4. Synthesis of Spiro-imidazole

This type of synthesis has been used in the middle of the 20th century as a method of producing various heterocyclic compounds[85] and in this particular case, resulted in the formation of the spiroimidazole compound, **3**, in good yield[84] **(Scheme 3.4).** One of the more noteworthy items about this reaction is that it can be done on a very large scale (easily up to 1 kg). Next, lithium metal was used to reduce both double bonds in the spiroimidazole, **3**. Four moles of lithium were needed, because lithium donates one electron per pi bond, which eventually resulted in the formation of a dianion **(Figure 3.2).** Spiroimidazole, **3**, is fused together; therefore no free rotation is allowed. The

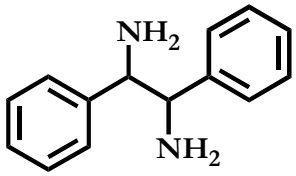

4

newly formed anions seek to oppose each other due to electron repulsion **(Figure 3.2)**, giving rise to a lower energy intermediate and upon protonation to produce only the *d,l* product, **4.** Spiro ring opening was accomplished by using 2 N HCl and upon basification with NaOH led to the racemic diamine. Finally, the *d,l* isomers were resolved with tartaric acid, where L-(+)-tartaric acid gave rise to the S,S-isomer and D-(-)-tartaric acid gave rise to the R,R isomer[84].

3.2 Diamine Mono-protection Strategies

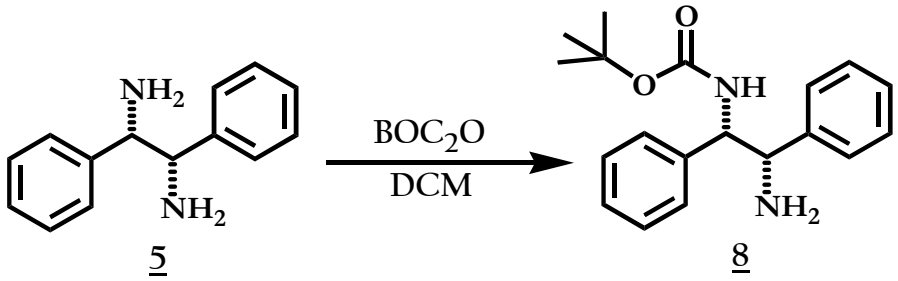

5 8

Scheme 3.5. Synthesis of Mono-Boc DPDA

At this point the DPDA needed to be protected, due to the eventual coupling of two separate DPDA molecules in a future step. Since the DPDA molecule possesses C_2 symmetry, orthogonal protecting groups must be used in this situation.

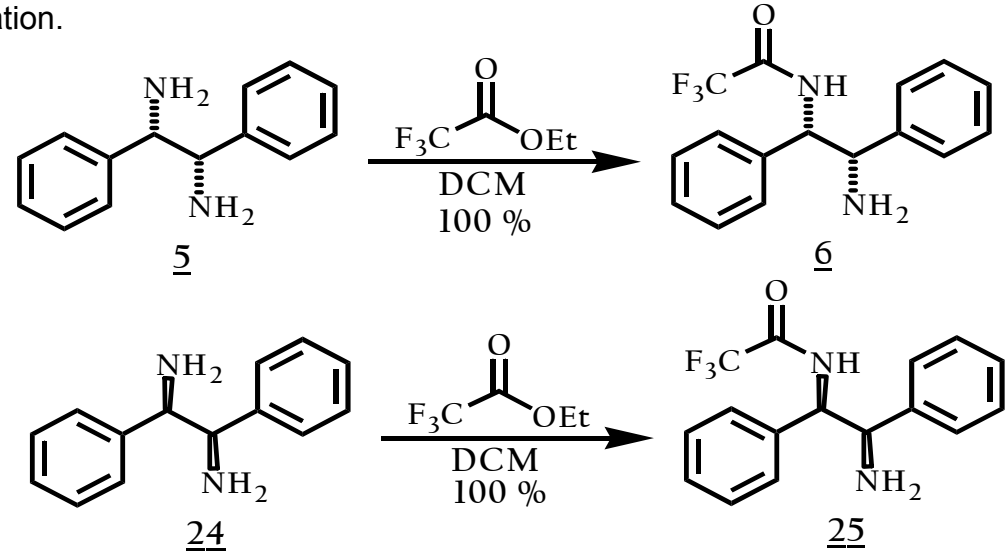

5 6

24 25

Scheme 3.6. Synthesis of Mono-TFA DPDA

At first, we thought the easiest mono-protected diamine to synthesize would be the BOC mono-protected diamine. In general, mono-protection of vicinal primary

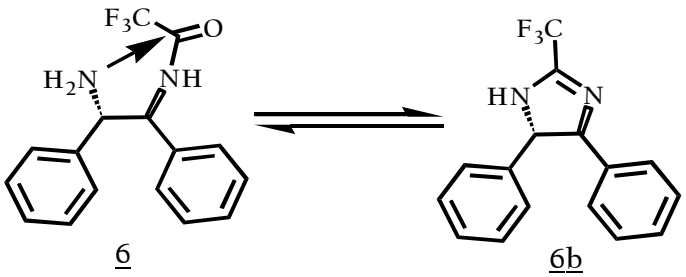

Figure 3.3. Formation of Cyclic Mono-TFA intermediate.

diamines is quite problematic, usually resulting in protection of both diamines. An attempt to synthesize a mono-Boc diamine was made, by carefully reacting 1 equivalent of BOC anhydride with the DPDA in DCM (Only the S enantiomer was tried). The yield of this reaction is quite low, which is characteristic of vicinal diamine mono-protection, with the majority of the product being the diprotected material. The literature shows that DPDA, (both enantiomers, respectively) can be mono-protected by using ethyl trifluoroacetate (excess amount) in THF affording 100 % yield of the mono-protected TFA compound.[86] In a similar manner, this was attempted using DCM as the solvent, instead of THF. This reaction still worked as the literature suggested. The authors of the paper gave no explanation why this reaction led to the mono-protected TFA amine. One hypothesis could be that the molecule undergoes a reversible cyclization **(Figure 3.3)** where the amino group attacks an electron poor carbonyl group in the same molecule leading to a 5-membered ring hydrate at low temperatures. Supporting evidence of this hypothesis comes from the attempted coupling of two mono TFA diamines in the presence of 1, 1-dicarbonyl imidazole. This reaction did not lead to the coupled urea product. Instead, a cyclic imidazoline compound formed **(Scheme 3.7)**.

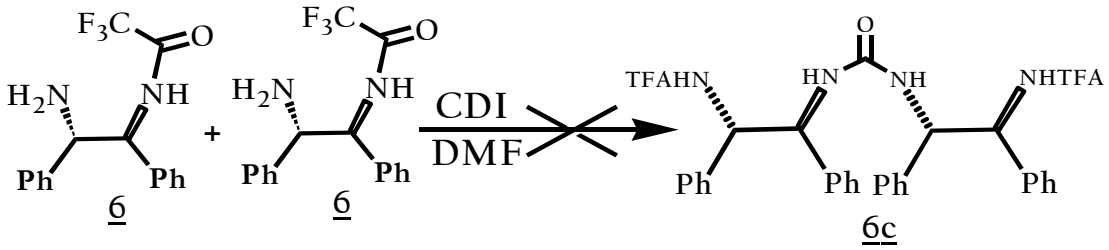

Scheme 3.7. Attempeted coupling of two Mono-TFA diamines

Out of curiosity, mono-TFA amine, **6**, was heated in DMF at 50 ^{o}C, without 1, 1-carbonyl diimidazole present resulting in the same product being formed. This suggests an intermolecular cyclization between the amino group and the carbonyl forming the initial hydrate. Water is eventually expelled to form the 5-membered imidazolidine product (**Fig. 3.4b).**

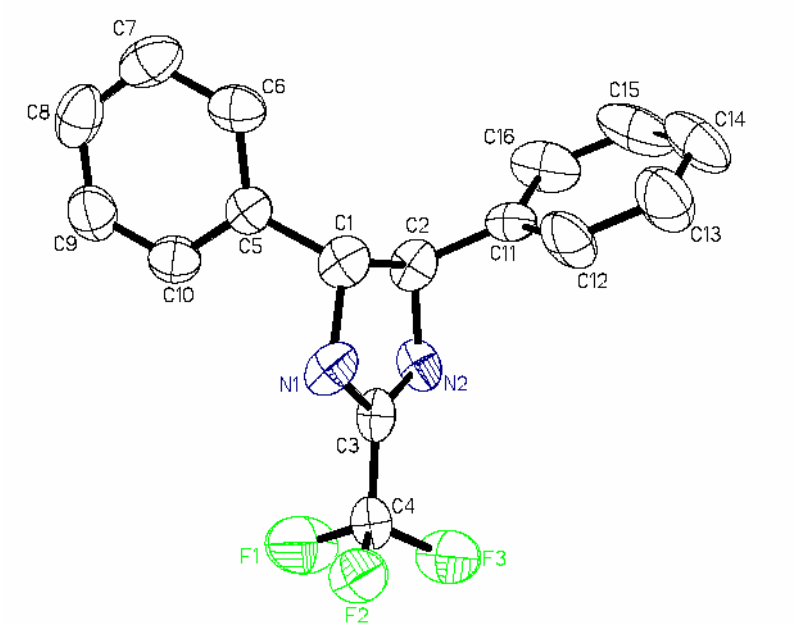

Figure 3.4b. X-ray crystal structure of compound 6b.

Another hypothesis to explain mono-protection occurs is due to the ability of the trifluoroacetyl group (when it is attached to the diamine) to withdraw electrons from an unprotected amino group, not allowing that amino group to be reactive enough to attack a different ethyl trifluoroacetate molecule. At this point, mono-TFA DPDA was synthesized in quantitative yield, but another mono-protected DPDA must be obtained, with its protecting group orthogonal to TFA. Earlier it was mentioned that attempting to mono-Boc DPDA lead to disastrous results, it was imagined that trying to mono-protect DPDA with other protecting groups would give the same outcome. However, an indirect method of making other mono-protected diamines can occur. We can use the mono-protected TFA molecule itself as a type of “intermediate” by protection of the free amine and then subsequent removal of the TFA protecting group[87] eventually leading to the desired mono-protected diamine.

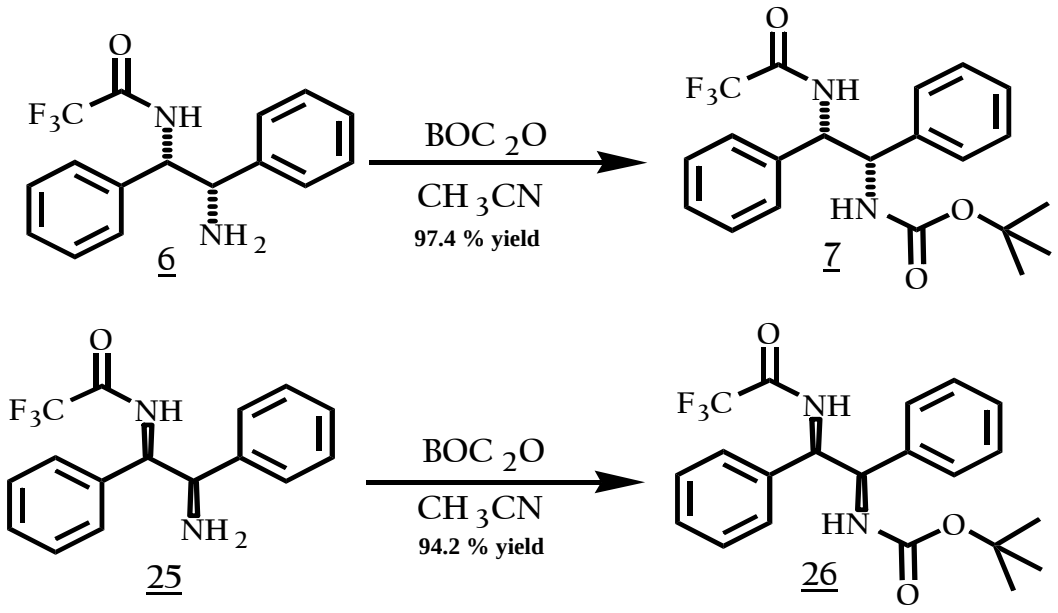

Scheme 3.8. Synthesis of the orthogonally protected monomer.

The BOC group seemed to be an ideal group due to it being orthogonal to a TFA group when it comes to deprotection. Treatment of the mono-protected-TFA diamine with Boc anhydride in acetonitrile, led to quantitative yield of the mixed orthogonally protected diamine, referred to as the "doubly protected monomer" **(Scheme 3.8)**. In order to obtain the mono-Boc diamine, the TFA protecting group needed to be removed. Such groups can be removed by reaction with a hydroxide base, such as LiOH or by using $NaBH_4$. Attempted removal of the protecting group with $NaBH_4$ (refluxing in MeOH) was not successful. Another approach to remove the TFA protecting group[87] utilized an excess of LiOH in MeOH **(Scheme 3.9)**. However, this reaction does not go to completion and it is not known why this reaction does so. The product was easily separated by column chromatography and the recovered starting material was resubmitted to the same reaction conditions. This was repeated until all of the starting material was consumed. Therefore, it is possible to generate the mono-Boc diamine indirectly though this method in high yields, rather than a direct synthesis of the mono-Boc diamine.

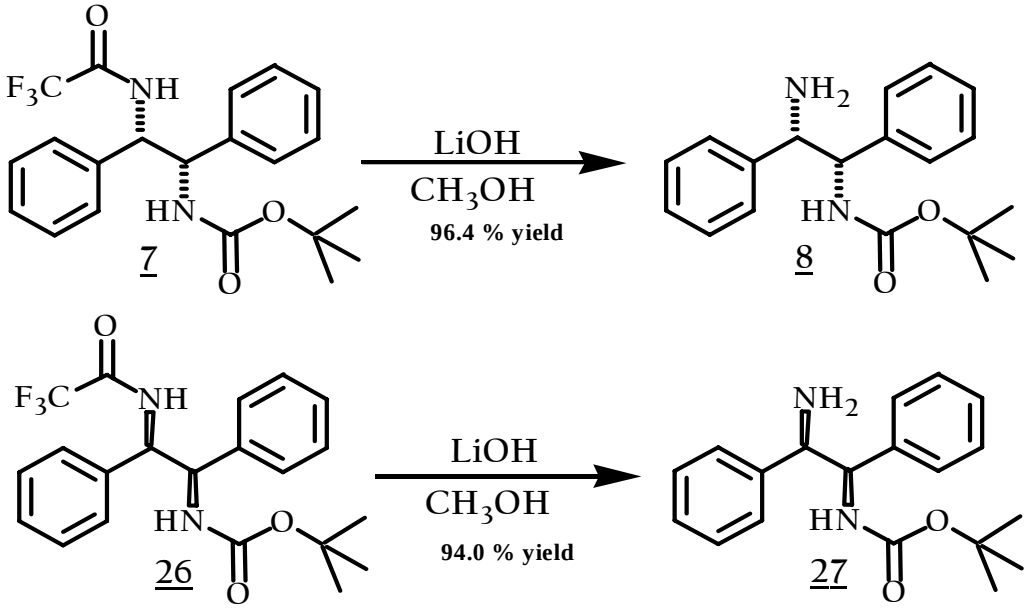

Scheme 3.9. Synthesis of Mono-BOC DPDA

3.3 Diamine Mono Activation Strategies and Diamine Coupling Reactions

In order to form a urea-linked dimer one of the carbonyl units must be activated towards coupling. The literature shows a few ways to accomplish this activation. Some of these methods include: formation of an isocyanate via triphosgene[88,89] **(Scheme 3.10)**; reaction with 1, 1-dicarbonyl imidazole[90] **(Scheme 3.11)** leading

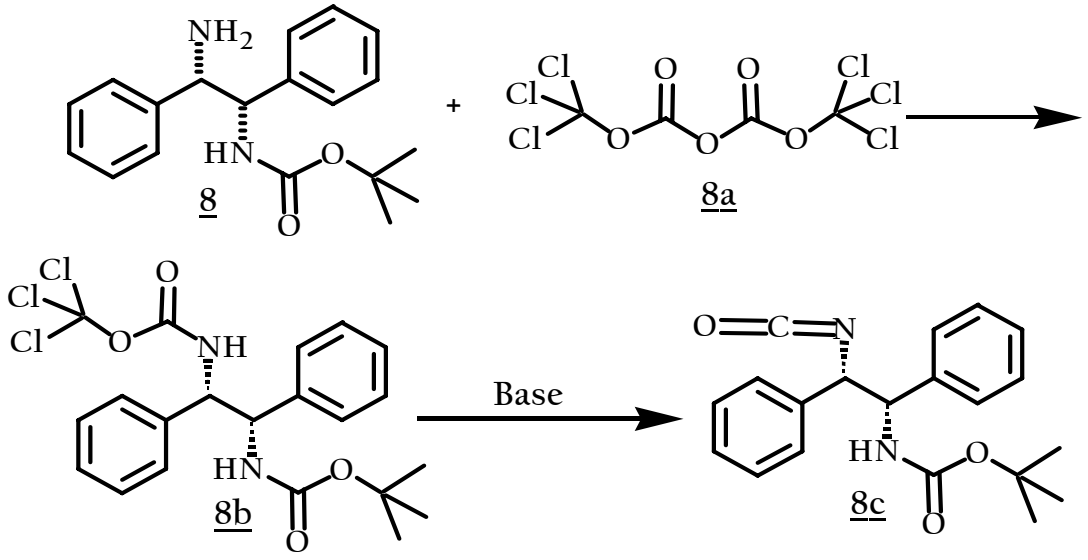

Scheme 3.10. Triphosgene Methodology.

to a reactive intermediate and the synthesis of a stable isocyanate precursor from *p*-nitrophenyl chloroformate **(Scheme 3.12).**[91] The problems with all

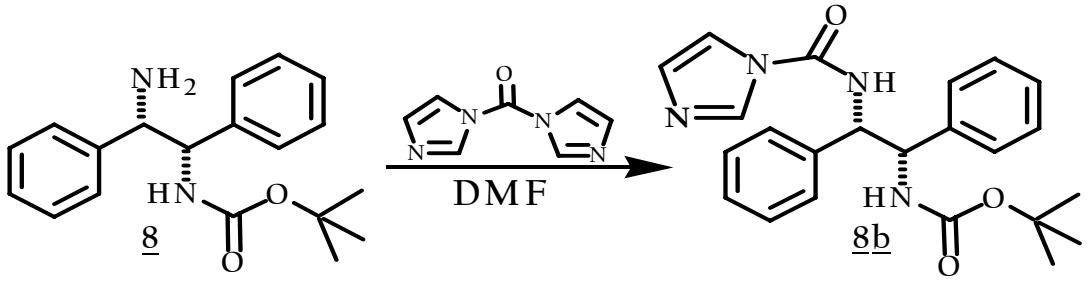

Scheme 3.11. Carbonyl imidazole methodology

the previously mentioned methods include handling of very reactive materials, use of anhydrous solvents (in the case of dicarbonyl imidazole) and not being able to control the reaction. Despite these drawbacks, the route utilizing *p*–nitrochloroformate[92] had distinct advantages over the other methods. One major advantage is the ease of purification of *p*-nitrophenyl carbamates, which

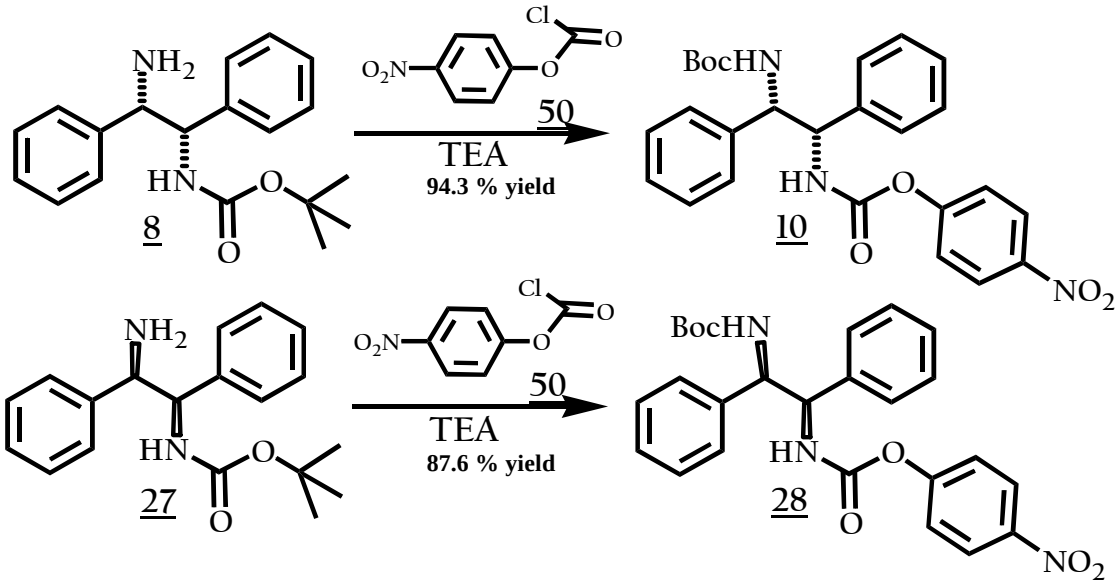

Scheme 3.12. Synthesis of *p*–nitrophenyl DPDA carbamate precursor

tends to form crystalline compounds. The literature shows that these types of compounds decompose over a time period of several months. At this point a crossroad was reached in the synthesis. Both the carbamates from the mono-Boc diamine and the TFA diamine could be made. Previous work from another project showed that reaction of 2 equivalents of the mono-TFA *p*-nitrophenyl

carbamate with DPDA led to both the desired product and also the transfer of the TFA group to another DPDA molecule. Use of the mono-Boc *p*-nitrophenyl carbamate did not lead to the transfer of the Boc group from on diamine to another **(Scheme 3.12)**. This led to the decision of use the mono-Boc DPDA carbamate as the coupling molecule. It is thought that the electron withdrawing *p*-nitrophenoxy moiety is responsible for this type of the transfer of the trifluoroacetyl group to a free amine. Earlier, it was mentioned that these types of molecules decompose over time. One very simple experiment to determine how long it would before the molecule, **10**, decomposed, was just to let it sit in solvent (this case $CHCl_3$) over a one week period. Three days later white needles began to form. It was determined the structure was, **10b**, by NMR.

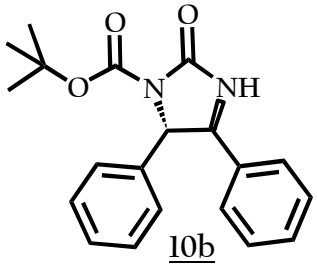

10b

Figure 3.5. An intermolecular cyclization product.

The *p* nitrophenyl carbamate decomposed, presumably forming the isocyanate in situ, which was subsequentially attacked by the BOC carbamate nitrogen. Therefore, reaction of a mono-BOC DPDA *p*-nitrophenyl carbamate with another mono-TFA protected DPDA molecule, **6 & 26**, in DMF lead to the orthogonally protected dimer, **11 & 29** , in good yields **(Scheme 3.13)**.Now that the orthogonal protected dimer, **11 & 29**, was in hand, the next step was the attachment of specific amino acid residues to the molecule. First, the dimer had to be deprotected and once again LiOH was used to carry out this task. Deprotection of the dimer was accomplished using excess LiOH in MeOH **(Scheme 3.14)**. This reaction was also observed to reach equilibrium. The starting material was separated from the deprotected TFA product and the starting material was subjected to the same reaction conditions.

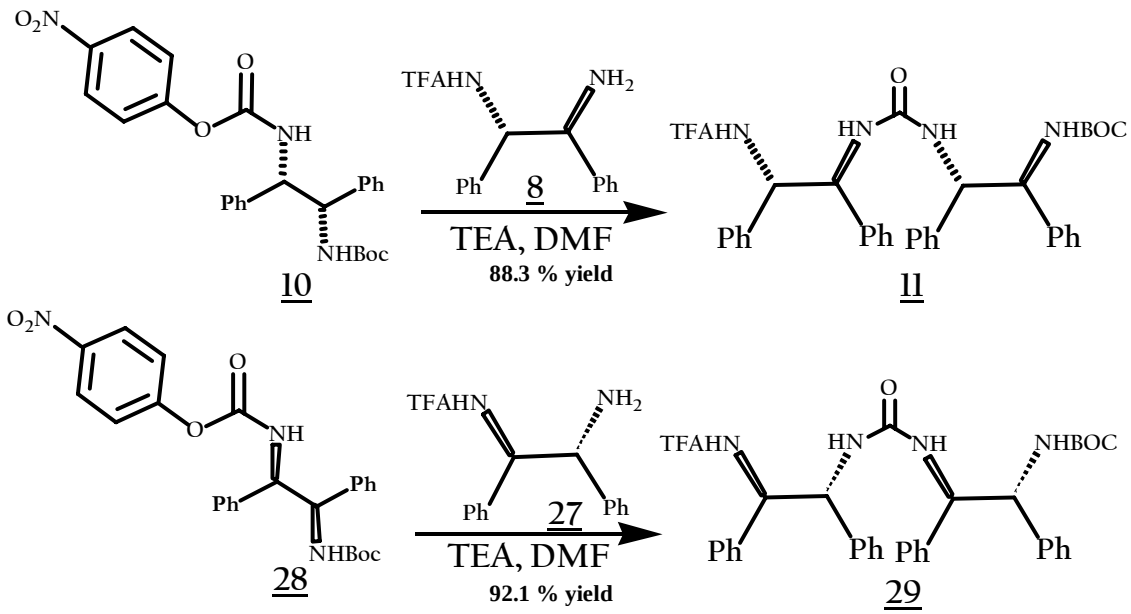

Scheme 3.13. Synthesis of orthogonal protected dimer.

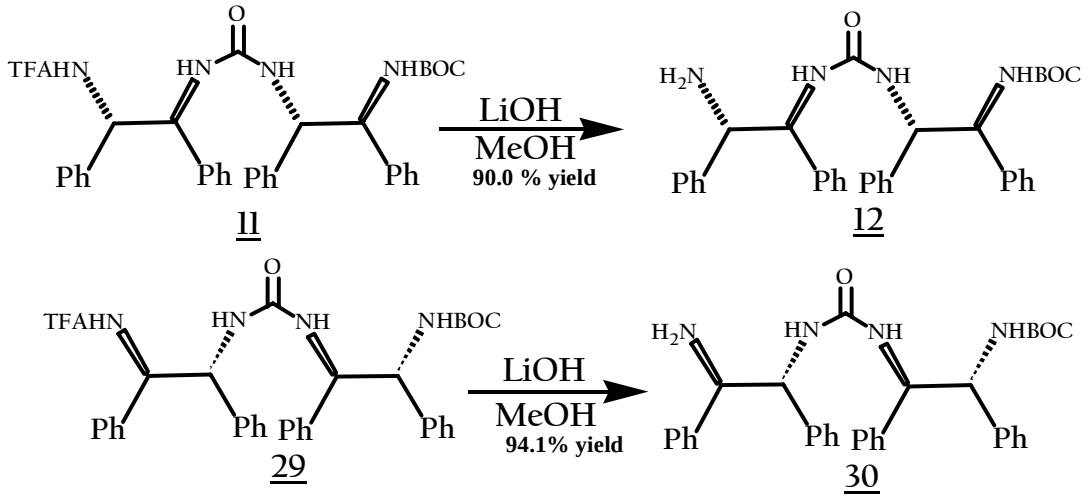

Scheme 3.14. TFA deprotection of dimer.

3.4 Activated Amino Acid Techniques and "Trimer" Synthesis

In order to introduce both diversity, as well as functionality into the peptidomimetic, two amino acids Lysine and Alanine, were chosen. Lysine allows the peptidomimetic to have the positive charge necessary for attraction to bacterial membranes and alanine was needed to act as a spacer and to provide

variability to our mimic. At this stage both amino acids (lysine and alanine) needed to be converted to their activated forms[93] (*p*-nitrophenyl carbamates) for coupling **(Scheme 3.15)**. Unfortunately, both amino acids needed to be protected as their methyl ester. If the carboxylic acid end of the amino acid is not protected as an ester, the molecule could close upon itself forming a cyclized product. The methyl esters of both amino acids (lysine also had its ε–amino group protected

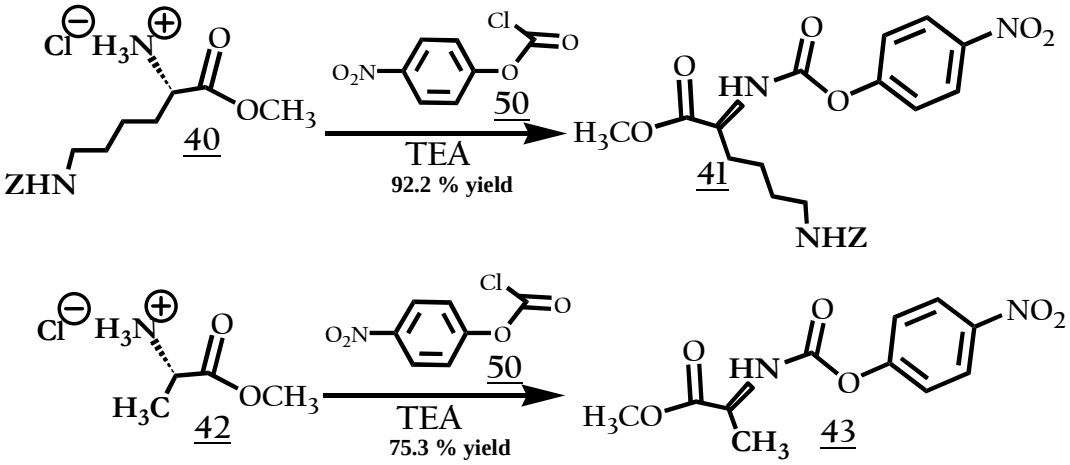

Scheme 3.15. Amino acid activation.

as a BOC carbamate) were reacted (individually) with *p*-nitrophenyl chloroformate affording the *p*-nitrophenyl carbamate of both amino acids esters in moderate yield **(Scheme 3.15)**. In the next step, these amino acid carbamates were reacted with the mono-protected dimer, respectively, to afford what we refer to as a Boc-protected "trimer" in moderate yields **(Scheme 3.16 - for Lys) (Scheme 3.17 - for Ala).**

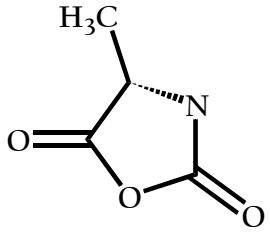

43b

Figure 3.6. Cyclized product from activated amino acid.

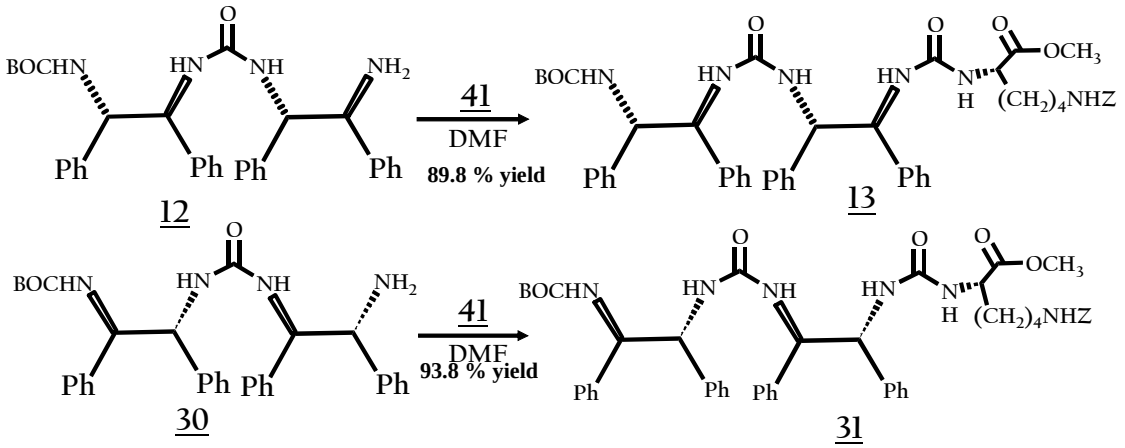

Scheme 3.16. Synthesis of protected lysine "trimers".

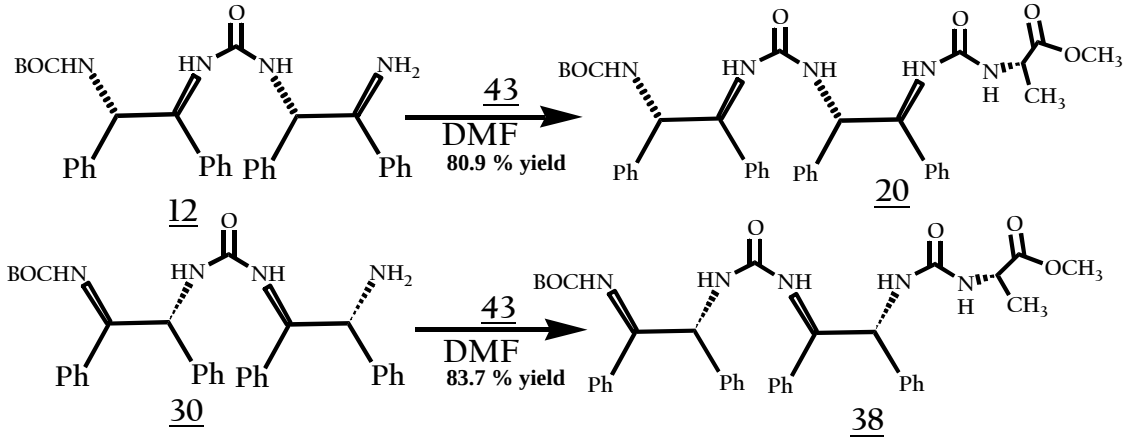

Scheme 3.17. Synthesis of protected alanine "trimers".

3.5 Protecting group modifications

Using the Boc protecting group allowed easy access to the trimeric units. However, it was found later that BOC protecting groups are not compatible with the solid phase resin (Knorr) that was used in this study. In order to prepare the molecule for solid phase synthesis it was decided to replace the BOC protecting

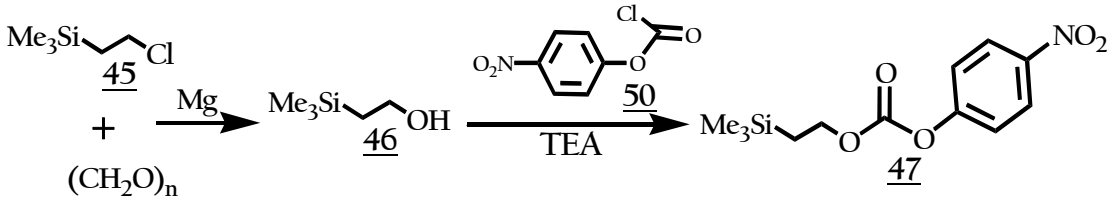

Scheme 3.18. Synthesis of Teoc carbonate.

group with a Teoc (Trimethylsilylethyl) group. Amines can be protected as a Teoc carbamate by their reaction with Teoc carbonate.[94] Teoc carbonate was prepared by reaction of trimethylsilyl ethanol with one equivalent of *p*-nitrophenyl chloroformate affording Teoc carbonate in good yield **(Scheme 3.18)**.

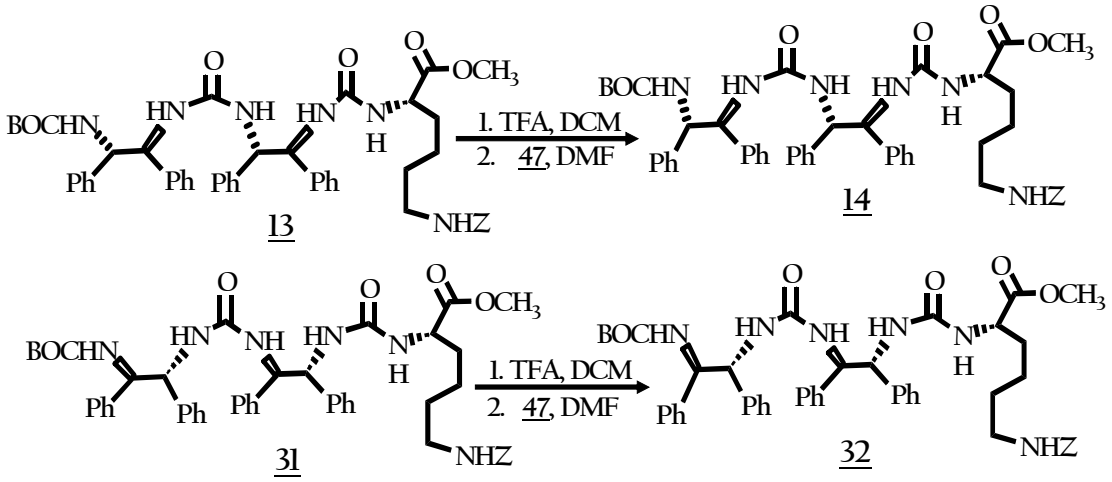

Scheme 3.19. Synthesis of Teoc protected lysine "trimers".

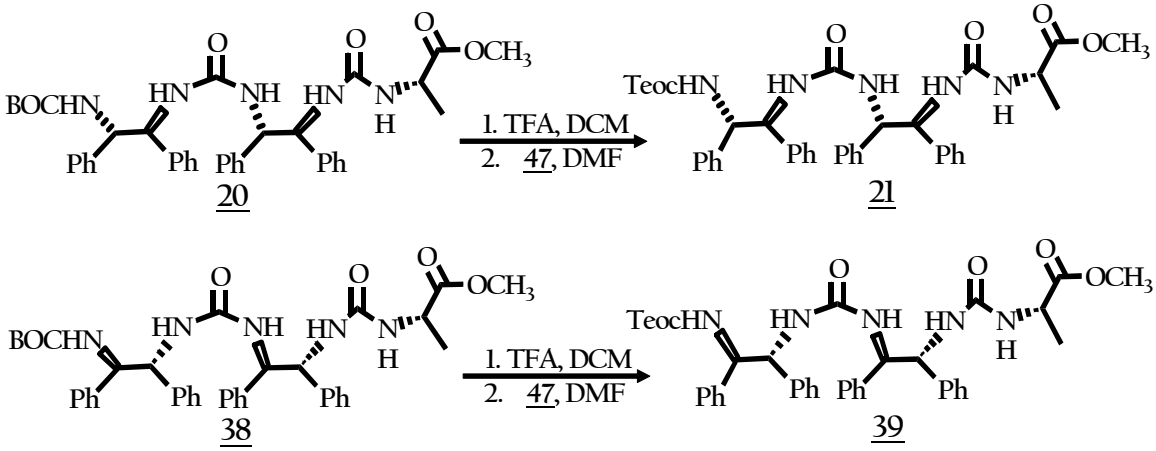

Scheme 3.20. Synthesis of Teoc protected alanine "trimers".

Teoc carbonate, **47**, was reacted with the Boc deprotected (by trifluoroacetic acid) trimer, effectively switching the terminal protection group **(Scheme 3.19 and Scheme 3.20)**. The obvious question here should be why Teoc protecting group strategy was not used from the very beginning of the synthesis. After asking ourselves this same question, a reaction of Teoc carbamate and the mono-TFA DPDA was attempted. This reaction lead to several different compounds being formed and the abandonment of this approach. To synthesize

the alanine trimeric precursor, **22** & **40**, the methyl ester was carefully saponified with ice cold 1M LiOH to avoid racemization **(Scheme 3.21)**.

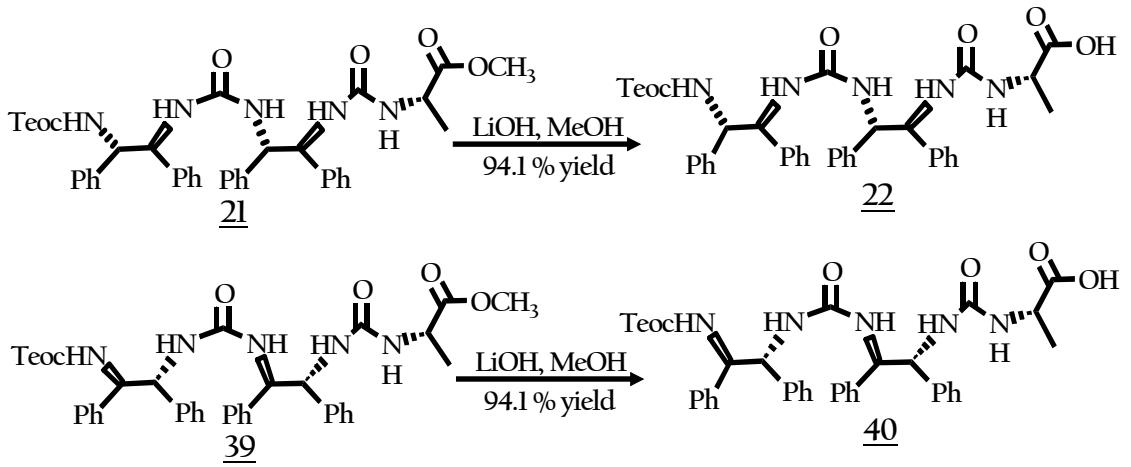

Scheme 3.21. Saponification of Alanine methyl ester.

For the ε–Z protected lysine trimer precursor more protecting group strategies had to be utilized. Therefore, the Z group was removed in via hydrogenolysis in the presence of BOC anhydride to directly convert the newly formed free amine to a tert-butyloxy carbamate **(Scheme 3.22)**. The final reaction was the careful hydrolysis of the protected lysine methyl ester with ice-cold 1M LiOH in methanol and with acidic workup of this basic mixture **(Scheme 3.23)** the carboxylic acid was formed in good yield.

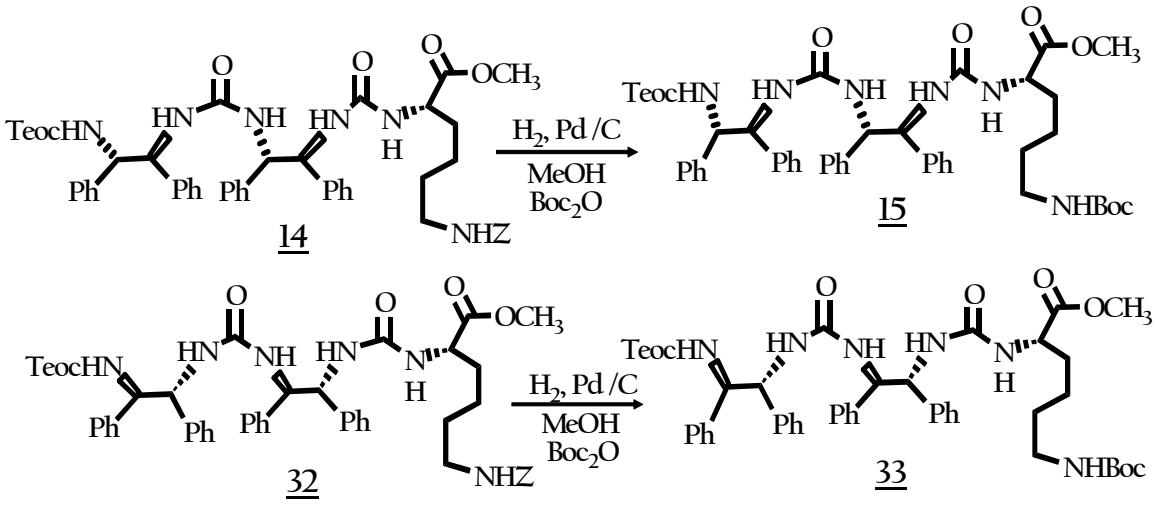

Scheme 3.22. Hydrogenation of Teoc protected "Trimer".

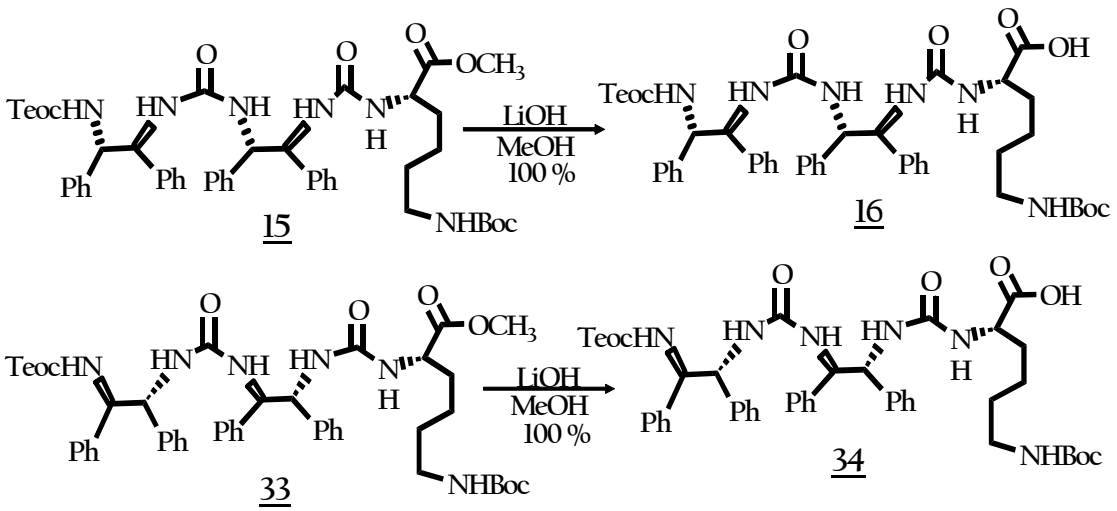

Scheme 3.23. Saponification of Teoc protected "Trimer".

3.6 Solid Phase Synthesis

The preceding reactions were used to generate the oligoureas (trimers), that are needed for fragment condensation on the solid phase.[95] One of the problems with solid phase synthesis is the costs of the solid phase resins themselves, with the Wang resin being the most cost effective. Since many different types of reactions can now be done on the solid support, including organometallic reactions, having a variety of different resins is important, because some reactions will only work on specific resins (due to their swelling capacity and solvent compatibility). In our situation, we used a polystyrene resin with Knorr's linker **(Fig. 3.7),** which is commonly referred to as Knorr's resin and is one of the traditional solid phase synthesis resins used in the synthesis of peptides.[96] The linker, protected by an Fmoc group, must be removed by washing 3 times with a piperidine/DMF solution, resulting in deprotection and the formation of a fulvene (**Scheme 3.24)**. After deprotection was completed; the resin was checked using the Kaiser test. The Kaiser test is a very sensitive colorimetric test, developed by Kaiser in the 70's to determine the

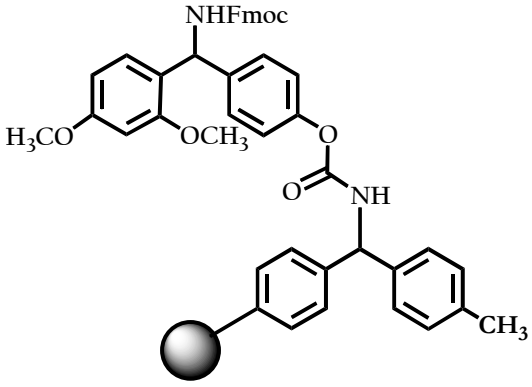

Figure 3.7. Knorr's linker

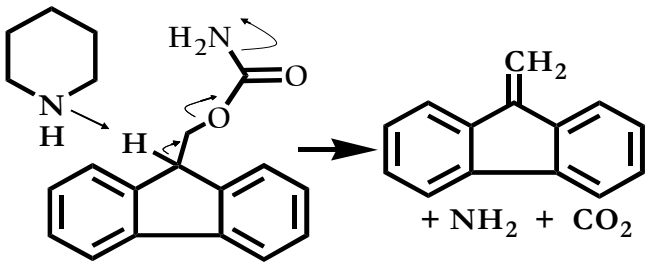

Scheme 3.24. Deprotection of FMOC amine.

presence of a primary amine.[97]

After detection of the free amine an attempt was made to couple an oligourea trimer to Knorr's resin.

Unfortunately, carboxylic acids do not react directly with amines. Therefore, carboxylic acids must be converted to an activated ester prior to use. There are many different approaches for making activated esters.[98] The goal of all of these different methods is to quickly make an activated ester and suppress any possible amino acid racemization. In our case, we decided to use Castro's Reagent (BOP) as the activating agent with HOBt to suppress any possible racemization.

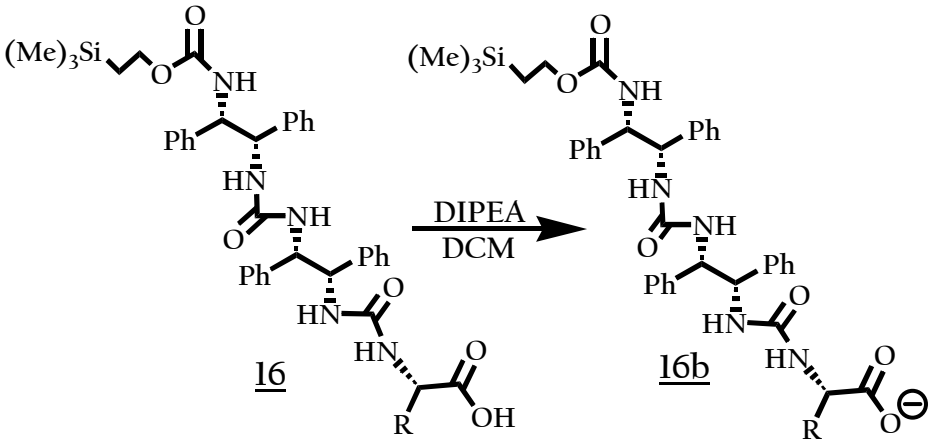

Scheme 3.25. First step in making an activated ester.

The first step in this process is the deprotonation of the carboxylic acid with Hunig's Base (DIPEA), **(Scheme 3.25)** then esterification with Castro's reagent in the presence of hydroxybenzotriazole (HOBt) (which suppresses racemization) **(Scheme 3.26)**. After the activated ester was formed, the mixture was added to the reaction vessel containing the deprotected solid phase resin and was allowed to react for several days at room temperature. The resin was tested under Kaiser conditions to determine if any free amine groups were present.

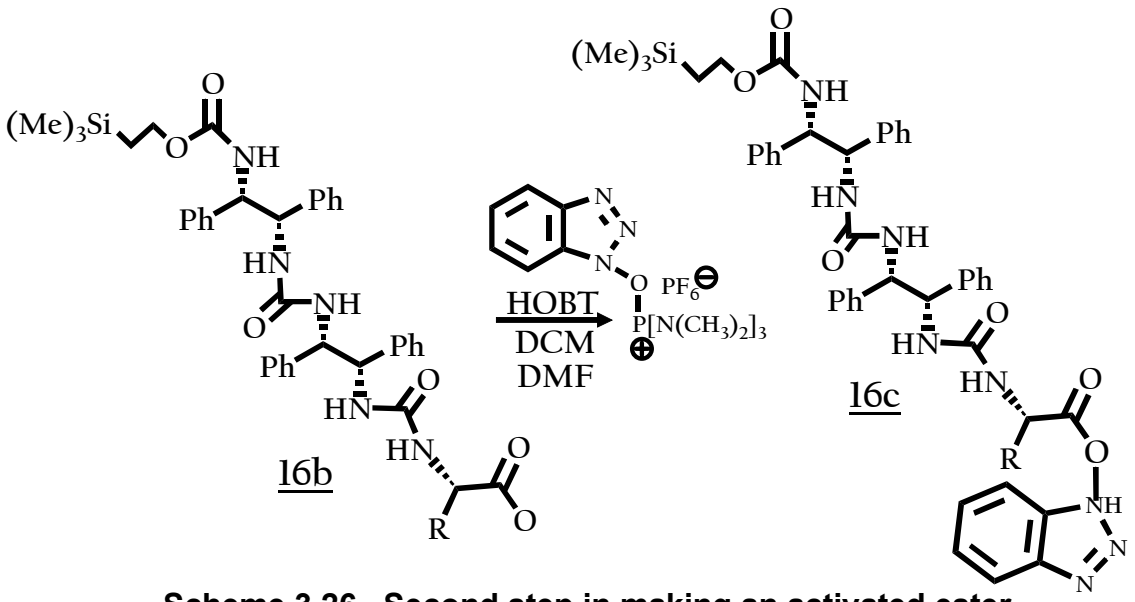

Scheme 3.26. Second step in making an activated ester.

The Kaiser test was positive, indicating the presence of a free amine. This shows that no coupling reactions had taken place; only starting material (activated ester) was recovered. This reaction was attempted several more times, only to end up unsuccessful. Other attempts were made, at slightly elevated temperatures. No coupling of the solid phase precursor to the resin occurred in this case as well. Two other oligourea trimers (the *R*,*R* diastereomer, **34** and the alanine containing oligourea **22**) were also tested as well. In these cases, no coupling occurred as well. One possible reason why coupling was not occurring could be caused by the actual solid phase resin itself. It could be that the Knorr resin is incompatible for this type of synthesis. Unfortunately, no other resins were used and there was not enough material to be used in future reactions at the time of this writing. Another possible reason why coupling did not occur could be related to the size of the solid phase precursors. There could be possible steric interactions influencing the approach of the activated ester to the resin, allowing a reaction not to occur. In order to continue this project, the problems associated with the solid phase must be corrected. Another student will carry on this project at this point. Next, the syntheses to the precursors used in this work will be described in the next section.

3.7 Experimental Procedure

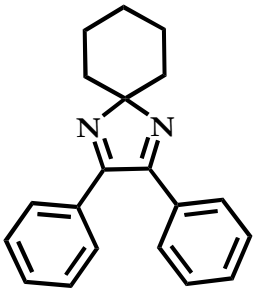

3

2, 2-Spirocyclohexane-4, 5-diphenyl-2H-imidazole[84]

A 2-L, three-necked, round-bottomed flask equipped with a mechanical stirrer and a reflux condenser is charged with 1.0 L of glacial acetic acid, 158 g (0.75 mol) of benzil, 400 g of ammonium acetate and 80 mL (0.77 mol) of cyclohexanone. The mixture is stirred and heated at reflux temperature for 1.5 hr and then, while hot, poured into 3 L of vigorously stirred water. The mixture is left overnight to cool to ambient temperature and crystals are collected by filtration, washed 4 times with 300 mL of water, crushed in a mortar and dried under reduced pressure to give 207 g (96 %) of the product as beige crystals, mp 105 – 106 °C; ^{1}**H** NMR (Varian 400 MHz; (DMSO–*d6*) δ: 1.65 – 1.92 (m, **6H**), 1.95 – 2.00 (m, **4H**), 7.33 – 7.53 (m, **10H**); ^{13}**C** NMR (Varian 400 MHz; (DMSO–*d6*) δ: 24.1, 25.7, 34.7, 104.1, 128.3, 128.9, 129.9, 133.1, and 164.0.

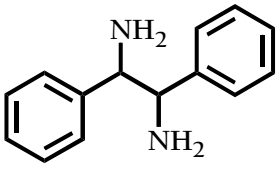

4

(±)–1, 2–Diphenyl–1, 2–ethylenediamine[84]

A 2 L, four-necked, round-bottomed flask equipped with a mechanical stirrer, thermometer and dry ice condenser is charged with 72.0 g (0.250 mol) of 2,2–spirocyclohexane–4,5–diphenyl–2*H*–imidazole, **3**. The flask is flushed with argon, and 400 mL of THF is added. The mixture is stirred until all solids dissolve, cooled to −78 °C (dry ice/acetone bath) and treated with a stream of

gaseous NH_3 until the volume of liquid increases by about 400 mL. One of the side necks is then equipped with a solids addition funnel and 6.94 g (1.00 mol) of lithium is slowly introduced by cutting the wire with scissors in a gentle stream of argon. The rate of lithium addition is such that the temperature does not rise above − 65 °C. Following the addition of lithium, the mixture is stirred for 30 min and 30 mL (1.0 mol) of ethanol is slowly added. The mixture is stirred for an additional 20 min and 70.0 g of NH_4Cl is added. The cooling bath is removed, the mixture is allowed to warm to 0 °C, 400 mL of water is carefully introduced, and the phases are separated. The aqueous phase is washed 3 times with 300 mL of ether and the combined organic extracts are washed with brine, dried over anhydrous sodium sulfate, filtered and concentrated with a rotary evaporator to about 200 mL. The solution is transferred to a 1 L, one-necked, round-bottomed flask equipped with a mechanical stirrer, cooled to 0 °C and treated with 300 mL of 2 N aqueous HCl. The biphasic mixture is vigorously stirred at ambient temperature for 1 hr, 500 mL of water is added and phases are separated. The organic phase is washed with 150 mL of water and the combined aqueous phases are extracted with 300 mL of DCM. The aqueous solution is then carefully treated with 300 mL of 2 M NaOH and the mixture is extracted 4 times with 150 mL of DCM. The combined organic extracts are washed with brine, dried over anhydrous $NaSO_4$, and filtered. Removal of volatile material under reduced pressure (water aspirator) gives 48.0 g (92.1 % yield) of racemic diamine as a pale yellow solid, mp 81 – 82 °C, lit.[84] mp 82 °C; ^{1}**H** NMR (Varian 400 MHz; (DMSO–*d6*) δ: 1.90 (s, **4H**), 3.82 (s, **2H**), 7.06 – 7.17 (m, **10H**); ^{13}**C** NMR (Varian 400 MHz; (DMSO–*d6*) δ: 61.9, 126.8, 126.9, 128.2, and 143.4.

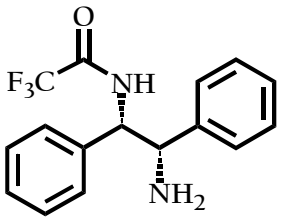

5

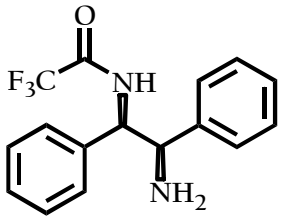

24

(1S, 2S)– (−) –and (1R, 2R)– (+)–1, 2–Diphenyl–1, 2–ethylenediamine[84]

"*S*,*S* and *R*,*R* Parent Diamine"

A 1 L, round-bottomed flask equipped with a mechanical stirrer is charged with 42.5 g (0.20 mol) of the racemic diamine, **4**, and 230 mL of ethanol. The solids are dissolved by heating the mixture to 70 °C whereupon a hot (70 °C), homogeneous solution, of 30.0 g (0.200 mol) of L–(+)–tartaric acid in 230 mL of ethanol is added. The tartrate salts precipitate immediately, and after the mixture is cooled to ambient temperature, the crystals are collected by filtration, washed twice with 60 mL of ethanol, and dried under reduced pressure. The solids are dissolved in 230 mL of boiling water, 230 mL of ethanol is added and the homogeneous solution is allowed to cool slowly to room temperature. The crystals are collected by filtration, washed with 40 mL of ethanol and dried under reduced pressure. The recrystallization procedure is then repeated twice using the same volumes of solvents (230 mL of water and 230 mL of ethanol) to give 23 – 25 g (63 – 69%) of the tartrate salt as colorless crystals, $[\alpha]^{23}D$ −10.8 ± 0.2° (H_2O, *c* 1.3). The salt is transferred to a 1 L, one-necked, round-bottomed flask equipped with a magnetic stirring bar and suspended in 300 mL of water. After the mixture is vigorously stirred and then cooled to 0 – 5°C, 23 mL of 50 % aqueous NaOH is added dropwise followed by 150 mL of DCM and stirring is continued for 30 min. The phases are separated, the aqueous phase is washed twice with 50 mL of DCM and the combined organic extracts are washed with brine, dried over anhydrous $NaSO_4$ and filtered. Removal of the volatile material under reduced pressure gives a colorless solid that is recrystallized from hexane to yield 12 – 14 g (57–66%) of (*S*,*S*)–(**−**)–diamine as colorless crystals, $[\alpha]^{23}D$ −106 ± 1° (MeOH, *c* 1.1) lit.[84] $[\alpha]^{23}D$ −106.5 ° (MeOH, *c* 1.09). The filtrates from all crystallizations are combined and the solvent is evaporated on a rotary

evaporator under vacuum (water aspirator). The residual solid is transferred to a 1 L, one-necked, round-bottomed flask equipped with a magnetic stirring bar, and suspended in 250 mL of water. To this vigorously stirred mixture is slowly added 25 mL of aqueous 50 % NaOH followed by 200 mL of DCM and the stirring is continued for 30 min. The phases are separated, the aqueous phase is washed twice with 50 mL of DCM and the combined organic extracts are washed with brine, dried over anhydrous $NaSO_4$ and filtered. Removal of volatile material under reduced pressure gives 24 – 27 g of the enriched (*R*,*R*)–diamine as pale yellow crystals. This material is treated with D–(**−**)–tartaric acid and the resulting salt is recrystallized in exactly the same manner as described for the other enantiomer to give 29 – 31 g (80 – 85%) of colorless crystals, $[\alpha]^{23}$ D +4 ± 0.5 ° (H_2O, *c* 1.3). Treatment with NaOH, as described above, followed by crystallization from hexane gives 11.5 – 13 g (54 – 61%) of (*R*,*R*)–(+)–diamine as colorless crystals, $[\alpha]^{23}$ D +106 ± 1° (MeOH, *c* 1.1); ^{1}**H** NMR (Varian 400 MHz; (DMSO–*d6*) δ: 1.65 – 1.92 (m, **6H**), 1.95 – 2.00 (m, **4H**), 7.33 – 7.53 (m, **10H**). ^{13}**C** NMR (Varian 400 MHz; (DMSO–*d6*) δ: 24.1, 25.7, 34.7, 104.1, 128.3, 128.9, 129.9, 133.1, and 164.10.

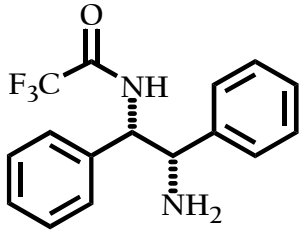

6

***N*–(2–Amino–*S*,*S*–1,2–diphenylethyl)–2, 2,2,trifluoroacetamide[86]**
"*S*,*S* – Mono TFA Diamine"

To a 250 mL round bottom flask was added 10.0 (32.5 mmol) of *S*,*S*–1,2–diphenyl–1,2–diamine in 100 mL of DCM. Next, the solution was cooled to 0 ^{o}C and a previously chilled solution of ethyl trifluoroacetate (5.00 mL, 35.0 mmol) in 10 mL of DCM was added dropwise with stirring. After a while a gel formed and stirring was increased. After addition, the solution was allowed to stir for 1 hr at 0 ^{o}C. The solvent was removed carefully under rotary evaporation then

placed under vacuum for 24 hrs, allowing for a quantitative yield (14.5 g) of the *S*, *S*–Mono–TFA protected diamine. Melting pt. = 182-183 ^{o}C.

^{1}**H** NMR (Varian 400 MHz; (DMSO–*d6*) δ: 4.22 (d, **1H**, *J* = 8.27 Hz); 4.92 (d, **1H**, *J* = 8.27 Hz); 7.09 – 7.22 (m, **10H**). ^{13}**C** NMR (Varian 400 MHz; (DMSO–*d6*) δ: 59.35, 61.06, 111.66, 114.53, 117.40, 120.27, 126.77, 127.08, 127.23, 127.57, 127.80, 128.02, 139.88, 143.07, 155.43, 155.79, 156.15, and 156.51.

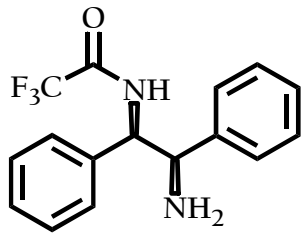

25

N–(2–Amino–*R*,*R*–1, 2–diphenylethyl)–2,2,2–trifluoroacetamide[86]
"R, R–Mono TFA Diamine"

To a 250 mL round bottom flask was added 9.00 (29.2 mmol) of *R,R*–1,2–diphenyl–1,2–diamine, **24**, in 100 mL of DCM. Next, the solution was cooled to 0 ^{o}C and a previously chilled solution of ethyl trifluoroacetate (4.50 mL, 31.7 mmol) in 10 mL of DCM was added dropwise with stirring. After a while a gel formed and stirring was increased. After addition, the solution was allowed to stir for 1 hr at 0 ^{o}C. The solvent was removed carefully under rotary evaporation, then placed under vacuum for 24 hrs, allowing for a quantitative yield (13.1 g) of the *R*,*R*–Mono–TFA protected diamine, **25**. ^{1}**H** NMR (Varian 400 MHz; (DMSO–*d6*) δ: 4.24 (d, **1H**, *J* = 8.27 Hz); 4.95 (d, **1H**, *J* = 8.27 Hz); 7.12 – 7.24 (m, **10H**). ^{13}**C** NMR (Varian 400 MHz; (DMSO–*d6*) δ: 59.50, 61.32, 111.72, 114.55, 117.42, 120.25, 126.78, 127.11, 127.26, 127.58, 127.84, 128.05, 139.92, 143.12, 155.47, 155.81, 156.19, and 156.55.

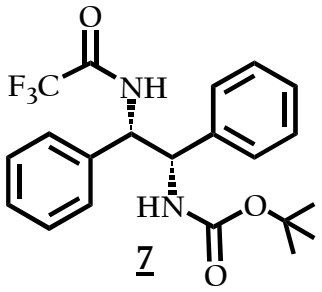

7

[*S*,*S*–1, 2–Diphenyl–2–(2, 2, 2–trifluoroacetylamino)–ethyl]–carbamic acid tert–butyl ester
"*S*,*S*–Mixed Monomer"

To a round bottom flask containing 7.25 g (23.5 mmol) of the *S*,*S*–mono TFA amine, **6**, was added 125 mL of MeCN, a stirring bar and 5.25 g (24.1 mmol) of Boc anhydride. The reaction was stirred at room temperature and after 30 min. a white precipitate began to form. The reaction was allowed to continue stirring overnight. The next day, the solution was filtered allowing the recovery of white solid material which was recrystallized from EtOAc affording white needle-like crystals, **7**. Yield = 9.35 g; % yield = 97.4; mp: 223-4 °C; ^{1}**H** NMR (Varian 400 MHz; (DMSO–*d6*)) δ: 1.27 (s, **9H**); 5.09 – 5.13 (dd**, 1H**); 5.26 – 5.30 (dd, **1H**); 7.12 – 7.29 (m**, 10H**); 7.66 – 7.69 (d, **1H**); 9.79 – 9.81 (d, **1H**). ^{13}**C** NMR (Varian 400 MHz; (DMSO–*d6*) δ: 28.117, 57.712, 58.008, 78.138, 111.75, 114.42, 117.29, 121.30, 127.02, 127.20, 127.3, 127.95, 128.09, 138.65, 140.15, 155.06, 155.24, 155.63, 155.98, 156.38. .***Anal. Calc*: C**, 61.76; **H**, 5.68; **N**, 6.86; **F**, 13.96; ***Found:*** C, 61.69; **H**, 5.53; **N**, 6.77; **F**, 13.98.

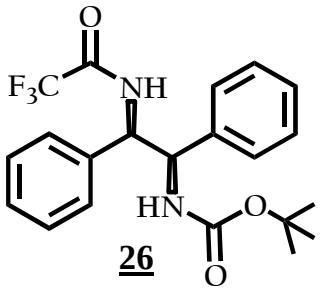

26

[*R*,*R*–1, 2–Diphenyl–2–(2, 2, 2–trifluoroacetylamino)–ethyl]–carbamic acid tert–butyl ester
"*R*,*R*–Mixed Monomer"

To a 250 mL round bottom flask containing 6.5 g (21.3 mmol) of the *R*,*R*–mono TFA amine was added 125 mL of MeCN, a stirring bar and 9.25 g (42.4 mmol) of BOC anhydride. The reaction was stirred at room temperature and after 30 min. a white precipitate began to form. The reaction was allowed to continue stirring overnight. The next day, the solution was filtered allowing the recovery of white solid material which was recrystallized from EtOAc affording white needle-like crystals. Yield = 8.12 g; Percent yield = 94.2 %. ^{1}**H** NMR (Varian 400 MHz; (DMSO–*d6*) δ: 1.28 (s, **9H**); 5.10 – 5.15 (dd, **1H**); 5.28 – 5.32 (dd**, 1H**); 7.14 – 7.31 (m, **10H**); 7.68 – 7.72 (d, **1H**); 9.81 – 9.83 (d, **1H**). ^{13}**C** NMR (Varian 400 MHz; (DMSO–*d6*) δ: 28.12, 57.73, 58.02, 78.16, 111.79, 114.42, 117.29, 121.32, 127.10, 127.20, 127.3, 127.95, 128.11, 138.65, 140.15, 155.10, 155.23, 155.63, 155.94, 156.34.

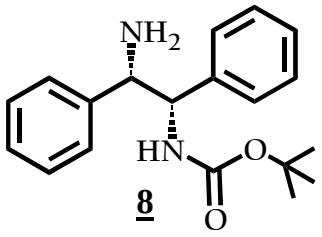

8

(2–Amino–*S*,*S*–1, 2–diphenylethyl)–carbamic acid tert–butyl ester
"*S*,*S*–Mono – BOC Diamine"

8.00 g (19.6 mmol) of the *S*, *S*-mixed monomer was added to a 250 mL round bottom flask and was suspended in 100 mL MeOH. 1.50 g (32.65 mmol) LiOH was added and the solution was brought to reflux and allowed to reflux overnight. The next day the solution was allowed to cool to room temperature and the

MeOH removed via rotary evaporation. The product was suspended in water and extracted with EtOAc. This was repeated two more times and the organic extracts were combined and dried over anhydrous Na_2SO_4. The salts were removed and EtOAc removed by rotary evaporation. The compound was purified by column chromatography using first 100 % $CHCl_3$ to remove any starting material and then with 100 % EtOAc to obtain the product as a pale yellow gummy solid. Unfortunately, this reaction reaches equilibrium and does not continue. This reaction was repeated with the remaining starting material until all the starting material was consumed and was worked up in the same manner (twice). Total yield for all combined reactions was 5.90 g (96.4 %) ^{1}**H** NMR (Varian 400 MHz (DMSO–*d6*) δ: 1.32 (s, **9H**); 4.08 (d, **1H**, *J* = 6.66 Hz); 4.70 (t, **1H**, *J* = 7.69 Hz, *J* = 7.80 Hz); 7.12 – 7.27 (m, **10H**); 7.38 (d, **1H**, *J* = 8.91 Hz). ^{13}**C** NMR (Varian 400 MHz; (DMSO–*d6*) δ: 28.23, 60.03, 61.20, 77.81, 126.47, 126.54, 127.06, 127.23, 127.67, 127.78, 142.08, 143.30, 155.27. ***Anal. Calc*: C**, 73.05; **H**, 7.74; **N**, 8.97. ***Found:* C**, 72.99; **H**, 8.53; **N**, 8.67.

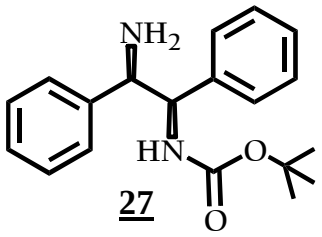

27

(2–Amino–*R*,*R*–1, 2–diphenylethyl)–carbamic acid tert–butyl ester
"*R,R*–Mono – BOC Diamine"

7.00 g (17.1 mmol) of the *R*, *R*-mixed monomer was added to a 250 mL round bottom flask and was suspended in 100 mL MeOH. 1.50 g (33.7 mmol) LiOH was added and the solution was brought to reflux and allowed to reflux overnight. The next day the solution was allowed to cool to room temperature and the MeOH removed via rotary evaporation. The product was suspended in water and extracted with EtOAc. This was repeated two more times and the organic extracts were combined and dried over anhydrous Na_2SO_4. The salts were removed and EtOAc removed by rotary evaporation. The compound was purified by column chromatography using first 100 % $CHCl_3$ to remove any starting

material and then with 100 % EtOAc to obtain the product as a pale yellow gummy solid. This reaction was repeated with the remaining starting material obtained from column chromatography until all the starting material was consumed and was worked up in the same manner. Total yield for all combined reactions was 94 % (5.02 g).

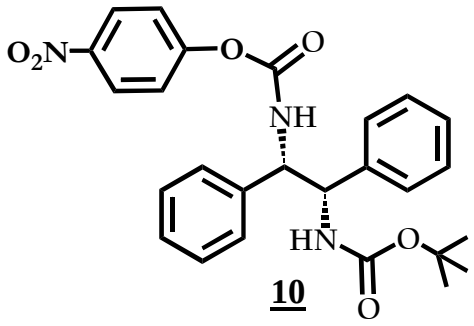

10

(2–tert–Butoxycarbonyl–1, 2–diphenylethyl)–
carbamic acid. 4–Nitrophenyl Ester
"*S,S*–Activated Boc Diamine"

A 100 mL round bottom flask was charged with 3.50 g (17.4 mmol) of *p*-nitrophenyl chloroformate in 50 mL THF. Next, the solution was cooled to 0 °C and a previously prepared solution containing 5.00 g of the mono-BOC diamine, **8**, 1.75 mL Et_3N in 10 mL of THF. This solution was added dropwise with stirring into the flask containing the *p*–nitrophenyl chloroformate. After addition was complete, the solution was allowed to warm to room temperature for 2 hrs. After this two hour period elapsed, the solution was allowed to reflux for 1 hr. After the reflux period expired, the solvent was removed by rotary evaporation leaving behind an off-white colored residue. Water was added to dissolve the $Et_3N^+ Cl^-$ salts, then $CHCl_3$ was added and the solution was shaken. The organic layer was dried over anhydrous Na_2SO_4. The salts were removed by filtration and the solvent removed by rotary evaporation affording 7.97 g of product. The compound was recrystallized from EtOAc affording 7.81 g (94.3%) of the monoactivated mono-Boc diamine. mp = 164 – 165 °C. ^{1}**H** NMR (Varian 400 MHz; (DMSO–*d6*) δ: 1.28 (s, **9H**); 4.99 – 5.05 (m, **2H**); 7.18 – 7.34 (m, **12H**); 7.52 – 7.54 (d, **1H** *J* = 9.11 Hz); 8.19 – 8.23 (dt, **2H**); 8.60 – 8.62 (d, **1H**, *J* = 8.88 Hz). ^{13}**C** NMR (Varian 400 MHz; (DMSO–*d6*) δ: 28.8; 59.08; 60.32; 78.72; 122.74;

125.84; 127.69; 128.65; 140.53; 141.34; 144.75; 153.36; 155.69; 156.63. ***Anal. Calc*: C**, 65.40; **H**, 5.70; **N**, 8.80. ***Found:*** C, 65.42; **H**, 5.53; **N**, 8.77.

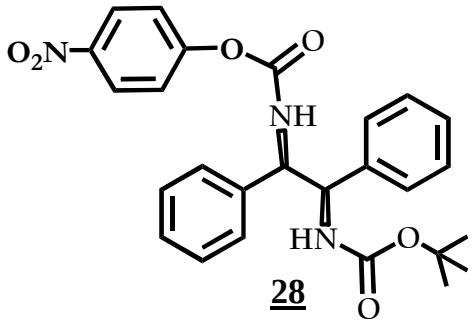

28

(2–tert–Butoxycarbonyl–1, 2–diphenylethyl)–carbamic acid. 4–Nitrophenyl Ester "*R*,*R*–Activated Boc Diamine"

A 100 mL round bottom flask was charged with 3.00 g (14.9 mmol) of *p*–nitrophenyl chloroformate in 35 mL THF. Next, the solution was cooled to 0 °C and a previously prepared solution containing 4.50 g of the *R*,*R*–Mono–BOC diamine, **27**, 1.50 mL Et_3N in 10 mL of THF. This solution was added dropwise with stirring into the flask containing the p–nitrophenyl chloroformate. After addition was complete, the solution was allowed to warm to room temperature for 2 hrs. After this two hour period elapsed, the solution was allowed to reflux for 1 hr. After the reflux period expired, the solvent was removed by rotary evaporation leaving behind an off-white colored residue. Water was added to dissolve the $Et_3N^+Cl^-$ salts, then $CHCl_3$ was added and the solution was shaken. The organic layer was dried over anhydrous Na_2SO_4. The salts were removed by filtration and the solvent removed by rotary evaporation affording 6.54 g of product. The compound was recrystallized from EtOAc affording 6.23 g (87.6 %) of the monoactivated Mono–Boc diamine. mp = 164 – 165 ^oC.

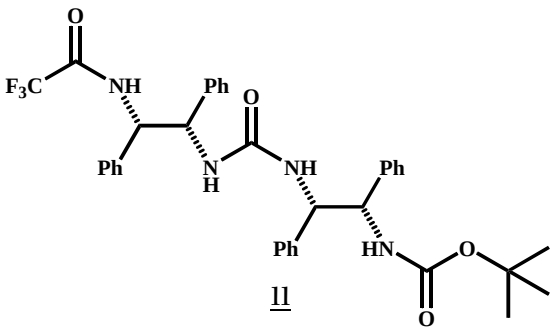

11

"Orthogonally Protected *S*,*S*–TFA/BOC Dimer"

To a round bottom flask containing 4.50 g (16.2 mmol) of the Mono–TFA compound, **6**, in 10 mL of DMF was added a THF solution of the *S*,*S*–Mono–BOC activated compound, **10**, was added dropwise with stirring. After addition was complete the solution was allowed to stir at room temperature overnight. The next day the solution was allowed to reflux for 1 hr. After the reflux period expired the solution was allowed to cool to room temperature and the DMF removed by high vacuum rotary evaporation. Next, the residue was dissolved in EtOAc and poured though a small pad of alumina (removes the nitrophenoxide anion). The product was chromatographed on silica eluting with 50/50 EtOAc/Pet ether affording 9.25 g (88.3 %). ^{1}**H** NMR (Varian 400 MHz; (DMSO–*d6*) δ: 1.28 (s, **9H**); 4.74 – 4.79 (dd, **1H,** *J* = 8.71 Hz, *J* = 8.71 Hz); 4.81 – 4.91 (dd, **1H,** *J* = 8.3 Hz, *J* = 8.3 Hz); 5.02 – 5.11 (m, **2H**); 6.70 (d, **1H**, *J* = 8.57 Hz); 6.82 (d, **1H**, *J* = 7.38 Hz); 7.02 – 7.14 (m, **20H**); 7.39 (d, **1H**, *J* = 9.12 Hz); 10.1 (d, **1H**, *J* = 7.55 Hz). ^{13}**C** NMR (Varian 400 MHz; (DMSO–*d6*) δ: 28.18, 28.29, 57.10, 57.58, 58.08, 58.48, 58.92, 59.23, 59.68, 77.98, 111.60, 114.47, 117.34, 120.21,126.31, 126.49, 126.75, 126.83, 127.10, 127.19, 127.27, 127.39, 127.52, 127.69, 127.79, 127.84, 127.90, 127.96, 128.10, 128.26, 138.87, 140.63, 140.87, 141.59, 155.35, 155.43, 155.79, 156.15, 156.52, 157.36. ***Anal. Calc*: C**, 66.86; **H**, 5.77; **N**, 8.66; **F**, 8.81. **Found: C**, 66.69; **H**, 5.65; **N**, 8.62; **F**, 8.76.

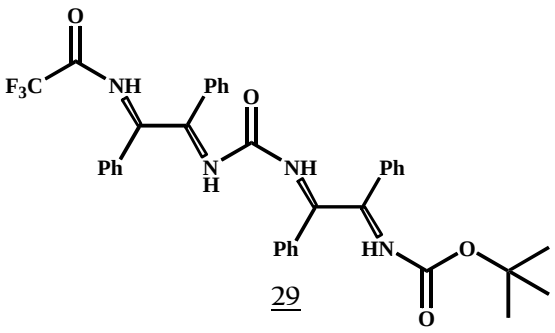

29

"Orthogonally Protected *R*,*R*–TFA/BOC Dimer"

To a round bottom flask containing 3.50 g of the mono TFA compound, **25**, in 10 mL of DMF was added a THF solution of the *R*,*R*–mono–BOC activated compound, **28**, was added dropwise with stirring. After addition was complete the solution was allowed to stir at room temperature overnight. The next day the solution was allowed to reflux for 1 hr. After the reflux period expired the solution was allowed to cool to room temperature and the DMF removed by high vacuum rotary evaporation. Next, the residue was dissolved in EtOAc and poured though a small pad of alumina (removes the nitrophenoxide). The product was chromatographed on silica eluting with 50/50 EtOAc/Pet ether affording 6.84 g of **29**. Percent yield = 92.1 %

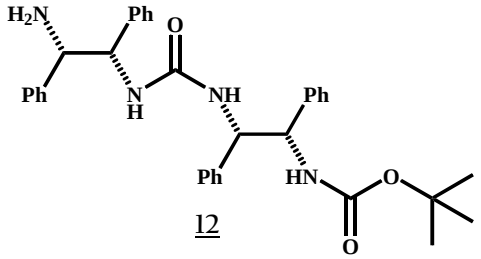

12

"*S*,*S*–Mono–Boc Dimer"

In a 100 ml round bottom flask was added 8.00 g (12.4 mmol) of the *S*,*S*–orthogonally protected dimer, **14**, in 30 mL methanol. 1.50 g (33.7 mmol) LiOH was added and the solution was brought to reflux and allowed to reflux overnight. The next day the solution was allowed to cool to room temperature and the MeOH removed via rotary evaporation. The product was suspended in water and extracted three times with 25 mL EtOAc. The organic extracts were combined and dried over anhydrous Na_2SO_4. The salts were removed and

EtOAc removed by rotary evaporation. The product was purified by column chromatography first using 50/50 $CHCl_3$/EtOAc to remove the starting material and then with 100 % EtOAc. The solvent was removed leaving behind a colorless oil. This reaction was repeated with the remaining starting material obtained from column chromatography until all the starting material was consumed and was worked up in the same manner. The total yield for all combined reactions is 90 % (6.15 g). ^{1}**H** NMR (Varian 400 MHz; (DMSO–*d6*) δ: 1.28 (s, **9H**); 4.14 (d, **1H**, *J* = 3 .79 Hz); 4.63 (dd, **1H**, *J* = 4.3 Hz, *J* = 8.2 Hz); 4.74 – 4.83 (m, **2H**); 6.48 (d, **1H**, *J* = 8.0 Hz); 7.04 (d, **1H**, *J* = 7.3 Hz); 7.15 – 7.26 (m, **20H**); 7.31 (d, **1H**, *J* = 7.1 Hz). ^{13}**C** NMR (Varian 400 MHz; (DMSO–*d6*) δ: 28.16; 57.82; 59.09; 59.40; 59.65; 77.95; 126.38, 126.48; 126.58; 126.61; 126.95; 127.10; 127.17; 127.65; 127.71; 127.84; 141.13; 141.50; 142.65; 143.56; 155.06; 156.95. ***Anal. Calc:*** **C**, 74.15; **H**, 6.96; **N**, 10.17. ***Found:*** **C**, 74.12; **H**, 6.89; **N**, 10.03.

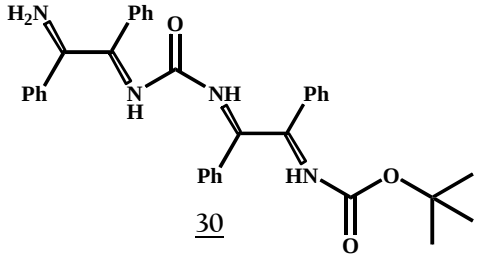

30

"*R*,*R*–Mono–Boc Dimer"

In a 100 mL round bottom flask was added 6.00 g (9.27 mmol) of the *R,R*–orthogonally protected dimer, **29**, in 25 mL methanol. 1.50 g (33.7 mmol) LiOH was added and the solution was brought to reflux and allowed to reflux overnight. The next day the solution was allowed to cool to room temperature and the MeOH removed via rotary evaporation. The product was suspended in water and extracted three times with 25 mL EtOAc. The organic extracts were combined and dried over anhydrous Na_2SO_4. The salts were removed and EtOAc removed by rotary evaporation. The product was purified by column chromatography first using 50/50 $CHCl_3$/EtOAc to remove the starting material and then with 100 % EtOAc. The solvent was removed leaving behind colorless oil. This reaction was repeated with the remaining starting material obtained from

column chromatography until all the starting material was consumed and was worked up in the same manner. Total yield for all combined reactions is 94 % (6.41 g).

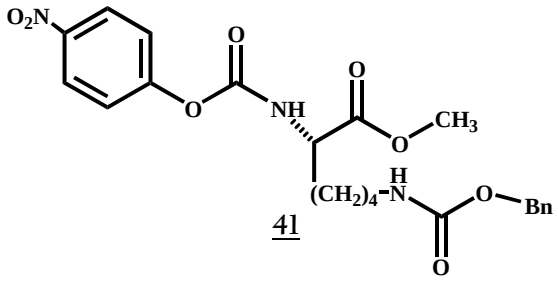

41

ε–Cbz –(*S*)–Lysine α–PNP Carbamate Methyl Ester

In a 250 mL round bottom flask was added 15.0 g of ε–Cbz–(*S*)–Lysine Methyl Ester, hydrochloride salt suspended in 50 mL THF. Next, 10 mL of TEA in 20 mL THF was added dropwise at room temperature. After addition was complete, the solution was allowed to stir for 1 hr. A white precipitate, the hydrochloride salt of TEA, precipitated out of solution. The white precipitate was filtered off and 5 mL of TEA was added to the remaining solution. Next, this solution was added dropwise into a different 250 mL round bottom containing 9.50 g (47.1 mmol) of *p̃*nitrophenyl chloroformate dissolved in 50 mL of THF. After addition was complete the solution was allowed to stir overnight. The next day a white precipitate that formed during the reaction was removed by filtration and the solvent was removed by evaporation, leaving behind a gummy residue. Hot ether was added and the mixture was triturated and then allowed to cool in a freezer. The product crystallized and was filtered giving a yield of 21.2 g (98.2 %). **^{1}H** NMR (Varian 400 MHz; (DMSO–*d6*) δ: 1.33 – 1.46 (m, **4H**); 1.62 – 1.79 (m, **2H**); 2.99 (q, **2H**, *J* = 6.2 Hz); 3.66 (s, **3H**); 4.05 – 4.10 (m, **1H**); 4.99 (s, **2H**); 7.25 – 7.35 (m, **5H**); 7.38 – 7.41 (m, **2H**); 8.24 – 8.28 (m, **2H**); 8.53 (d, **1H**, *J* = 7.6 Hz). **^{13}C** NMR (Varian 400 MHz; (DMSO–*d6*) δ: 22.74, 28.94, 30.27, 52.07, 54.14, 65.17, 122.37, 125.25, 127.75, 128.36, 137.30, 144.27, 153.31, 155.96, 156.15, 172.35. ***Anal. Calc:*** **C**, 57.51; **H**, 5.48; **N**, 9.15; ***Found*****:** C, 57.00; **H**, 5.53; **N**, 9.03.

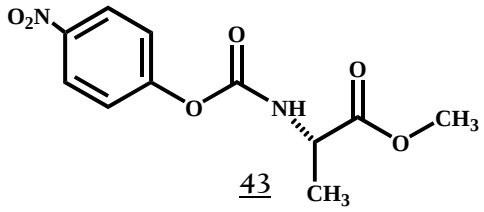

43

Alanine α–PNP Carbamate Methyl Ester

5.0 g (35.8 mmol) of (*S*)–Alanine Methyl Ester, Hydrochloride salt and 7.50 g (37.2 mmol) of *p̃* nitrophenyl chloroformate were suspended in 100 mL DCM. Next, 3.50 mL of TEA mixed in 10 mL DCM was added dropwise at room temperature. After addition was complete, the solution was allowed to stir overnight. The next day, the mixture was washed with 25 mL of a saturated $NaHCO_3$ solution and dried over anhydrous Na_2SO_4. The salts were removed by filtration and the amount of solvent was reduced to 15 mL. The solution was chromatographed over Silica, eluting with DCM (R_f = 0.25). The solvent was removed affording 7.23 g (75.3 %) of a pale yellow-green compound. **^{1}H** NMR (Varian 400 MHz; (DMSO–*d6*) δ: 1.35 (d, **3H**, *J* = 7.3 Hz); 3.67 (s, **3H**); 4.19 (dt, **1H**, *J* = 7.31 Hz, *J* = 7.32 Hz); 7.37 – 7.41 (m, **2H**); 8.24 – 8.28 (m, **2H**); 8.57 (d, **1H**, *J* = 7.3 Hz). **^{13}C** NMR (Varian 400 MHz; (DMSO–*d6*) δ: 16.80, 52.13, 49.54, 122.38, 125.24, 144.27, 152.95, 155.93, 172.75.

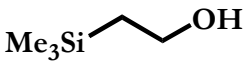

46

2–(Trimethylsilyl) ethanol[17]

A solution of 40 g of ethyl 2–(trimethylsilyl) acetate (0.25 mol) in 50 ml THF was cooled to –10 °C. Over a 2 hour period, 0.30 L of 1.02 M BH_3·THF complex (0.30 mol) was added through the septum with the aid of slight nitrogen pressure. The colorless solution was allowed to warm to room temperature and was left for 2 days. The contents of the reaction vessel were transferred to a flask containing 0.75 L of MeOH. After being stirred for 20 hours under nitrogen, the solution was concentrated at 25 – 28 °C until only 140 mL remained. This was distilled under vacuum through a Vigreux column affording 25.0 g of the alcohol, **46**.

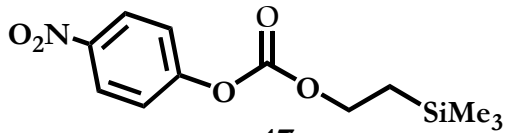

47

Teoc Carbonate[17]

In a 250 mL round bottom flask were added 20.0 g of *p*– nitrophenyl chloroformate (99.2 mmol) and 11.0 g of 2–(trimethylsilyl) ethanol in 150 mL of DCM. A solution of 9.5 mL of TEA and 20 mL of DCM was added dropwise into the solution containing the silyl compound. After addition, the solution was allowed to stir overnight at room temperature. The next day the solution was extracted with 0.5 M HCl and the organic layer was neutralized with $NaHCO_3$. The organic layer was dried over anhydrous Na_2SO_4. Trituration of this residue with hexane yielded a white precipitate (p– nitrophenyl carbonate). Evaporation of the hexane solution, after filtration of the solid left behind an oil, which was stirred with 250 mL of ice-cold water containing 5 drops of formic acid. The white precipitate that formed was filtered and dried overnight affording 21.1 g (79.6 %) of 2–(Trimethylsilyl)–ethyl–4–nitrophenyl carbonate, **47**.

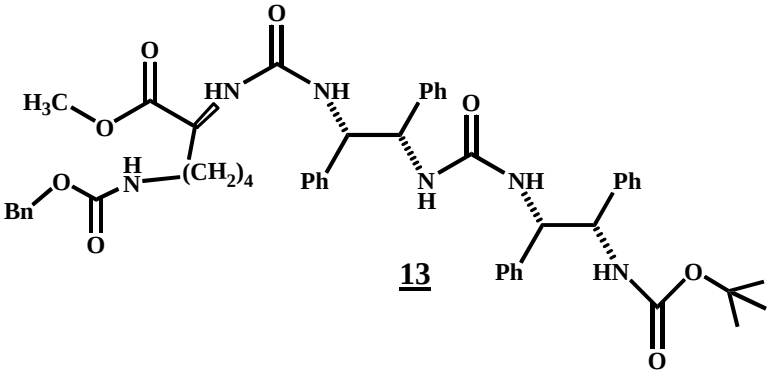

13

***S*,*S*–Cbz–Boc–Lys–Trimer**

In a 100 mL round bottom flask charged with 25 mL DMF was added 5.50 g (6.31 mmol) of ε–Cbz–(*S*)–Lysine α–PNP Carbamate Methyl Ester, **41**, along with 5.00 g (10.9 mmol) of Mono–Boc dimer, **12**. A solution of TEA in 5 mL DMF was added dropwise into the previously mentioned flask. After addition was complete, the solution was warmed to 50 °C with stirring for a 24 hr period. After the period elapsed, DMF was removed via high vacuum rotary evaporation. The residue

was suspended in EtOAc and passed through a short pad of Alumina, which traps the *p*-nitrophenoxide ion. EtOAc was reduced to 10 mL and the mixture was chromatographed over silica eluting with a 60:40 mixture of EtOAc/hexanes. R_f = 0.22 The organic portions were combined; the solvents removed affording 4.93 g (89.8 %) of the fully protected trimer, **13**. ^{1}**H** NMR (Varian 400 MHz; (DMSO–*d6*) δ: 1.13 – 1.20 (m, **2H**); 1.23 (s, **9H**); 1.29 – 1.36 (m, **2H**); 1.44 – 1.60 (m, **2H**); 2.90 (dd, **1H**; *J* = 6.7 Hz, *J* = 12. 9 Hz); 3.60 (s, **3H**); 4.09 (dd, **1H**, *J* = 7.7 Hz, *J* = 13.3 Hz); 4.74 (t, **1H**, *J* = 8.3 Hz); 4.80 – 4.82 (m, **2H**); 4.88 (t, **1H**, *J* = 8.1 Hz); 4.97 (s, **2H**); 6.39 – 6.41 (d, **1H,** *J* = 7.76 Hz); 6.57 (d, **1H**, *J* = 7.5 Hz); 6.78 (d, **1H**, *J* = 8.8 Hz); 6.89 – 6.91 (m, **4H**); 7.10 – 7.37 (m, **25H**). ^{13}**C** NMR (Varian 400 MHz; (DMSO–*d6*) δ: 22.34, 28.14, 29.01, 31.65, 51.70, 52.41, 57.93, 58.00, 58.32, 59.45, 65.10, 77.67, 126.60, 126.77, 127.19, 127.25, 127.41, 127.47, 127.61, 127.72, 127.76, 128.35, 137.27, 140.48, 141.06, 141.44, 155.06, 156.05, 156.95, 157.19, 173.57. MALDI–TOF–MS: m/z 771 [M-Boc], 772[M+H–Boc], 793 [M+H–Boc], 871 [M+], 872 [M+H], 893 [M+Na], 894 [M+H+Na], 909 [M+K], 910 [M+H+K]. ***Anal. Calc*: C**, 68.95; **H**, 6.71; **N**, 9.65. ***Found:*** C, 68.69; **H**, 6.53; **N**, 9.60.

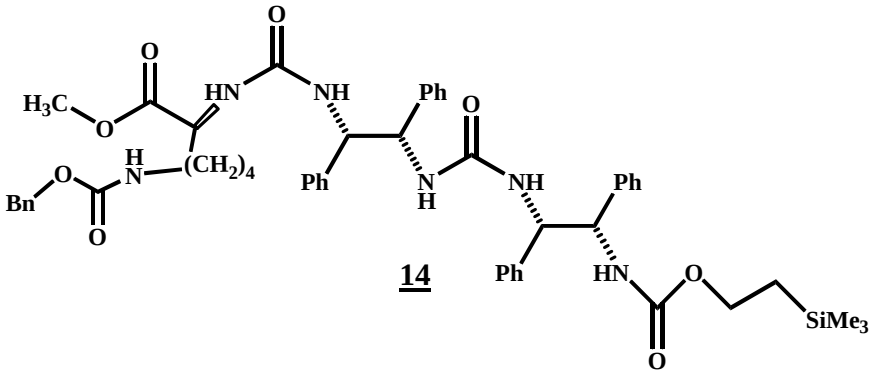

14

Teoc–*S*,*S*–Cbz–Lys–Trimer

The previously synthesized *S*,*S*–Cbz–Lys–Trimer, **13**, in the amount of 4.00 g (4.59 mmol) was submitted to deprotection conditions using 3 eq. of TFA in 10 mL DCM for a 24 hr period. Afterwards, excess TFA and DCM were removed by rotary evaporation leaving behind a syrupy residue. This residue was dissolved 10 mL of DCM and washed 5 times with saturated $NaHCO_3$ solution. The organic

layer was saved and dried over anhydrous $NaSO_4$. The salts were filtered and DCM removed. Next, 10 mL of DMF were added along with 3 eq. of Teoc Carbonate, **47** and allowed to stir at room temperature for 24 hrs. The next day, DMF was removed via high vacuum rotary evaporation. The resulting residue was taken up in EtOAc and chromatographed over alumina, eluting with 50/50 EtOAc/hexane. The solvents were removed affording 4.05 g of Teoc–*S*,*S*–Cbz–Lys-Trimer, **14**, with a yield of 96.5 %. ^{1}**H** NMR (Varian 400 MHz; (DMSO–*d6*) δ: –0.05 (s, **9H**); 0.78 – 0.82 (m, **2H**), 1.19 – 1.24 (m, **2H**); 1.34 – 1.41 (m, **2H**); 1.45 – 1.60 (m, **2H**), 2.94 – 2.99 (q, **2H**, *J* = 6.67 Hz, *J* = 13.04 Hz); 3.53 (s, **3H**); 3.87 – 3.91 (t, **2H**, *J* = 7.92 Hz); 4.04 – 4.09 (q, **1H**, *J* = 7.47 Hz, *J* = 13.67 Hz); 4.72 – 4.76 (t, **1H**, *J* = 8.48 Hz); 4.81 – 4.83 (m, **2H**); 4.84 – 4.89 (t, **1H**, *J* = 8.28 Hz); 5.00 (s, **2H**); 6.37 – 6.39 (d, **1H**, *J* = 7.96 Hz); 6.41 – 6.43 (d, **1H**, *J* = 7.80 Hz); 6.53 – 6.55 (d, **1H**, *J* = 7.50 Hz); 6.80 – 6.82 (d, **1H**, *J* = 8.26 Hz); 6.92 – 6.94 (m, **2H**); 7.05 – 7.38 (m, **25H**); 7.55 – 7.57 (d, **1H**, *J* = 8.87 Hz). ^{13}**C** NMR (Varian 400 MHz; (DMSO-*d6*) δ: –1.46, 17.28, 22.31, 28.29, 29.19, 31.61, 51,59, 52.28, 52.55, 57.82, 57.99, 58.37, 58.45, 61.61, 77.41, 126.64, 126.65, 127.13, 127.22, 127.25, 127.38, 127.48, 127.60, 127.66, 127.76, 127.88, 139.92, 140.55, 141.03, 141.42, 155.58, 157.12, 157.69, 159.22, 173.56. MALDI–TOF–MS: m/z 915 [M+], 916 [M+H], 937 [M+Na], 938 [M+H+K]. ***Anal. Calc*: C**, 66.93; **H**, 6.83; **N**, 9.18; **Si**, 3.07. ***Found:*** **C**, 66.69; **H**, 6.83; **N**, 9.20; **Si**, 2.96.

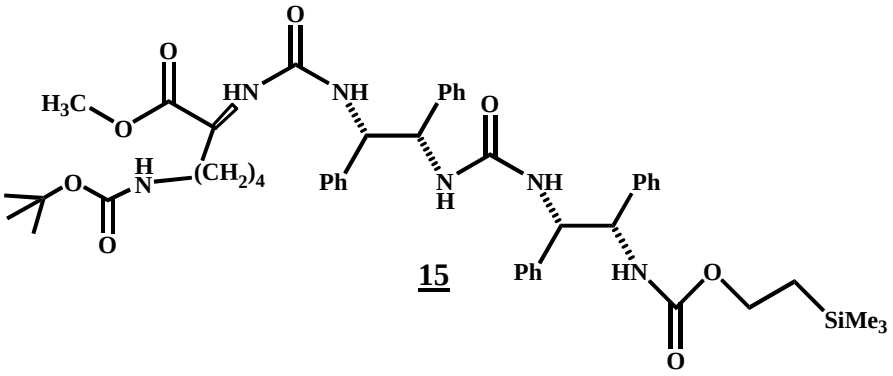

15

Teoc–*S*,*S*–Boc–Lys–Trimer

In a small hydrogenation flask were added, 3.00 g (3.28 mmol) of the Teoc–*S*,*S*–Cbz–Lys–Trimer, **14**, 10 mL of anhydrous MeOH, 0.75 g of BOC anhydride and 0.10 g of 5 % Pd/C. This solution was hydrogenated for 30 minutes, at a pressure of 40 psi. After hydrogenation was completed, the solution was passed thought Celite to remove the Pd/C. The solvent was evaporated and the compound was purified by column chromatography to remove any excess BOC anhydride, eluting with EtOAc to afford 2.90 g of pure product, **15**. ^{1}**H** NMR (Varian 400 MHz; (DMSO–*d6*) δ: –0.07 (s, **9H**); 0.77 – 0.83 (m, **2H**), 1.16 – 1.22 (m, **2H**); 1.27 (s, **9H**); 1.35 – 1.41 (m, **2H**); 1.46 – 1.61 (m, **2H**), 2.91 – 2.97 (dd, **2H**, *J* = 6.66 Hz, *J* = 13.0 Hz); 3.57 (s, **3H**); 3.88 – 3.90 (t, **2H**, *J* = 7.90 Hz); 4.03 – 4.10 (dd, **1H**, *J* = 7.45 Hz, *J* = 13.5 Hz); 4.72 – 4.76 (t, **1H**, *J* = 8.46 Hz); 4.80 – 4.83 (m, **2H**); 4.84 – 4.90 (t, **1H**, *J* = 8.30 Hz); 6.39 – 6.41 (d, **1H**, *J* = 7.95 Hz); 6.43 – 6.45 (d, **1H**, *J* = 7.83 Hz); 6.55 – 6.57 (d, **1H**, *J* = 7.49 Hz); 6.82 – 6.84 (d, **1H**, *J* = 8.27 Hz); 6.94 – 6.96 (m, **2H**); 7.07 – 7.36 (m, **20H**); 7.54 – 7.56 (d, **1H**, *J* = 8.88 Hz). ^{13}**C** NMR (Varian 400 MHz; (DMSO-*d6*) δ: –1.50, 17.29, 22.41, 28.29, 29.18, 31.61, 51.60, 52.51, 57.80, 57.99, 58.44, 59.94, 61.66, 77.36, 126.52, 126.64, 126.80, 127.13, 127.24, 127.37, 127.48, 127.60, 127.68, 127.75, 127.84, 128.35, 140.55, 140.57, 141.01, 141.42, 155.58, 155.85, 157.03, 157.26, 173.56. MALDI–TOF–MS: m/z 781 [M–Boc], 782 [M+H–Boc], 881 [M+], 903 [M+Na], 904 [M+H+Na], 919 [M+K]. ***Anal. Calc*: C**, 65.43; **H**, 7.32; **N**, 9.54; **O**, 14.53; **Si**, 3.19. ***Found:* C**, 65.01; **H**, 7.23; **N**, 9.51; **Si**, 3.17.

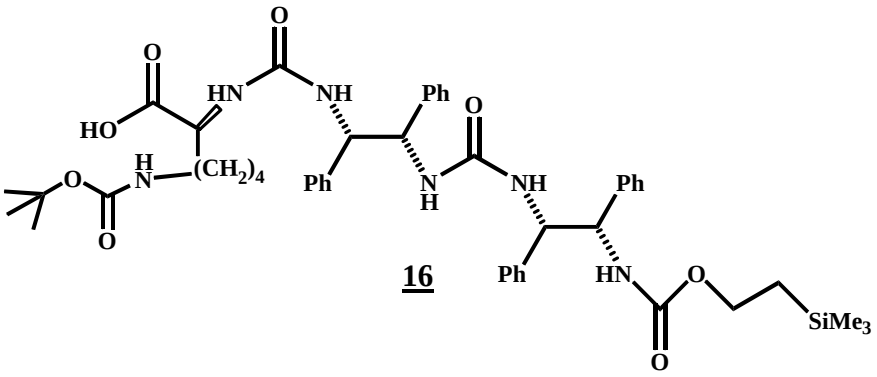

Teoc–*S*,*S*–Boc–Lys–Trimer Acid

2.50 g (2.83 mmol) of Teoc–*S*,*S*–Boc–Lys–Trimer, **15**, was dissolved in 5 mL of MeOH. The resulting solution was chilled to – 10 °C and 2.27 mL of ice-cold 1.00 M LiOH was carefully added dropwise with vigorous stirring. After addition of LiOH was completed, the reaction was warmed to 0 °C and was allowed to stir for 30 minutes. Next, 1.00 M of ice–cold HCl was added dropwise to neutralize the LiOH. After complete addition of HCl and white precipitate fell out of solution and the pH of solution was checked to ensure its acidic nature. The white solid was filtered to afford 2.03 g (96.9 %) of the carboxylic acid product, **16**. ^{1}**H** NMR (Varian 400 MHz; (DMSO–*d6*)δ: –0.06 (s, **9H**); 0.75 – 0.82 (m, **2H**), 1.14 – 1.21 (m, **2H**); 1.26 (s, **9H**); 1.34 – 1.40 (m, **2H**); 1.44 – 1.60 (m, **2H**), 2.90 – 2.97 (dd, **2H**, *J* = 6.63 Hz, *J* = 13.1 Hz); 3.89 – 3 .91 (t, **2H**, *J* = 7.88 Hz); 4.02 – 4.09 (dd, **1H**, *J* = 7.43 Hz, *J* = 13.2 Hz); 4.73 – 4.77 (t, **1H**, *J* = 8.46 Hz); 4.81 – 4.84 (m, **2H**); 4.86 – 4.93 (t, **1H**, *J* = 8.35 Hz); 6.40 – 6.42 (d, **1H**, *J* = 7.93 Hz); 6.45 – 6.47 (d, **1H**, *J* = 7.81 Hz); 6.55 – 6.57 (d, **1H**, *J* = 7.50 Hz); 6.83 – 6.85 (d, **1H**, *J* = 8.28 Hz); 6.95 – 6.98 (m, **2H**); 7.09 – 7.36 (m, **20H**); 7.55 – 7.57 (d, **1H**, *J* = 8.84 Hz). ^{13}**C** NMR (Varian 400 MHz; (DMSO–*d6*) δ: –1.44, 17.22, 22.04, 28.19, 29.18, 31.60, 51.59, 52.51, 57.79, 57.98, 58.34, 59.84, 77.32, 126.52, 126.64, 126.80, 127.13, 127.24, 127.40, 127.43, 127.61, 127.67, 127.75, 127.84, 128.35, 140.05, 140.47, 140.96, 141.45, 155.60, 155.75, 157.15, 157.30. MALDI-TOF-MS: m/z 721 [M–Boc–CO_2], 749 [M–Boc–H_2O], 750 [M+H–Boc–H_2O], 849

[M–H_2O], 871 [M–H_2O+Na], 872 [M+H–H_2O+Na]. ***Anal. Calc*: C**, 65.10; **H**, 7.21; **N**, 9.69; **Si**, 3.24. ***Found:*** **C**, 64.97; **H**, 7.53; **N**, 9.77; **Si**, 3.26.

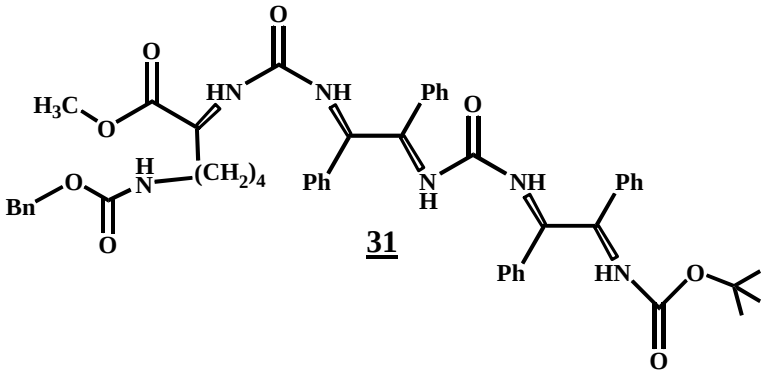

31

R, R–Cbz–Boc–Lys–Trimer

In a 100 mL round bottom flask charged with 25 mL DMF was added 2.30 g (5.54 mmol) of ε–Cbz–(S)–Lysine α–PNP Carbamate Methyl Ester, 2.80 g (5.23 mmol) of *R,R*-Mono-Boc dimer. A solution of TEA in 5 mL DMF was added dropwise into the previously mentioned flask. After addition was complete, the solution was warmed to 50 °C with stirring for a 24 hr period. After the period elapsed, DMF was removed via high vacuum rotary evaporation. The residue was suspended in EtOAc and passed through a short pad of Alumina, which traps the *p*–nitrophenoxide anion. EtOAc was reduced to 10 mL and the mixture was chromatographed over silica eluting with a 55:45 mixture of EtOAc/hexanes. R_f = 0.30 The organic portions were combined; the solvents removed affording 4.27 g (93.8 %) of the fully protected trimer. ^{1}**H** NMR (Varian 400 MHz; (DMSO–*d6*) δ: 1.15 – 1.21 (m, **2H**); 1.26 (s, **9H**); 1.30 – 1.36 (m, **2H**); 1.46 – 1.61 (m, **2H**); 2.95 (dd, **1H**; *J* = 6.73 Hz, *J* = 12. 8 Hz); 3.52 (s, **3H**); 4.60 (dd, **1H**, *J* = 7.77 Hz, *J* = 13.5 Hz); 4.76 (t, **1H**, *J* = 8.6 Hz); 4.82 – 4.84 (m, **2H**); 4.90 (t, **1H**, *J* = 8.4 Hz); 5.01 (s, **2H**); 6.46 – 6.48 (d, **1H**, *J* = 7.51 Hz); 6.78 – 6.81 (d, **1H**, *J* = 8.83 Hz); 6.82 – 6.85 (d, **1H**, *J* = 8.85 Hz); 6.92 – 6.95 (m, **4H**); 7.10 – 7.37 (m, **25H**). ^{13}**C** NMR (Varian 400 MHz; (DMSO–*d6*) δ: 22.54, 28.34, 29.11, 31.74, 51.88 52.43, 57.99, 58.00, 58.42, 59.55, 65.29, 77.83 126.62, 126.78, 127.29, 127.29, 127.53, 127.47, 127.65, 127.79, 127.76, 128.45, 137.32, 140.48, 141.16, 141.52, 155.17,

156.14, 156.99, 157.26, 173.62. MALDI–TOF–MS: m/z 771 [M–Boc], 793 [M+H–Boc], 871 [M+], 872 [M+H], 893 [M+Na], 894 [M+H+Na], 909 [M+K], 910[M+H+K]. ***Anal. Calc*: C**, 68.95; **H**, 6.71; **N**, 9.65. ***Found:* C**, 68.89; **H**, 6.61; **N**, 9.58.

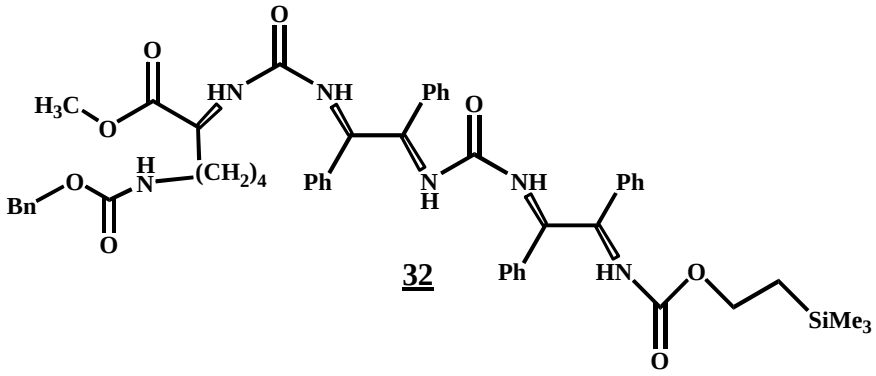

32

Teoc–R, R–Cbz–Lys–Trimer

The previously synthesized R,R–Cbz–Lys–Trimer, **31**, in the amount of 2.50 g (2.87 mmol) was submitted to deprotection conditions using 3 eq. of TFA in 10 mL DCM for a 24 hr period. Afterwards, excess TFA and DCM were removed by rotary evaporation leaving behind a syrupy residue. This residue was dissolved 10 mL of DCM and washed 5 times with saturated $NaHCO_3$ solution. The organic layer was saved and dried over anhydrous $NaSO_4$. The salts were filtered and DCM removed. Next, 10 mL of DMF were added along with 3 eq. of Teoc Carbonate, **47** and allowed to stir at room temperature for 24 hrs. The next day, DMF was removed via high vacuum rotary evaporation. The resulting residue was taken up in EtOAc and chromatographed over alumina, eluting with 50/50 EtOAc/hexane. The solvents were removed affording 2.45 g of Teoc–*R, R*–Cbz–Lys–Trimer, **32**, with a yield of 93.2 %. ^{1}**H** NMR (Varian 400 MHz; (DMSO–*d6*) δ: –0.07 (s, **9H**); 0.79 – 0.85 (m, **2H**); 1.12 – 1.20 (m, **2H**); 1.28 – 1.37 (m, **2H**); 1.42 – 1.60 (m, **2H**); 2.87 – 2.94 (q, **2H**, *J* = 6.68 Hz, *J* = 13.0 Hz); 3.60 (s, **3H**); 3.88 – 3.92 (t, **2H**, *J* = 5.45 Hz, *J* = 10.3 Hz); 4.05–4.12 (q, **1H**, *J* = 7.44 Hz, *J* = 13.5 Hz); 4.72 – 4.77 (t, **1H**, *J* = 8.43 Hz); 4.79 – 4.83 (m, **2H**); 4.85 - 4.88 (t, 1H, *J* = 8.28 Hz); 4.97 (s, 2H); 6.39 – 6.41 (d, **1H**, *J* = 7.97 Hz); 6.43 – 6.47 (d, **1H**, *J* = 7.76 Hz); 6.45 – 6.58 (d, **1H**, *J* = 7.49 Hz); 6.77 – 6.81 (d, **1H**, *J*

= 8.30 Hz); 6.87 – 6.96 (m, **2H**); 7.20 – 7.36 (m, **25H**); 7.53 – 7.58 (d, **1H**, *J* = 8.87 Hz). ^{13}**C** NMR (Varian 400 MHz; (DMSO–*d6*) δ: –1.40, 17.32, 22.32, 28.33, 29.22, 31.61, 51.59, 52.32, 52.58, 57.81, 57.95, 58.40, 58.48, 61.62, 77.45, 126.63, 126.67, 127.15, 127.24, 127.27, 127.40, 127.45, 127.61, 127.67, 127.77, 127.90, 139.96, 140.53, 141.03, 141.44, 155.57, 157.15, 157.72, 159.25, 173.59. MALDI–TOF–MS: m/z 915 [M+], 916 [M+H], 937 [M+Na], 938 [M+H+K]. ***Anal. Calc*: C**, 66.93; **H**, 6.83; **N**, 9.18; **Si**, 3.07. ***Found:*** C, 66.90; **H**, 6.73; **N**, 9.16; **Si**, 3.00.

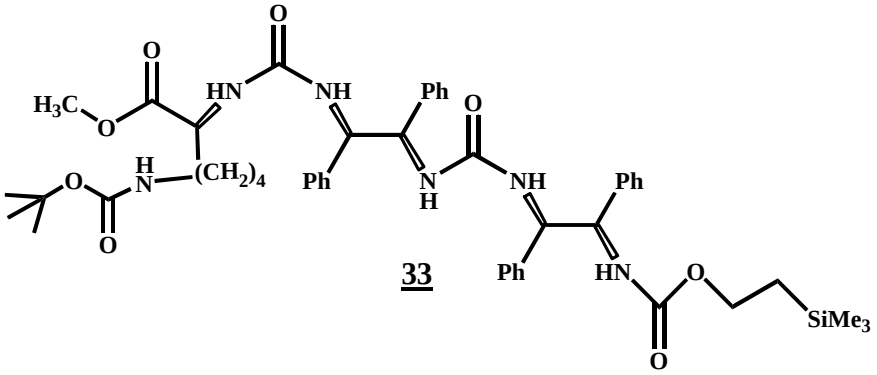

Teoc–R, R–Boc–Lys–Trimer

In a small hydrogenation flask were added, 1.75 g (1.91 mmol) of the Teoc–*R,R*–Cbz-Lys-Trimer, **32** along with 10 mL of anhydrous MeOH, 0.50 g (2.28 mmol) of BOC anhydride and 0.10 g of 5 % Pd/C. This solution was hydrogenated for 30 minutes, at a pressure of 40 psi. After the reaction was completed, the solution was passed through Celite (filtering aid) to remove the Pd/C. The solvent was evaporated and the compound was purified by column chromatography to remove any excess BOC anhydride, eluting with EtOAc to afford quantitatively, 1.69 g of **33**. ^{1}**H** NMR (Varian 400 MHz; (DMSO–*d6*) δ: –0.09 (s, 9H); 0.89 – 0.93 (m, **2H**); 1.14 – 1.23 (m, **2H**); 1.26 (s, **9H**); 1.30 – 1.37 (m, **2H**); 1.43 – 1.62 (m, **2H**), 2.85 – 2.97 (dd, **2H**, *J* = 6.63 Hz, *J* = 12.8 Hz); 3.60 (s, **3H**); 3.92 – 3.94 (t, **2H**, *J* = 7.92 Hz J = 10.43); 4.07 – 4.15 (dd, **1H**, *J* = 7.48 Hz, *J* = 13.2 Hz); 4.76 – 4.80 (t, **1H**, *J* = 8.42 Hz); 4.80 – 4.84 (m, **2H**); 4.89 – 4.95 (t, **1H**, *J* = 8.33 Hz); 6.42 – 6.44 (d, **1H**, *J* = 7.95 Hz); 6.47 – 6.51 (d, **1H**, *J* = 7.88 Hz); 6.57 – 6.59 (d, **1H**, *J* = 7.47 Hz); 6.85 – 6.88 (d, **1H**, *J* = 8.31

Hz); 6.90 – 6.97 (m, **2H**); 7.10 – 7.34 (m, **20H**); 7.57 – 7.60 (d, **1H**, *J* = 8.89). ^{13}**C** NMR (Varian 400 MHz; (DMSO–*d6*) δ: –1.47, 17.32, 22.45, 28.31, 29.23, 31.62, 51.62, 52.53, 57.85, 58.00, 58.46, 59.99, 62.00, 77.40, 126.57, 126.69, 126.86, 127.18, 127.30, 127.40, 127.48, 127.59, 127.66, 127.75, 127.86, 128.39, 140.72, 140.62, 141.05, 141.47, 155.59, 155.87, 157.06, 157.30, 173.59. MALDI–TOF–MS: m/z 781 [M–Boc], 782 [M+H–Boc], 881[M+], 903 [M+Na], 904 [M+H+Na], 919 [M+K]. ***Anal. Calc*: C**, 65.43; **H**, 7.32; **N**, 9.54; **Si**, 3.19. ***Found:*** **C**, 65.36; **H**, 7.33; **N**, 9.50; **Si**, 3.19.

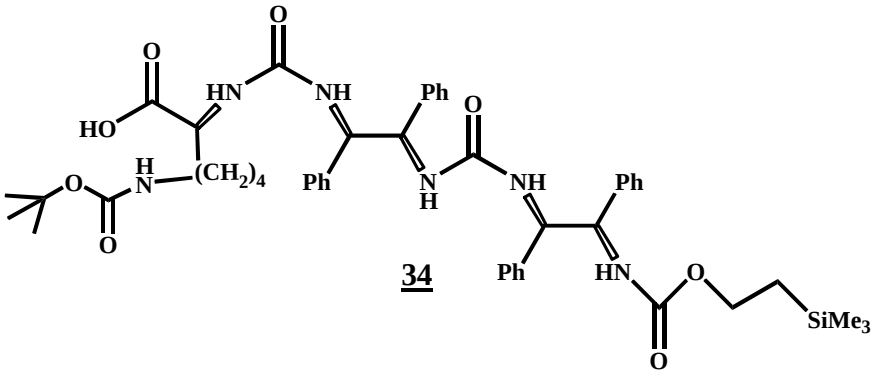

34

Teoc–R, R–Boc–Lys–Trimer Acid

1.25 g (1.41 mmol) of Teoc-*R, R*–Boc–Lys–Trimer, **33**, was dissolved in 5 mL of MeOH. The resulting solution was chilled to –10 °C and 2.27 mL of ice–cold 1.00 M LiOH was carefully added dropwise with vigorous stirring. After addition of LiOH was completed, the reaction was warmed to 0 °C and was allowed to stir for 30 minutes. Next, 1.00 M of ice–cold HCl was added dropwise to neutralize the LiOH. During the process of neutralization a white precipitate fell out of solution. After HCl addition was completed, the pH of solution was checked to ensure its acidic nature. The white solid was filtered to yield 1.00 g (96.9 %) of the carboxylic acid, **34**. ^{1}**H** NMR (Varian 400 MHz; (DMSO–*d6*) δ: –0.06 (s, **9H**); 0.85 – 0.92 (m, **2H**), 1.14 – 1.21 (m, **2H**); 1.27 (s, **9H**); 1.34 – 1.40 (m, **2H**); 1.44 – 1.60 (m, **2H**), 2.90 – 2.95 (dd, **2H**, *J* = 6.63 Hz, *J* = 13.1 Hz); 3.89 – 3.91 (t, **2H**, *J* = 7.88 Hz; *J* = 10.40 Hz); 4.02 – 4.09 (dd, **1H**, *J* = 7.43 Hz, *J* = 13.2 Hz); 4.73 – 4.77 (t, **1H**, *J* = 8.46 Hz); 4.81 – 4.84 (m, **2H**); 4.86 – 4.93 (t, **1H**, *J* = 8.35 Hz); 6.40 – 6.42 (d, **1H**, *J* = 7.93 Hz); 6.45 – 6.47 (d, **1H**, *J* = 7.81 Hz); 6.55 – 6.57 (d,

1H, *J* = 7.50 Hz); 6.83 – 6.85 (d, **1H**, *J* = 8.28 Hz); 6.95 – 6.98 (m, **2H**); 7.09 – 7.36 (m, **20H**); 7.55 – 7.57 (d, **1H**, *J* = 8.84 Hz). ^{13}**C** NMR (Varian 400 MHz; (DMSO–*d6*) δ: –1.44, 17.22, 22.04, 28.19, 29.18, 31.60, 51.59, 52.51, 57.79, 57.98, 58.34, 59.84, 77.32, 126.52, 126.64, 126.80, 127.13, 127.24, 127.40, 127.43, 127.61, 127.67, 127.75, 127.84, 128.35, 140.05, 140.47, 140.96, 141.45, 155.60, 155.75, 157.15, 157.30. MALDI–TOF–MS: m/z 721 [M–Boc–CO_2], 749 [M–Boc–H_2O], 750 [M+H–Boc–H_2O], 849 [M–H_2O], 871 [M–H_2O+Na], 872 [M+H–H_2O+Na]. *Anal. Calc*: **C**, 65.10; **H**, 7.21; **N**, 9.69; **O**, 14.76; **Si**, 3.24. ***Found:*** **C**, 64.99; **H**, 7.15; **N**, 9.65; **Si**, 3.20.

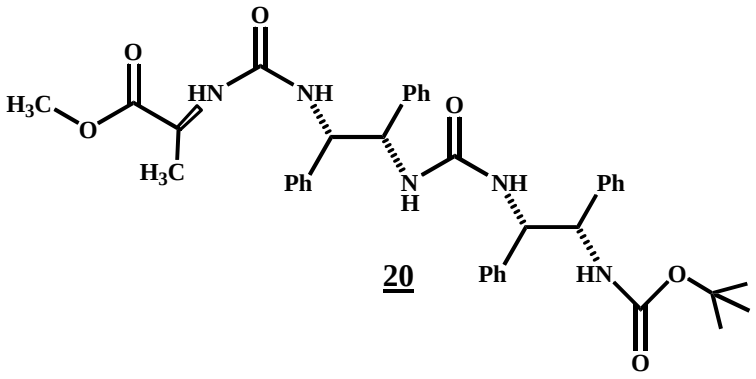

20

S, S–Boc–Ala–Trimer–Ester

In a 50 mL round bottom flask charged with 15 mL DMF was added 2.00 g (7.5 mmol) of alanine carbamate, **43** and 4.00 g (7.32 mmol) of *S*,*S*–Mono–BOC dimer. A solution of 0.80 mL TEA in 5 mL DMF was added dropwise into the flask containing the dimer and activated amino acid. After addition was complete, the solution was warmed to 50 °C with stirring for a 24 hr. period. The solvent, DMF was removed via high vacuum rotary evaporation. The residue was suspended in 10 mL EtOAc and passed through a short pad of alumina, trapping the *p*–nitrophenoxide anion. The mixture, now devoid of the yellow *p*–nitrophenoxide anion was chromatographed over silica eluting with 80:20 mixture of EtOAc/hexane affording 3.83 (80.9 % yield) of **20**. ^{1}**H** NMR (Varian 400 MHz; (DMSO–*d6*) δ: 1.17 – 1.19 (d, **3H**, *J* = 7.24 Hz); 1.23 (s, **9H**); 3.60 (s, **3H**); 4.09 – 4.17(m, **1H**); 4.73 – 4.76 (t, **1H**, *J* = 8.03 Hz); 4.79 – 4.82 (m, **2H**); 4.86 – 4.91 (t, **1H**, *J* = 8.10 Hz, *J* = 8.10 Hz); 6.38 – 6.40 (d, **1H**, *J* = 6.90 Hz); 6.56 – 6.60 (d,

1H, *J* = 7.76 Hz); 6.81 – 6.83 (d, **1H,** *J* = 8.1 Hz); 6.86 – 6.89 (d, **1H**, *J* = 7.60 Hz); 6.90 – 6.95 (d, **1H,** *J* = 7.57 Hz); 7.09 – 7.25 (m, **20H**). ^{13}**C** NMR (Varian 400 MHz; (DMSO–*d6*) δ: 17.1, 28.7, 50.4, 53.6, 56.9, 58.2, 59.4, 61.65, 77.4, 126.24, 127.33, 127.38, 127.43, 127.59, 127.68, 141.02, 141.35, 155.22, 156.05, 156.95, 173.97. MALDI–TOF–MS: m/z 680 [M+], 681 [M+1], 703 [M+Na], 704 [M+H+Na], 720 [M+K]. ***Anal. Calc*: C**, 68.90; **H**, 6.67; **N**, 10.30. *Found:* C, 68.09; H, 6.53; N, 10.20.

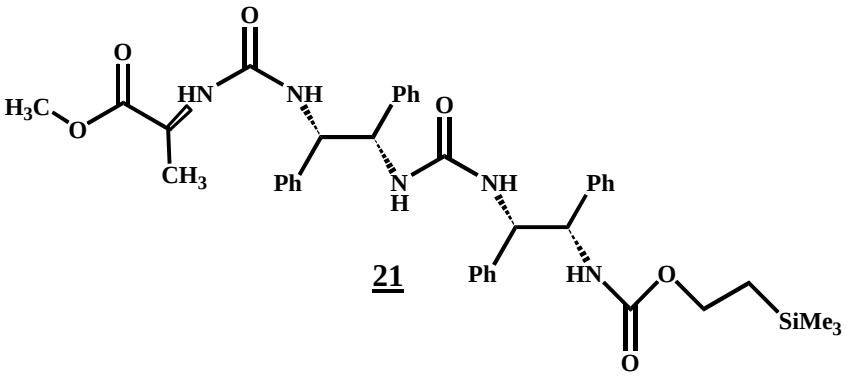

21

Teoc–S, S–Ala–Trimer Ester

2.75 g (4.24 mmol) of compound **20** was submitted to deprotection conditions using 3.0 eq of TFA in 10.0 mL DCM for a 24 hour period. After the period elapsed, excess TFA and DCM were removed by rotary evaporation leaving behind a residue. The residue was dissolved in 10.0 mL DCM and washed 3 times with saturated $NaHCO_3$ solution. The organic layer was dried over anhydrous Na_2SO_4. The salts were filtered and solvent removed. Next, DMF was added along with 3 eq. of Teoc carbonate, **47**. This solution was allowed to stir at room temperature for 24 hrs. The next day, DMF was removed via high vacuum rotary evaporation. The resulting residue was taken up in EtOAc and chromatographed over alumina, eluting with 40/60 EtOAc/hexane. The solvents were removed affording 2.80 g, 91.8 % of Teoc–*S*, *S*–Ala–Trimer, **21**. ^{1}**H** NMR (Varian 400 MHz; (DMSO–*d6*) δ: –0.04 (s, **9H**); 0.0782 – 0.823 (m, **2H**); 1.18 – 1.20 (d, **3H**, *J* = 7.22 Hz); 3.55 (s, **3H**); 3.87 – 3.92 (m, **2H**); 4.09 – 4.17 (m, **1H**); 4.73 – 4.77 (dd, **1H**, *J* = 8.59 Hz, *J* = 8.30 Hz); 4.79 – 4.83 (m, **2H**); 4.85 – 4.89 (dd, **1H,** *J* = 8.14 Hz, *J* = 8.14 Hz); 6.34 – 6.38 (d, **1H**, *J* = 7.53 Hz); 6.42

– 6.45 (d, **1H**, *J* = 7.41 Hz); 6.57 – 6.59 (d, **1H**, *J* = 7.97 Hz); 6.80 – 6.84 (d, **1H**, *J* = 8.45 Hz); 7.08 – 7.20 (m, **20H**); 7.55 – 7.58 (d, **1H**, *J* = 8.98 Hz). ^{13}**C** NMR (Varian 400 MHz; (DMSO–*d6*) δ: –1.47, 17.24, 18.07, 48.20, 57.96, 58.77, 59.96, 61.65, 79.17, 126.64, 127.13, 27.34, 127.49, 127.68, 127.78, 141.03, 141.43, 155.83, 157.06, 157.14, 174.06. MALDI–TOF–MS: 680 [M+], 681 [M+1], 703 M+Na], 704 [M+H+Na], 720 [M+K]. ***Anal. Calc***: **C**, 66.36; **H**, 6.82; **N**, 9.67; **Si**, 3.88. ***Found:*** **C**, 66.26; **H**, 6.77; **N**, 9.63; **Si**, 3.86.

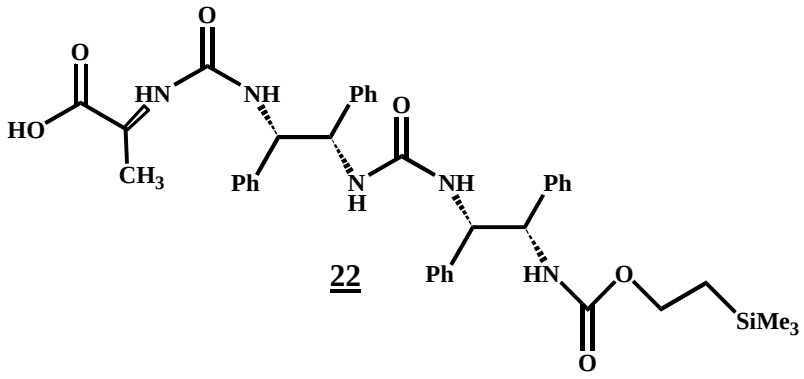

22

Teoc–S,S–Ala–Trimer Acid

2.00 g (2.77 mmol) of Teoc-*S, S*-Ala-Trimer, **21** was dissolved in 5 mL of MeOH. The resulting solution was chilled to –10 °C and 2.77 mL of ice–cold 1.00 M LiOH was carefully added dropwise with vigorous stirring. After addition of LiOH was completed, the reaction was warmed to 0 °C and was allowed to stir for 30 minutes. Next, 1.00 M of ice-cold HCl was added dropwise to neutralize the LiOH. After complete addition of HCl and white precipitate fell out of solution and the pH of solution was checked to ensure its acidic nature. The white solid was filtered to afford 1.84 g (94.1 %) of **22**. ^{1}H NMR (Varian 400 MHz; (DMSO–*d6*) δ: –0.05 (s, **9H**); 0.081 – 0.83 (m, **2H**); 1.28 – 1.30 (d, **3H**, *J* = 7.21 Hz); 3.88 – 3.92 (m, **2H**); 4.19 – 4.22 (m, **1H**); 4.76 – 4.80 (dd, **1H**, *J* = 8.61 Hz, *J* = 8.32 Hz); 4.83 – 4.87 (m, **2H**); 4.89 – 4.91 (dd, **1H**, *J* = 8.16 Hz, *J* = 8.16 Hz); 6.37 – 6.41 (d, **1H**, *J* = 7.54 Hz); 6.45 – 6.48 (d, **1H**, *J* = 7.43 Hz); 6.59 – 6.61 (d, **1H**, *J* = 8.00Hz); 6.82 – 6.87 (d, **1H**, *J* = 8.46 Hz); 7.10 – 7.21 (m, **20H**); 7.57 – 7.60 (d, **1H**, *J* = 8.97 Hz). ^{13}**C** NMR (Varian 400 MHz; (DMSO–*d6*) δ: –1.44, 17.22, 18.10, 48.23, 58.00, 58.77, 59.98, 79.15, 126.62, 127.16, 27.31, 127.52, 127.69, 128.01,

141.07, 141.48, 155.86, 157.11, 157.17. MALDI–TOF–MS: m/z 664[M–CO_2], 692[M–H_2O], 693 [M+H–H_2O], 714 [M+Na–H_2O], 715 [M+H+Na–H_2O]. ***Anal. Calc*: C**, 65.98; **H**, 6.67; **N**, 9.87; **Si**, 3.96. ***Found:* C**, 65.90; **H**, 6.59; **N**, 9.67; **Si**, 3.89.

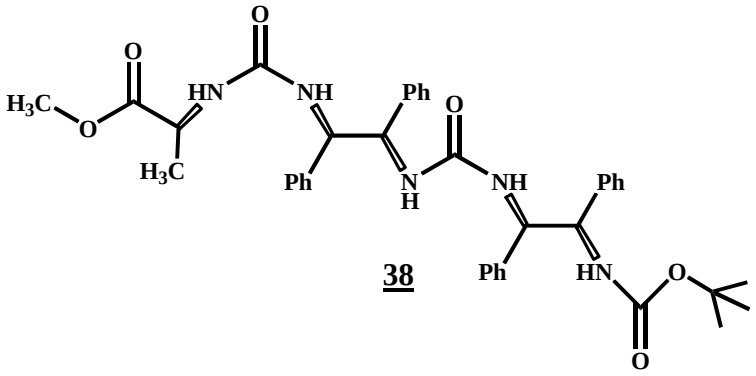

38

R, R–Boc–Ala–Trimer–Ester

In a 50 mL round bottom flask charged with 15 mL DMF was added 1.60 g (6.0 mmol) of alanine carbamate, **43** and 3.21 g (5.88 mmol) of *R, R*–Mono–BOC dimer, **30**. A solution of 0.80 mL TEA in 5 mL DMF was added dropwise into the flask containing the dimer and activated amino acid. After addition was complete, the solution was warmed to 50 °C with stirring for a 24 hr. period. The solvent, DMF was removed via high vacuum rotary evaporation. The residue was suspended in 10 mL EtOAc and passed through a short pad of alumina, trapping the *p*-nitrophenoxide anion. The mixture, now devoid of the yellow *p*–nitrophenoxide anion was chromatographed over silica eluting with 80:20 mixture of EtOAc/hexanes affording 3.34 (83.7 % yield) of **38**. ^{1}**H** NMR (Varian 400 MHz; (DMSO–*d6*) δ: 1.20 – 1.23 (d, **3H**, *J* = 7.27 Hz); 1.26 (s, **9H**); 3.58 (s, **3H**); 4.11–4.18 (m, **1H**); 4.76 – 4.79 (t, **1H**, *J* =8 .03); 4.82 – 4.84 (m, **2H**); 4.88 – 4.93 (t, **1H**, *J* = 8.00 Hz, *J* = 8.00 Hz); 6.40 – 6.42 (d, **1H**, *J* = 6.93 Hz); 6.62 – 6.66 (d, **1H**, *J* = 8.02 Hz); 6.85 – 6.87 (d, **1H,** *J* = 8.3 Hz); 6.89 – 6.82 (d, **1H**, *J* = 7.63 Hz); 6.91 – 6.96 (d, **1H,** *J* **=** 7.57 Hz); 7.11 – 7.23 (m, **20H**). ^{13}**C** NMR (Varian 400 MHz; (DMSO–*d6*) δ: 17.5, 29.0, 50.7, 53.6, 57.3, 58.9, 60.4, 62.3, 78.4, 126.64, 127.13, 127.34, 127.49, 127.68, 127.78, 141.02, 141.36, 157.11, 156.98, 174.0 MALDI–TOF–MS: m/z 680 [M+], 681 [M+1], 703 [M+Na], 704

[M+H+Na], 720 [M+K]. ***Anal. Calc*: C**, 68.90; **H**, 6.67; **N**, 10.30. *Found:* C, 68.77; H, 6.52; N, 10.11.

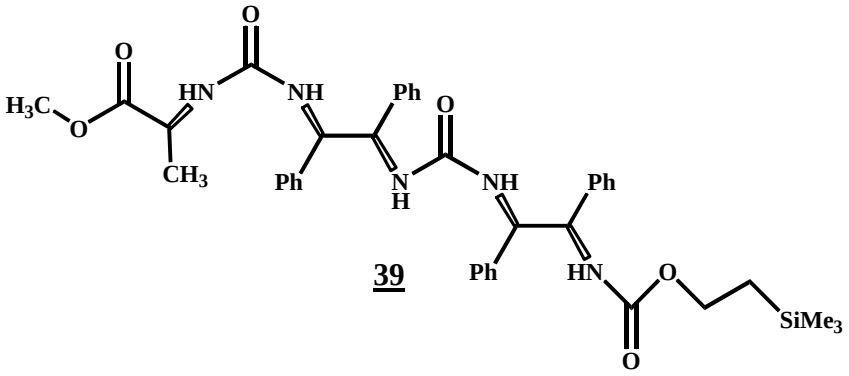

Teoc–R, R–Ala–Trimer Ester

2.75 g (4.24 mmol) of compound **38** was submitted to deprotection conditions using 3.0 eq of TFA in 10.0 mL DCM for a 24 hour period. After the period elapsed, excess TFA and DCM were removed by rotary evaporation leaving behind a residue. The residue was dissolved in 10.0 mL DCM and washed 3 times with saturated $NaHCO_3$ solution. The organic layer was dried over anhydrous Na_2SO_4. The salts were filtered and solvent removed. Next, DMF was added along with 3 eq. of Teoc carbonate, **47**. This solution was allowed to stir at room temperature for 24 hrs. The next day, DMF was removed via high vacuum rotary evaporation. The resulting residue was taken up in EtOAc and chromatographed over alumina, eluting with 40/60 EtOAc/hexane. The solvents were removed affording 2.82 g, 92.0 % of Teoc–*R, R*–Ala–Trimer, **39**. ^{1}**H** NMR (Varian 400 MHz; (DMSO–*d6*) δ: –0.06 (s, **9H**); 0.08 – 0.83 (m, **2H**); 1.24 – 1.32 (d, **3H**, *J* = 7.27 Hz); 3.59 (s, **3H**); 3.91 – 3.96 (m, **2H**); 4.11 – 4.19 (m, **1H**); 4.76 – 4.80 (dd, **1H**, *J* = 8.56 Hz, *J* = 8.27 Hz); 4.82 – 4.85 (m, **2H**, *J* = 8.17 Hz, *J* = 8.17 Hz); 4.89 – 4.92 (dd, **1H**); 6.38 – 6.42 (d, **1H**, *J* = 7.53 Hz); 6.45 – 6.48 (d, **1H**, *J* = 7.43 Hz); 6.60 – 6.62 (d, **1H**, *J* = 7.98 Hz); 6.83 – 6.86 (d, **1H**, *J* = 8.43 Hz); 7.09 – 7.20 (m, **20H**); 7.60 – 7.63 (d, **1H**, *J* = 8.90 Hz). ^{13}**C** NMR (Varian 400 MHz; (DMSO-*d6*) δ: –1.50, 17.28, 18.16, 48.27, 58.00, 59.02, 59.99, 61.72, 79.37, 126.66, 127.11, 127.38, 127.52, 127.73, 127.83, 141.13, 141.48, 155.93, 157.13, 157.34, 174.16. ***Anal. Calc***: **C**, 66.36; **H**, 6.82; **N**, 9.67; **Si**, 3.88. ***Found:***

C, 66.16; **H**, 6.78; **N**, 9.60; **Si**, 3.80. MALDI–TOF–MS: m/z 680 [M+], 681 [M+1], 703 [M+Na], 704 [M+H+Na], 720 [M+K]. ***Anal. Calc*: C**, 66.36; **H**, 6.82; **N**, 9.67; **Si**, 3.88. ***Found:*** **C**, 66.14; **H**, 6.65; **N**, 9.58; **Si**, 3.86.

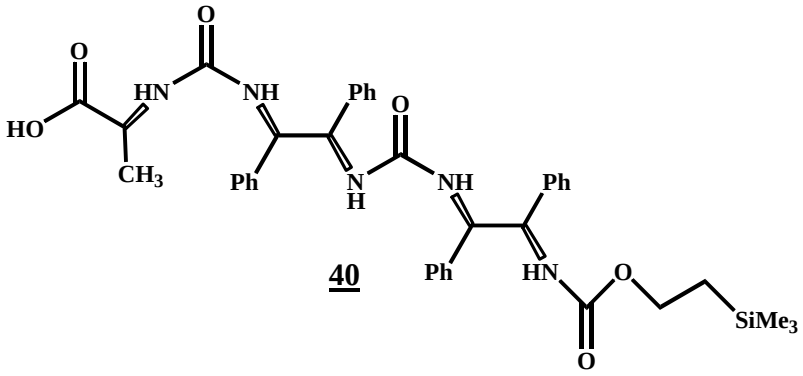

40

Teoc–R, R–Ala–Trimer Acid

2.00 g (2.77 mmol) of **39** was dissolved in 5 mL of MeOH. The resulting solution was chilled to –10 °C and 2.77 mL of ice–cold 1.00 M LiOH was carefully added dropwise with vigorous stirring. After addition of LiOH was completed, the reaction was warmed to 0 °C and was allowed to stir for 30 minutes. Next, 1.00 M of ice–cold HCl was added dropwise to neutralize the LiOH. After complete addition of HCl and white precipitate fell out of solution and the pH of solution was checked to ensure its acidic nature. The white solid was filtered to afford 1.88 g (95.7 %) of **41**. ^{1}H NMR (Varian 400 MHz; (DMSO–*d6*) δ: –0.05 (s, **9H**); 0.081–0.83 (m, **2H**); 1.27 – 1.30 (d, **3H**, *J* = 7.21 Hz); 3.88 – 3.92 (m, **2H**); 4.19 – 4.24 (m, **1H**); 4.80 – 4.84 (dd, **1H**, *J* = 8.65 Hz, *J* = 8.36 Hz); 4.83 – 4.87 (m, **2H**); 4.89 – 4.91 (dd, **1H**, *J* = 8.16 Hz, *J* = 8.16 Hz); 6.37 – 6.41 (d, **1H**, *J* = 7.54 Hz); 6.46 – 6.50 (d, **1H**, *J* = 7.45 Hz); 6.59 – 6.61 (d, **1H**, *J* = 8.00 Hz); 6.82 – 6.87 (d, **1H**, *J* = 8.46 Hz); 7.10 – 7.21 (m, **20H**); 7.57 – 7.60 (d, **1H**, *J* = 8.93 Hz). ^{13}**C** NMR (Varian 400 MHz; (DMSO–*d6*) δ: –1.49, 17.24, 18.10, 48.23, 58.01, 58.77, 59.98, 79.15, 126.67, 127.16, 127.31, 127.52, 127.69, 128.81, 141.07, 141.48, 155.96, 157.14, 157.37. MALDI–TOF–MS: m/z 692 [M–H_2O], 693 [M+H–H_2O], 714 [M+Na–H_2O], 715 [M+H+Na–H_2O]. ***Anal. Calc*: C**, 65.98; **H**, 6.67; **N**, 9.87; **Si**, 3.96. ***Found:*** **C**, 65.87; **H**, 6.59; **N**, 9.77; **Si**, 3.90.

3.8 Solid Phase Synthesis Protocols

3.8.1 First Attempt

In a solid phase synthesizer reaction vessel was added 0.20 g (0.84 mmol active sites) of Knorr resin, which was deprotected with treatment with three 30 minute washings with 20 % piperidine in DMF. Upon completion of the deprotection protocol, the resin beads were washed with MeOH for 10 minutes and then DCM for 2 minutes (for swelling). A small portion of beads were submitted to Kaiser test protocols to ensure that deprotection had taken place. Next, a previously prepared solution containing 0.50 g (0.576 mmol) of compound **16**, 100 μL of Hunig's base, 250 μL of DCM, 0.210 g (0.50 mmol) of Castro's reagent and 0.08 g (0.60 mmol) of HOBt in 1 mL DMF. This solution was warmed to 50 °C and placed directly on the deprotected solid phase resin beads. The reaction vessel was carefully shaken for 24 hrs and after this period elapsed, a small sample of beads were removed, then washed with a 50/50 mixture of DCM/DMF and submitted for Kaiser testing. The Kaiser tests on the beads were positive, indicating that coupling did not take place. The reaction was allowed to continue for 2 more days and a small portion of beads were removed and washed and submitted for Kaiser testing. Unfortunately, the test was positive, indicating that no reaction had taken place. The remaining solution was removed from the beads and the solution components checked by TLC to make sure that compound **16** had been completely converted to its active ester, which is needed for coupling.

3.8.2 Second Attempt

In a solid phase synthesizer reaction vessel was added 0.20 g (0.84 mmol active sites) of Knorr resin, which was deprotected with treatment with three 30 minute washings with 20 % piperidine in DMF. Upon completion of the deprotection protocol, the resin beads were washed with MeOH for 10 minutes and then DCM for 2 minutes (for swelling). A small portion of beads were submitted to Kaiser test protocols to ensure that deprotection had taken place. Next, a previously prepared solution containing 0.50 g (0.576 mmol) of compound **16**, 100 μL of Hunig's base, 250 μL of DCM, 0.210 g (0.50 mmol) of

Castro's reagent and 0.08 g (0.60 mmol) of HOBt in 1 mL DMF. This solution was warmed to 50 °C and placed directly on the deprotected solid phase resin beads. The reaction vessel was carefully shaken for 1 week. After this period elapsed, a small sample of beads were removed, then washed with a 50/50 mixture of DCM/DMF and submitted for Kaiser testing. The Kaiser tests on the beads were positive, indicating that coupling did not take place. No further attempts were taken with this material.

3.8.3 Third Attempt

In a solid phase synthesizer reaction vessel was added 0.20 g (0.84 mmol active sites) of Knorr resin, which was deprotected with treatment with three 30 minute washings with 20 % piperidine in DMF. Upon completion of the deprotection protocol, the resin beads were washed with MeOH for 10 minutes and then DCM for 2 minutes (for swelling). A small portion of beads were submitted to Kaiser test protocols to ensure that deprotection had taken place. Next, a previously prepared solution containing 0.50 g (0.576 mmol) of compound **34**, 100 μL of Hunig's base, 250 μL of DCM, 0.210 g (0.50 mmol) of Castro's reagent and 0.08 g (0.60 mmol) of HOBt in 1 mL DMF. This solution was warmed to 50 °C and placed directly on the deprotected solid phase resin beads. The reaction vessel was carefully shaken for 3 days at room temperature. After this period elapsed, a small sample of beads were removed, then washed with a 50/50 mixture of DCM/DMF and submitted for Kaiser testing. The Kaiser tests on the beads were positive, indicating that coupling did not take place. No further attempts were taken with this material.

3.8.4 Fourth Attempt

In a solid phase synthesizer reaction vessel was added 0.15 g (0.84 mmol active sites) of Knorr resin, which was deprotected with treatment with three 30 minute washings with 20 % piperidine in DMF. Upon completion of the deprotection protocol, the resin beads were washed with MeOH for 10 minutes and then DCM for 2 minutes (for swelling). A small portion of beads were submitted to Kaiser test protocols to ensure that deprotection had taken place. Next, a previously prepared solution containing 0.268 g (0.377 mmol) of compound **22**, 50 μL of

Hunig's base, 200 μL of DCM, 0.157 g (0.378 mmol) of Castro's reagent and 0.051 g (0.377 mmol) of HOBt in 0.75 mL of DMF. This solution was warmed to 50 °C and placed directly on the deprotected solid phase resin beads. The reaction vessel was carefully shaken for 2 days at room temperature. After this period elapsed, a small sample of beads were removed, then washed with a 50/50 mixture of DCM/DMF and submitted for Kaiser testing. The Kaiser tests on the beads were positive, indicating that coupling did not take place. No further attempts were taken with this material.

Chapter 4
Conclusion

The work presented in this dissertation was designed to elucidate the parameters necessary to create a novel helical-like peptidomimetic motif, which was based on the naturally occurring α–helical antibiotic peptide, Magainin. Also, presented in this work were the solution phase syntheses of small oligoureas (trimers) and various attempts to connect these "trimers" together using solid phase synthesis. This project surfaced from earlier studies which utilized short oligoureas sequences which contained the C_2 symmetric *trans*–1, 2–diaminocyclohexane. The results from those earlier studies suggested oligoureas derived from C_2 symmetric diamines would lead to a helical–like motif.

The first step towards our peptidomimetic was to utilize molecular modeling to predict which oligourea conformations would be best, in terms of helicity and the periodic disposition of the basic side chains. Unfortunately, because of the way modeling programs find energy minima, the carbonyl groups in the *S, S* and *R, R* conformers were pointed in the same direction, helping the conformational search to avoid producing a local mimina. Next, Monte Carlo searches were used to explore the molecular dynamics on the potential molecules.[19] These searches were initiated from helical–like conformations, consisting of 12 monomer units, with the carbonyl groups pointed in the same direction. The best results from this conformational search, which used the force field, Amber (CH_3Cl continuum dielectric field) produced, within a window of 25 kJ/mol (1000 max iterations for each cycle), 48 possible lowest energy structures. These results gave indication of an energetic preference for a right-handed helical-like motif. This right handed motif was composed mainly of C_2 symmetric diamine molecules that possess *S, S* stereochemistry. As shown in (Figures 1.12 a–d), the right handed helical-like motif is more ordered with the carbonyls pointing generally in the same direction. This allows for ease of hydrogen bonding and cooperativity between different subunits, eventually leading to stabilization of the structure and positioning of the amino acid side chain preferentially on one side. However, the left handed helical-like motif

(Figures 1.12 e–f) is not ordered and does not have the carbonyl groups pointing in one direction and it does not have the lysine side chains positioned preferentially on one side of the motif.

Using the results of the conformational search, a synthetic plan was implemented to make the small oligoureas. Unfortunately, two major problems needed to be overcome. One problem was the need for large quantities of the parent compound 1,2-diphenyl–1,2–diamine (DPDA), due to the many protecting group manipulations required in the synthesis. The second problem was wasting half of the diamine material for mono-protection. Luckily, in both cases, there existed, in the literature, procedures to produce mass quantities of the parent diamine (both enantiomers), as well as a method to mono-protect the diamine. Next, two orthogonally protected C_2 symmetric diamines were successfully coupled via a urea linkage (*R,R* and *S,S* diamines were used), leading to an orthogonally protected molecule (dimer). These dimers were deprotected on one end and eventually coupled to either a protected and activated lysine or a protected and activated alanine, creating a short sequence of oligoureas (trimers), containing an amino acid residue. The last step was connection of the various trimers together by an amide bond linkage. Solution phase syntheses of these compounds are quite problematic due to purification and overall yield of the synthesis. However, a solid–phase synthetic approach has worked quite well, for peptides and other oligomers. Therefore, attempts to connect the oligourea trimers were attempted using a solid–phase synthesis approach to generate a functional magainin mimic. Several attempts were tried; unfortunately none of the solid phase couplings worked. One of the possible reasons why coupling did not occur could have been caused by the nature of the solid phase resin itself. It is known that certain solid phase resins are incompatible with different types of molecules, as well as synthetic procedures due to the size, solubility and other resin characteristics. Another possible reason why coupling did not occur could have been related to the size of the trimers themselves. Steric interactions between the trimer and the resin could prevent the coupling of the trimer and the functionalized resin.

Appendix

A. 1 Crystal coordinates for structure 6b.

Atomic coordinates (x 10^4) and equivalent isotropic displacement parameters (A^2 x 10^3) for 6b.
U(eq) is defined as one third of the trace of the orthogonalized Uij tensor.

	x	y	z	U(eq)
N(1)	11251(3)	234(3)	1193(1)	45(1)
N(2)	11421(3)	703(3)	441(1)	42(1)
C(1)	12720(4)	98(4)	1059(1)	43(1)
C(2)	12942(4)	592(4)	540(1)	43(1)
C(3)	10637(4)	531(3)	824(1)	36(1)
C(4)	9046(4)	618(3)	838(1)	42(1)
F(1)	7720(3)	-858(3)	744(1)	102(1)
F(2)	8768(2)	1083(2)	1238(1)	56(1)
F(3)	9037(3)	1688(3)	539(1)	73(1)
C(5)	12515(4)	-1603(4)	1151(1)	37(1)
C(6)	13906(4)	-1770(4)	1250(1)	49(1)
C(7)	13732(5)	-3337(5)	1329(1)	61(1)
C(8)	12161(5)	-4751(4)	1308(1)	62(1)
C(9)	10773(5)	-4610(4)	1202(1)	60(1)
C(10)	10956(4)	-3048(4)	1128(1)	49(1)
C(11)	14539(3)	2225(4)	434(1)	40(1)
C(12)	15059(4)	3612(5)	706(1)	62(1)
C(13)	16494(5)	5101(5)	610(1)	77(1)
C(14)	17460(4)	5245(6)	239(1)	77(1)
C(15)	16955(5)	3882(7)	-34(1)	85(2)
C(16)	15498(5)	2333(6)	63(1)	69(1)

A. 2 Mono–TFA Diamine, 6, ^{1}H NMR

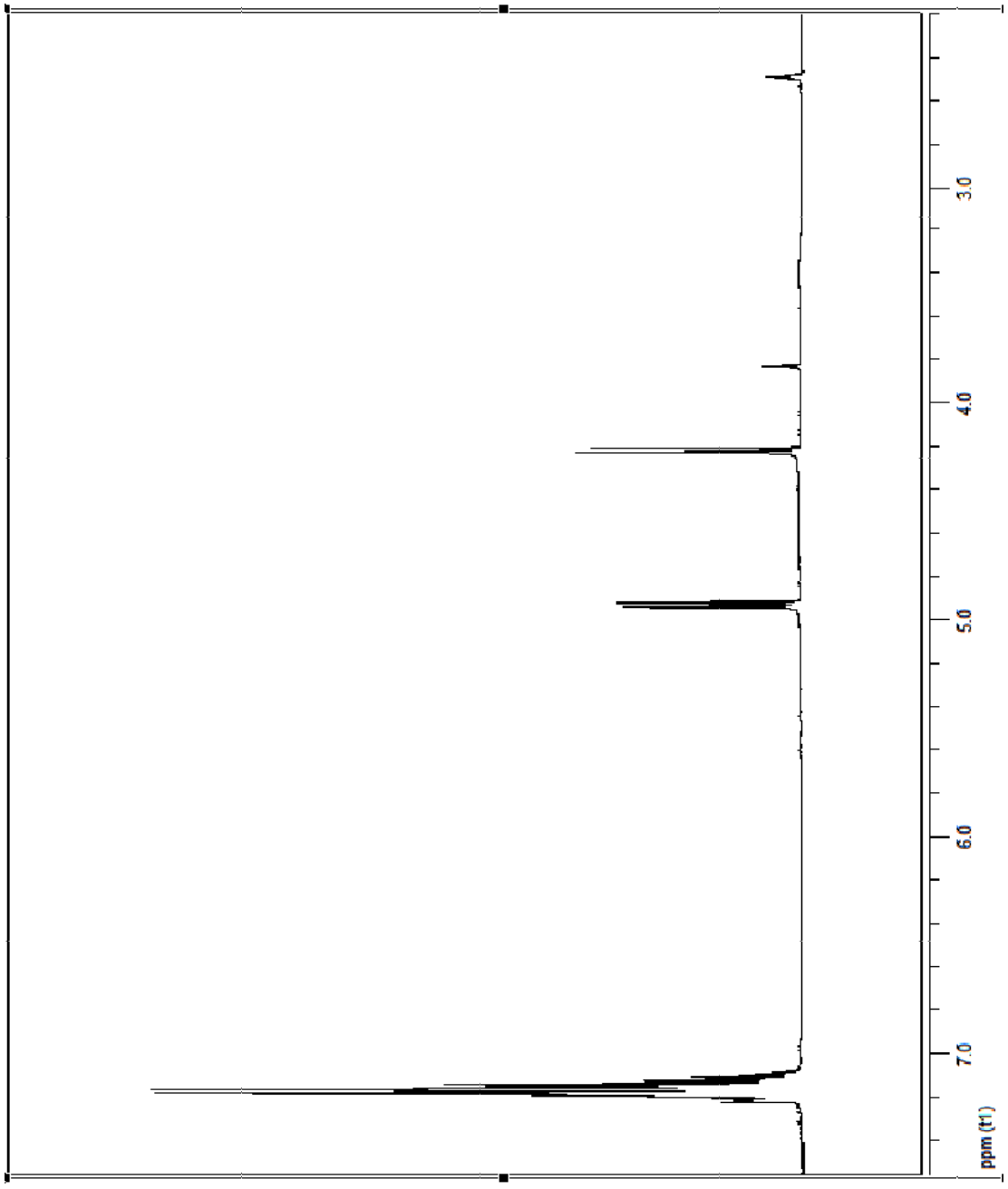

A. 3 Mono–TFA Diamine, 6, ^{13}C NMR

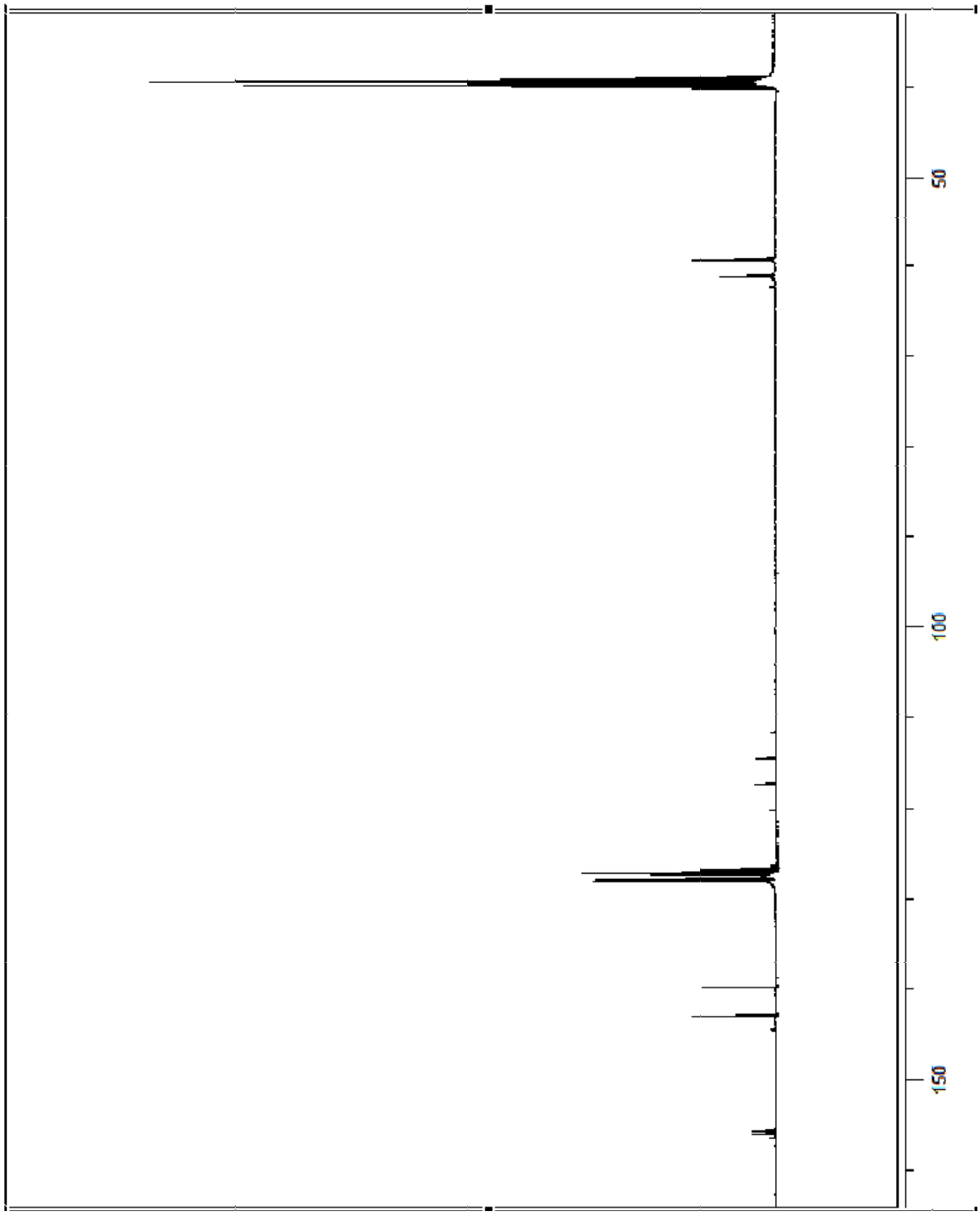

A. 4 Orthogonally Protected S,S–TFA/BOC Dimer, 11, ^{1}H NMR

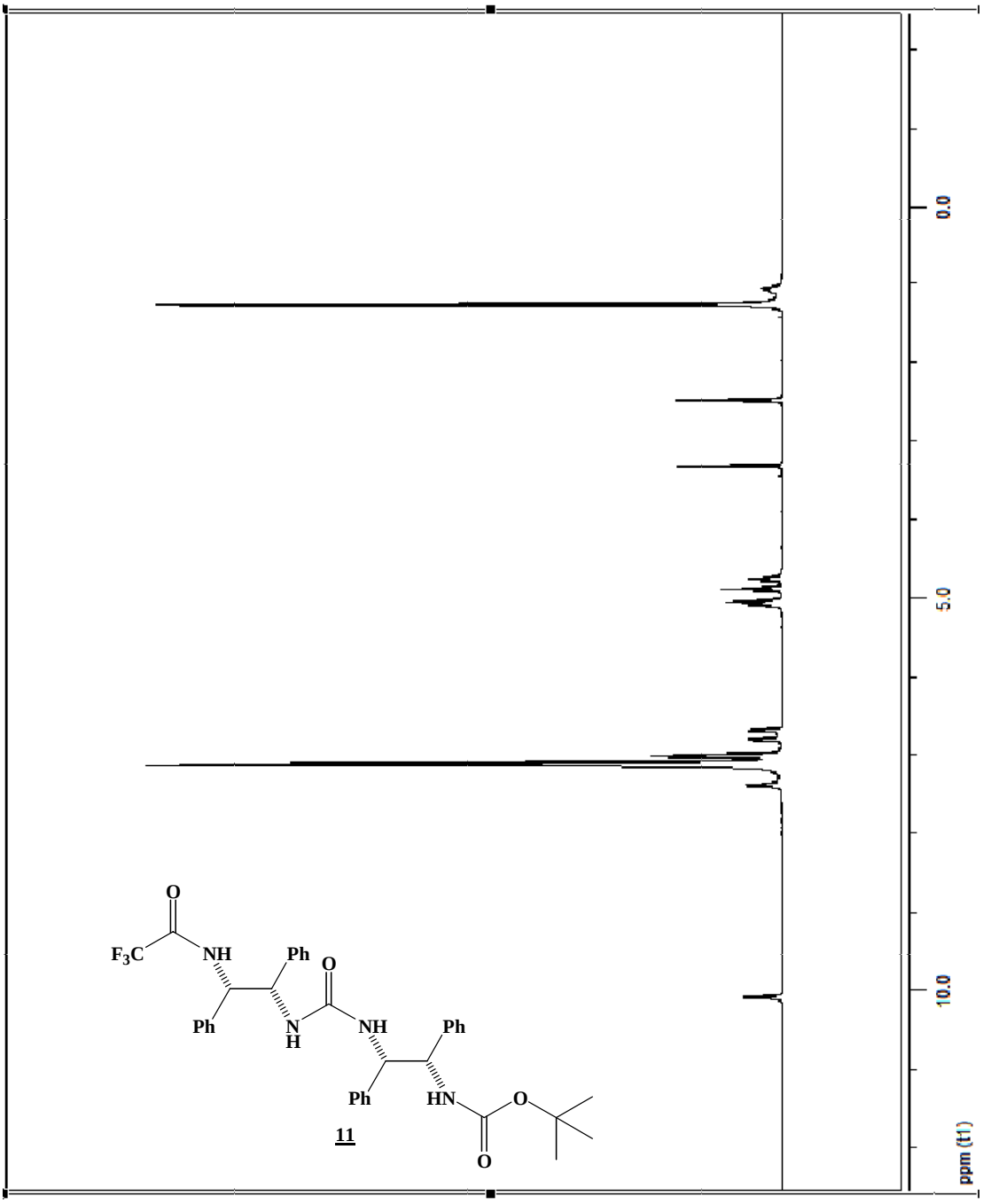

A. 5 Orthogonally Protected S,S–TFA/BOC Dimer, 11, ^{13}C NMR

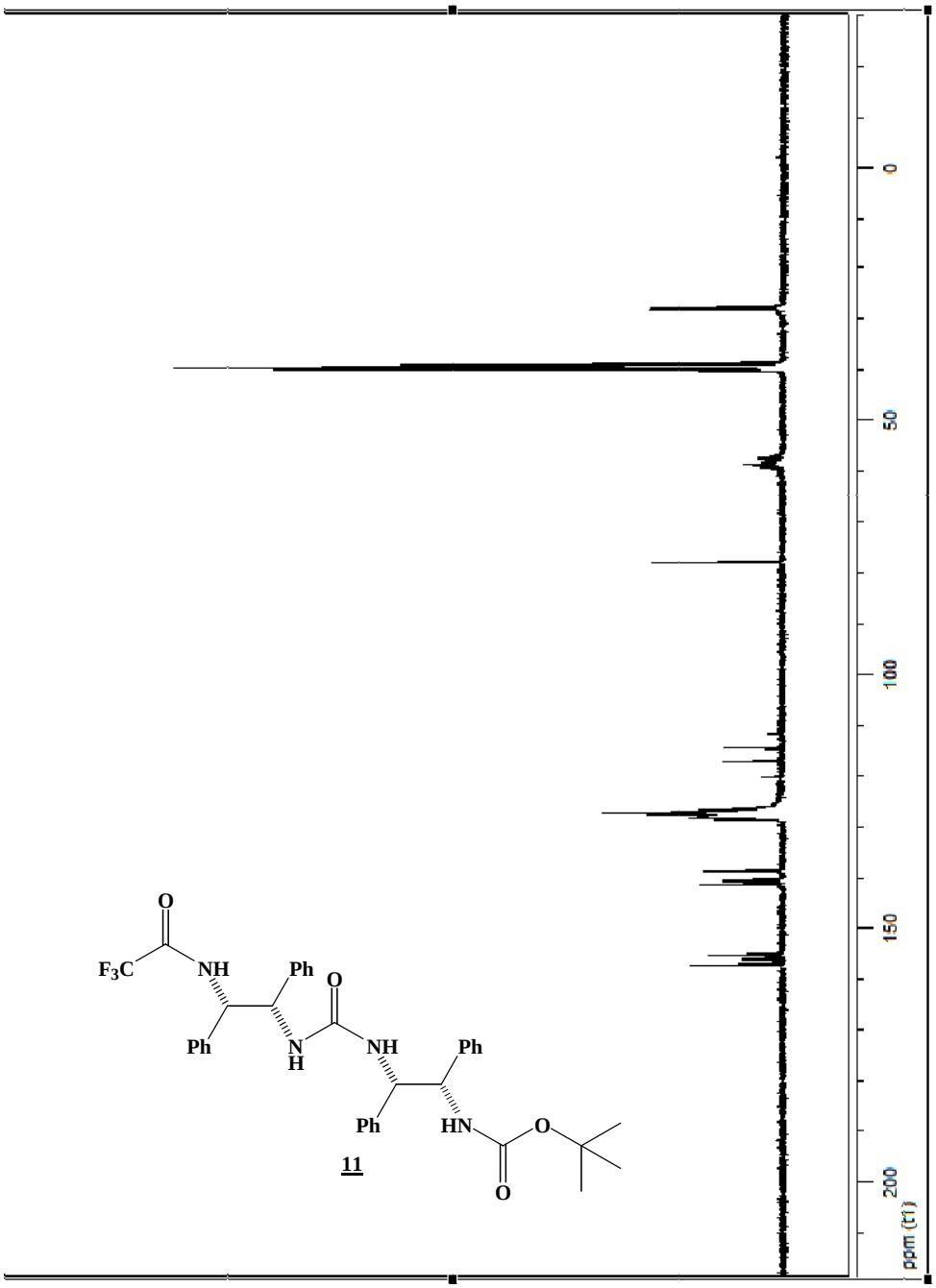

11

A. 6 ε–Cbz–(S)–Lysine–α–PNP Carbamate Methyl Ester, <u>41</u>, ^{1}H NMR

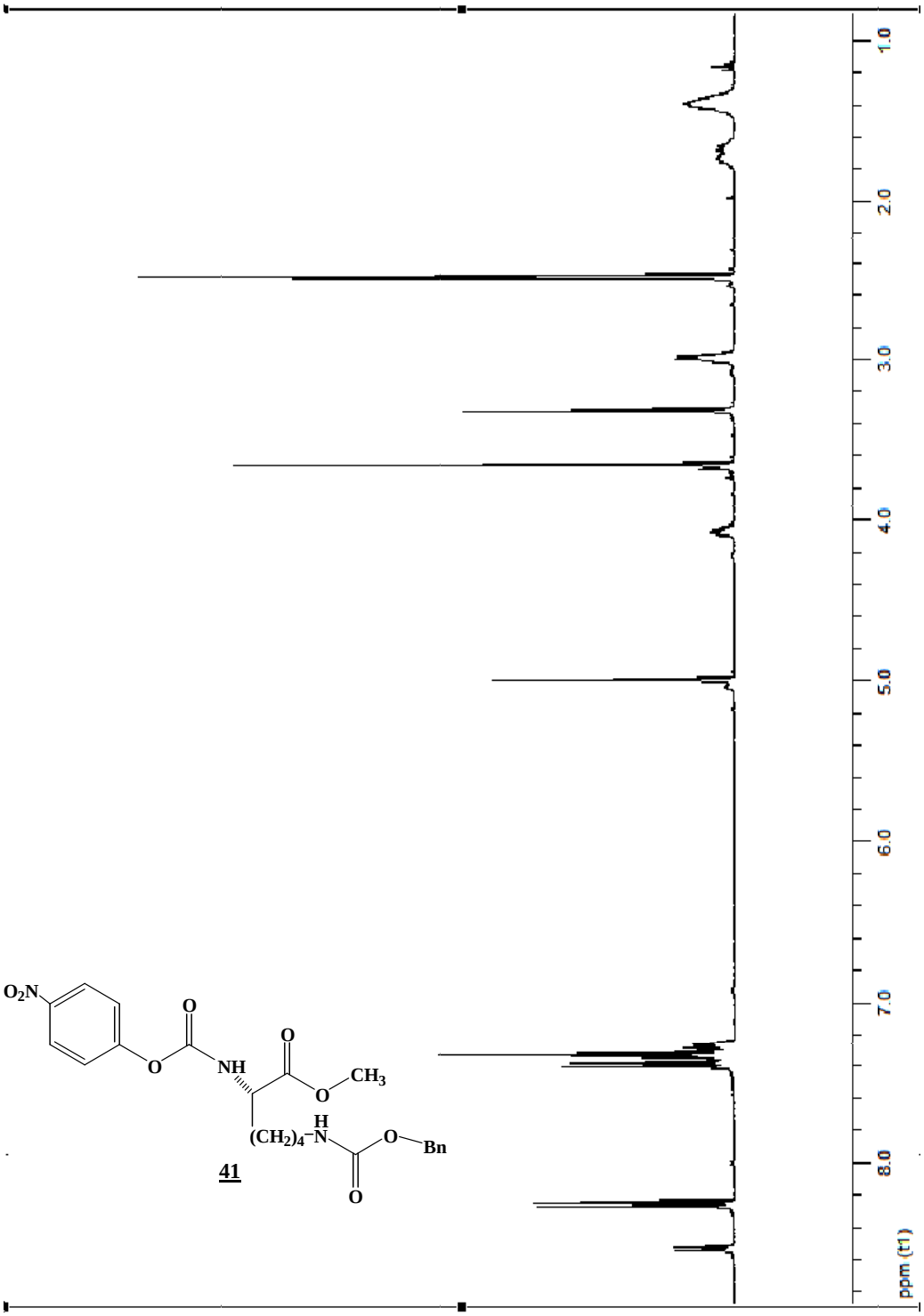

A. 7 ε–Cbz–(S)–Lysine–α–PNP Carbamate Methyl Ester, 41, ^{13}C NMR

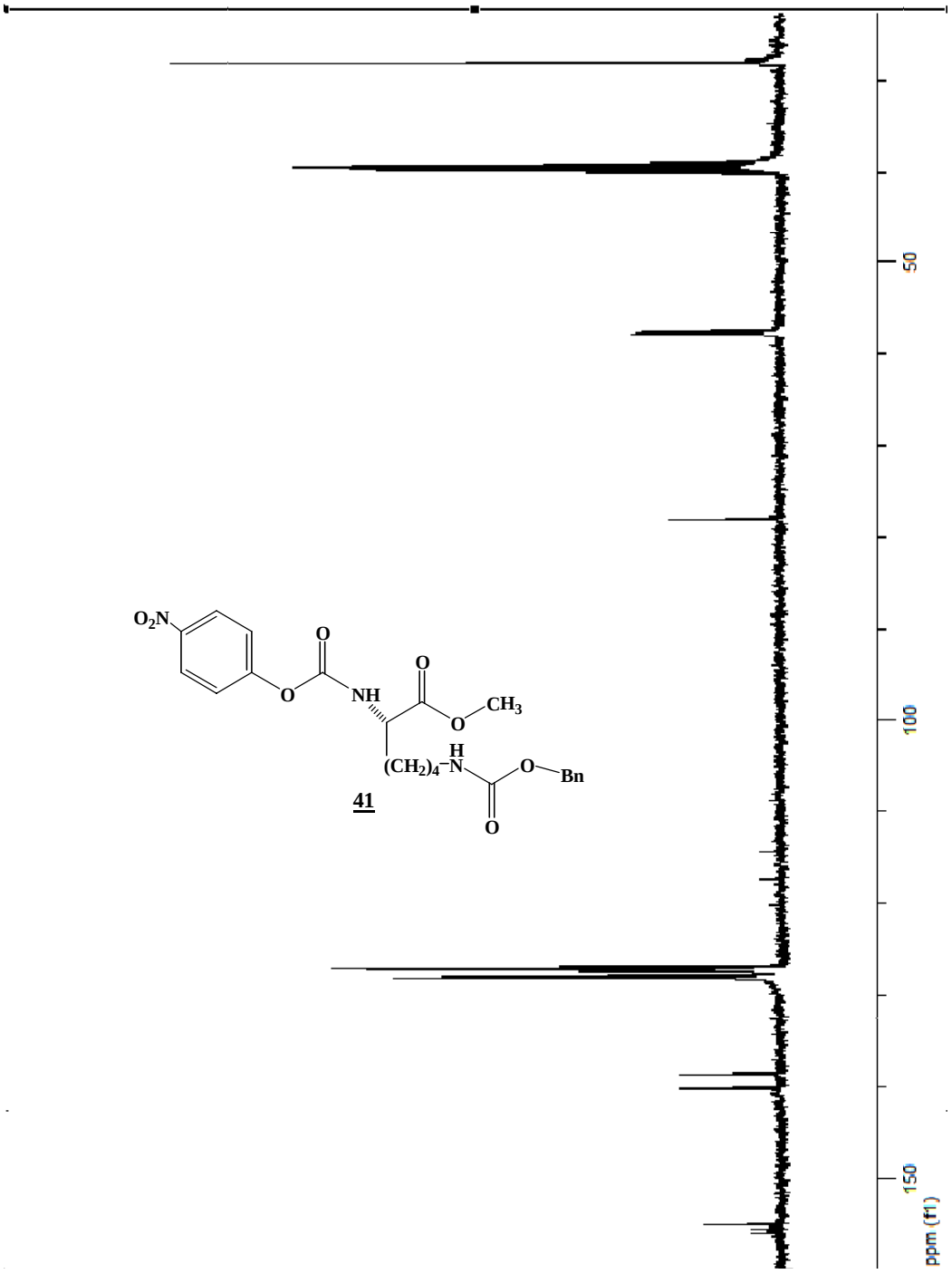

A. 8 Boc–*S*,*S*–(Z)–Lys–Trimer, 13, ^{1}H NMR

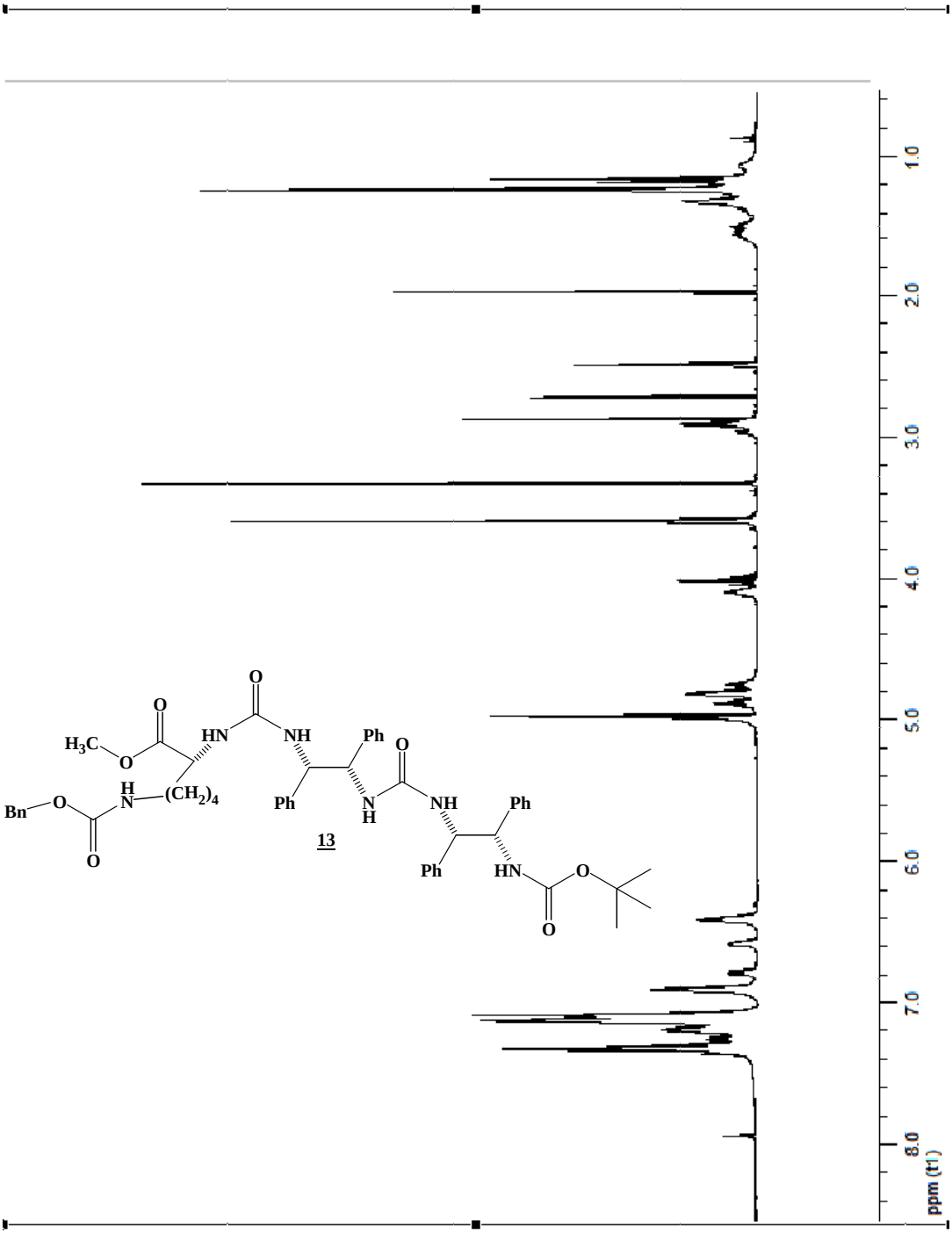

A. 9 Boc–*S*,*S*–(Z)–Lys–Trimer, 13, ^{13}C NMR

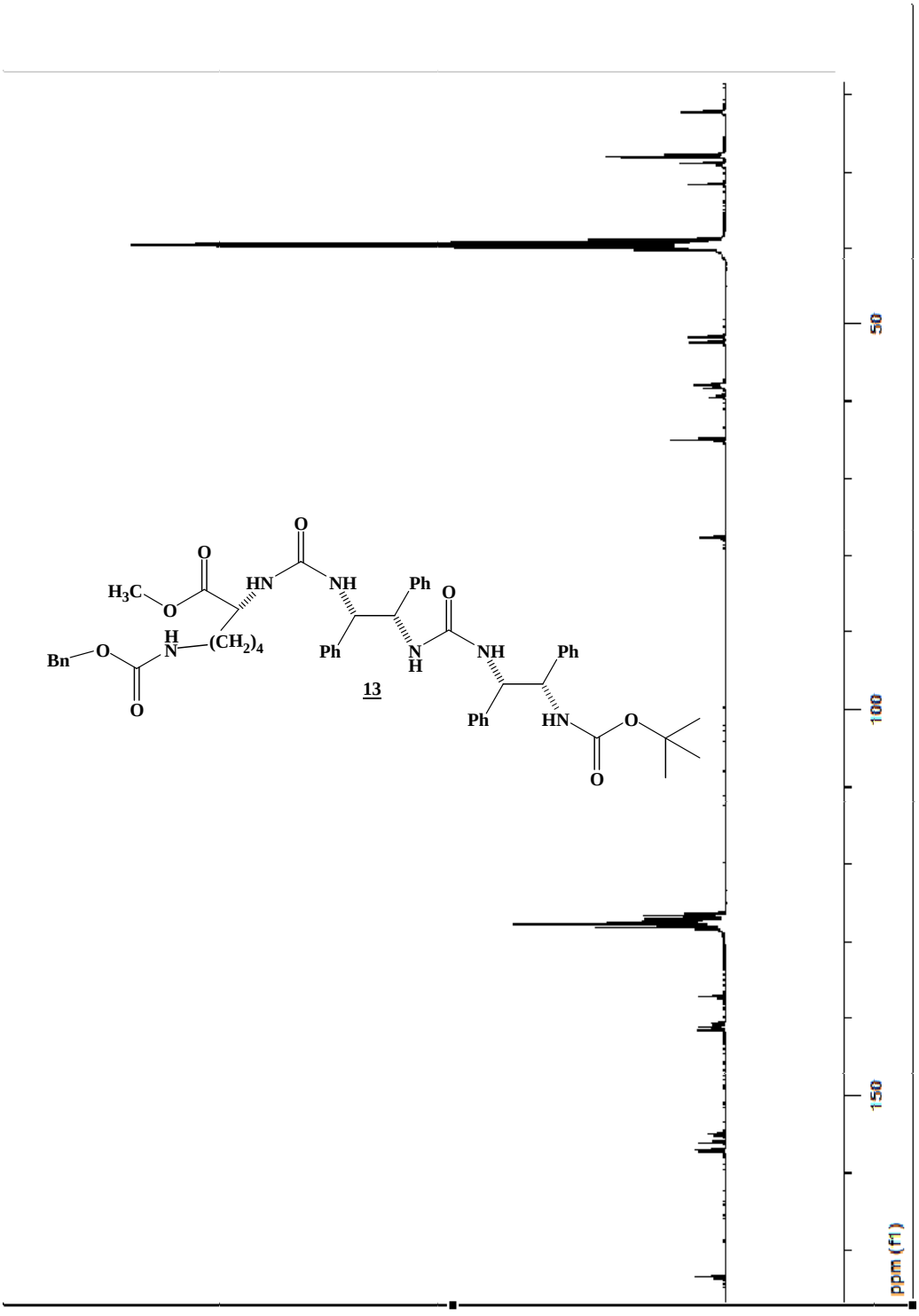

13

A. 10 Boc–*S*,*S*–(Z)–Lys–Trimer, <u>13</u>, MALDI–TOF–MS

A. 11 Teoc–*S*,*S*–(Z)–Lys–Trimer, 14, ^{1}H NMR

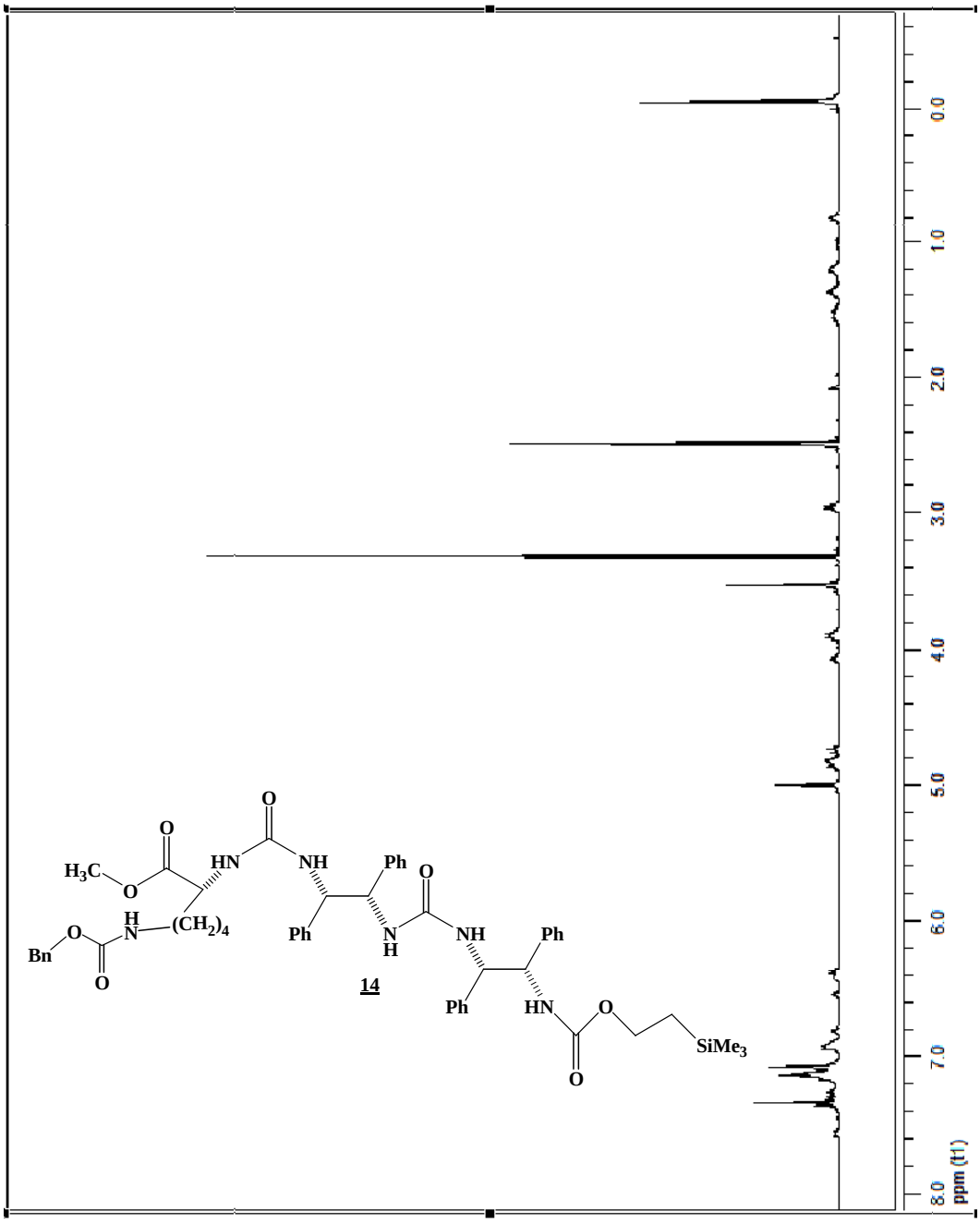

A. 12 Teoc–*S*,*S*–(Z)–Lys–Trimer, <u>14</u>, ^{13}C NMR

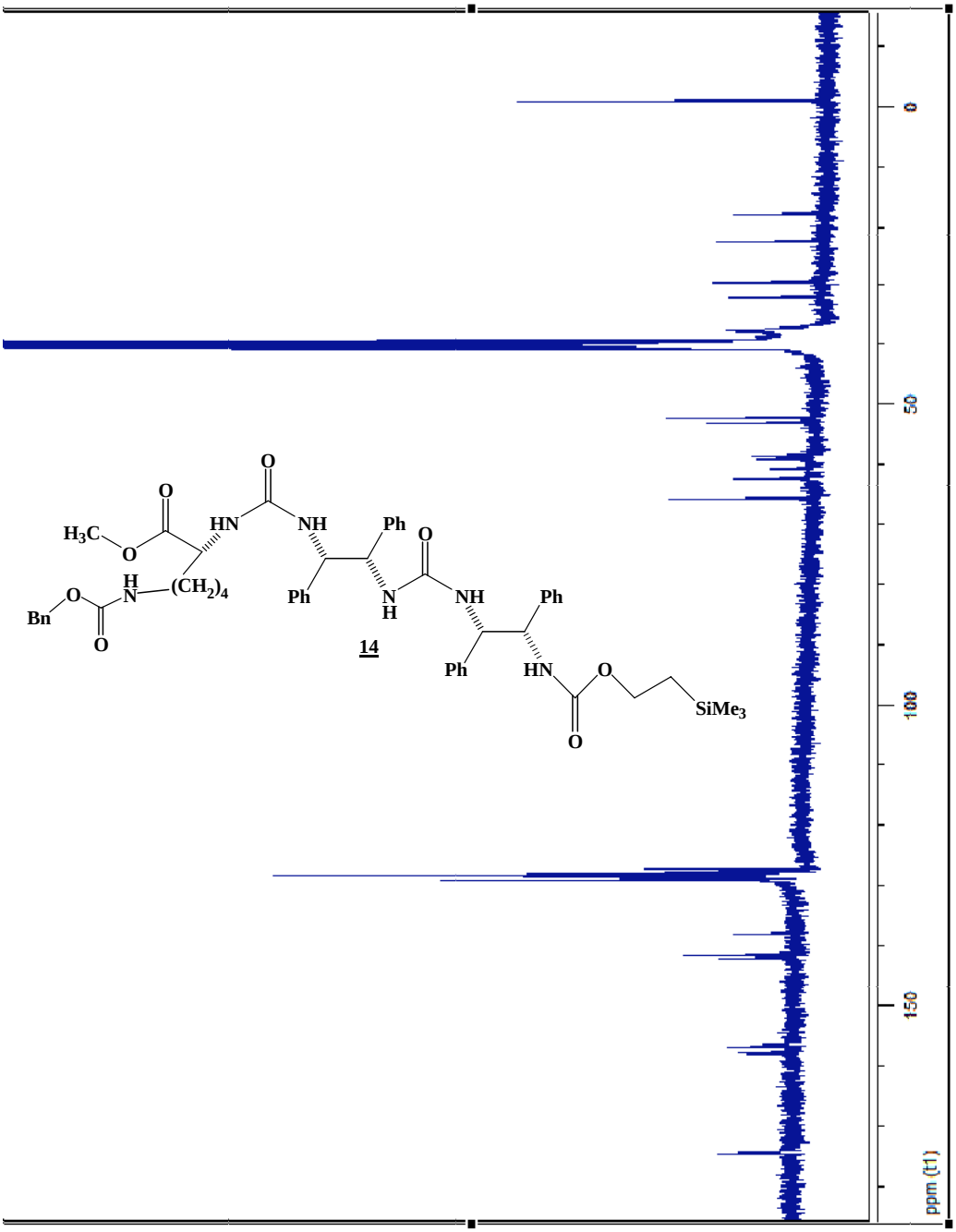

A. 13 Teoc–*S*,*S*–(Z)–Lys–Trimer, 14, MALDI–TOF–MS

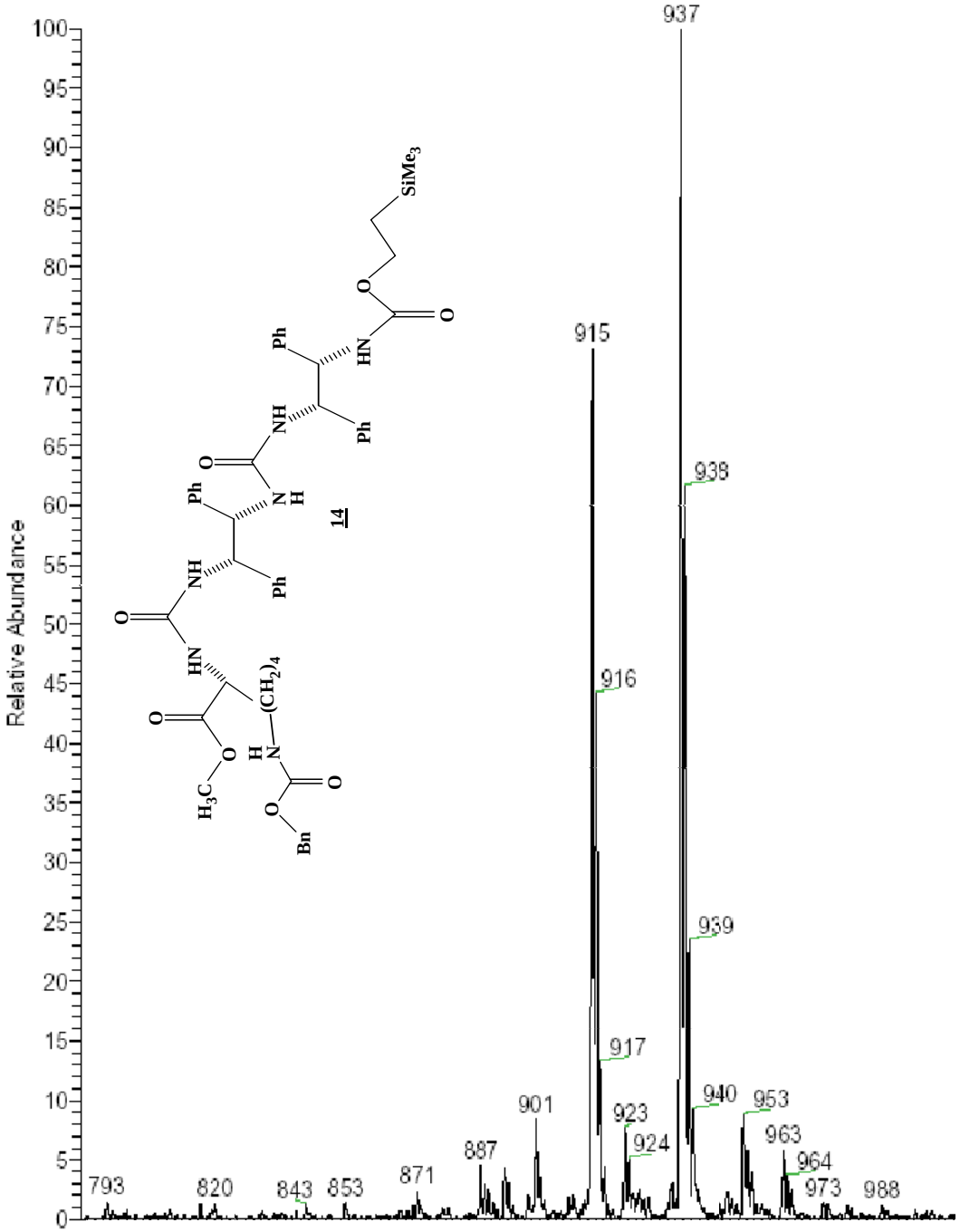

A. 14 Teoc–*S*,*S*–Boc–Lys–Trimer Acid, 16, MALDI–TOF–MS

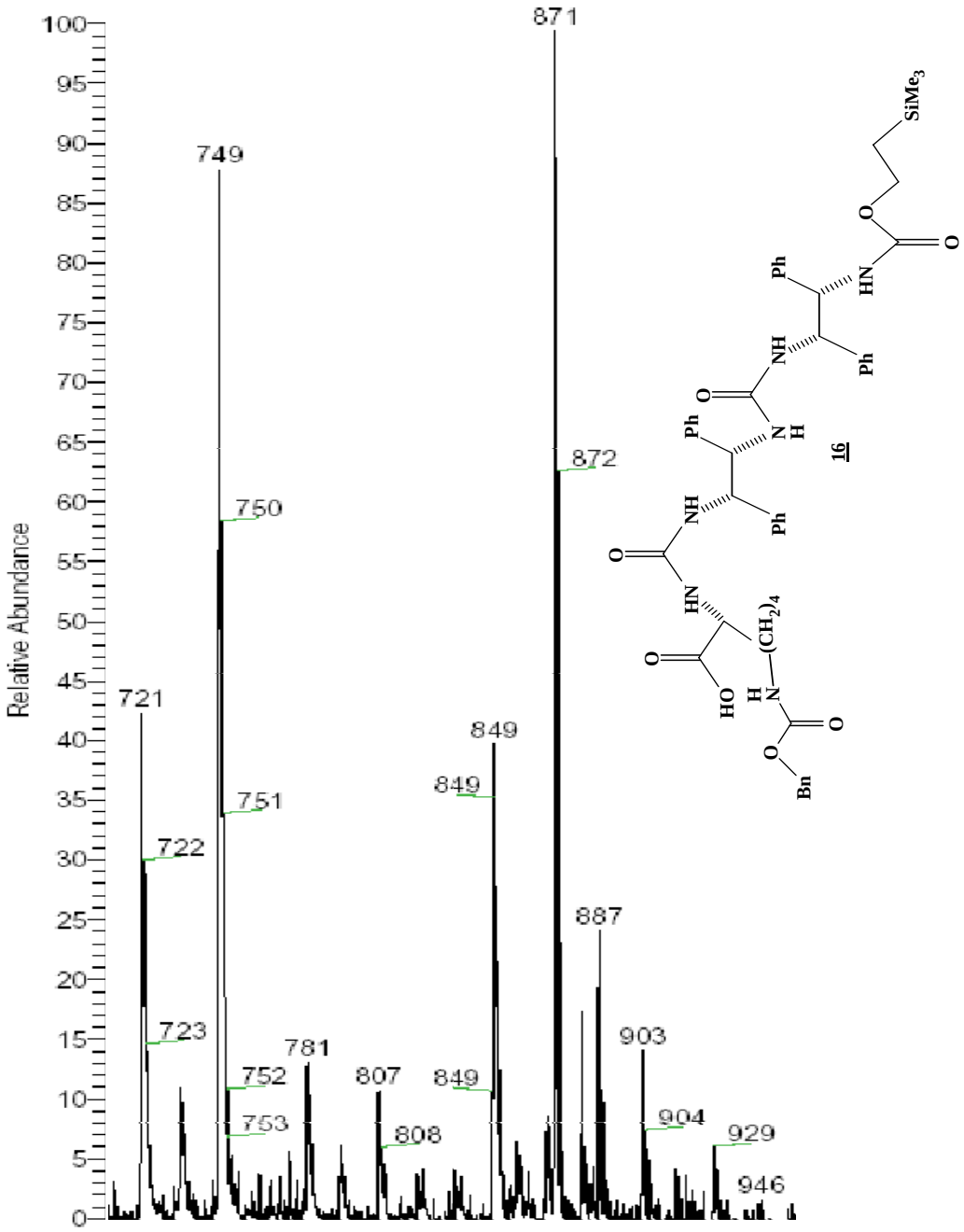

A. 15 *S,S*– Teoc–Ala–Trimer, 21, ^{1}H NMR

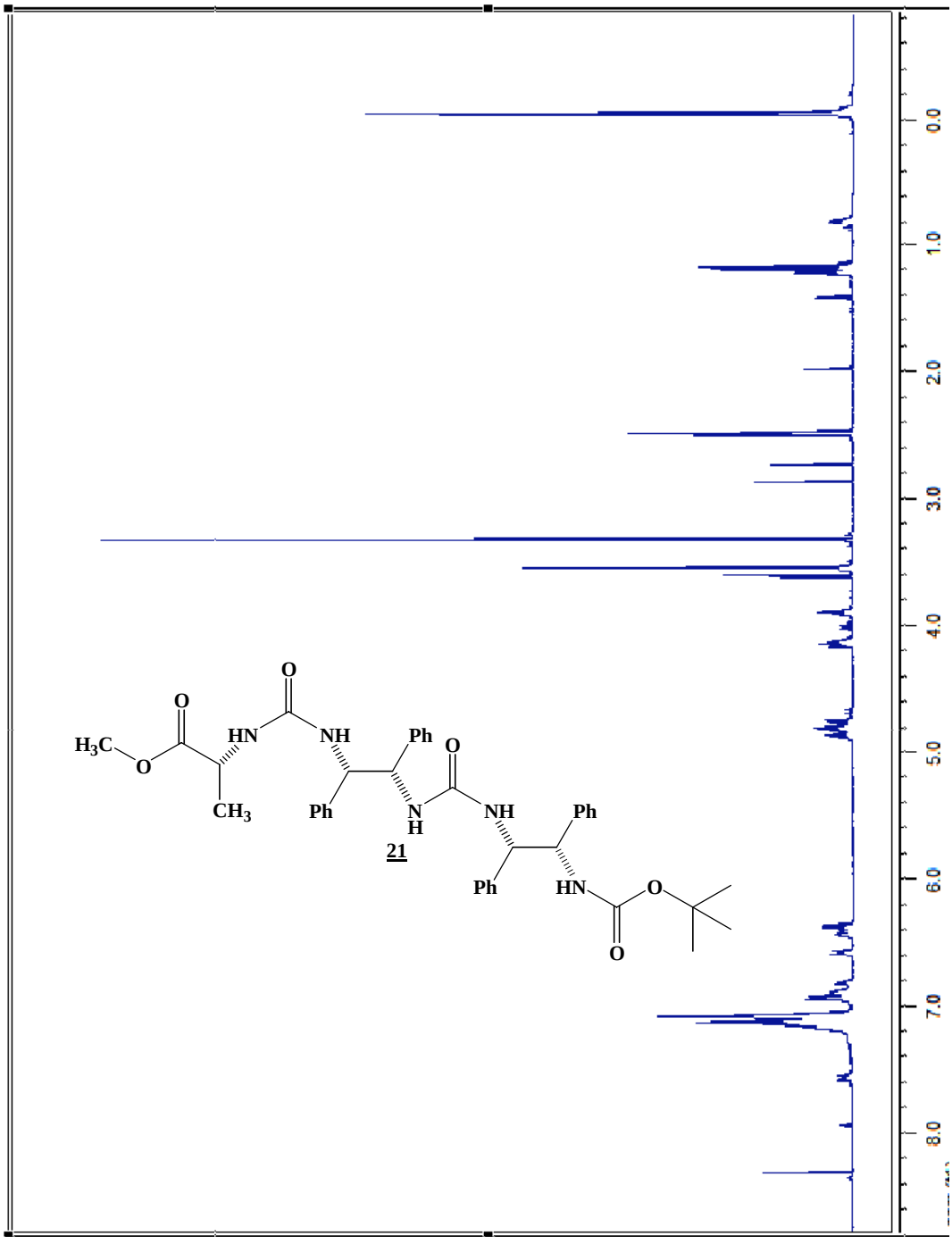

A. 16 *S*, *S*–Teoc–Ala–Trimer, 21, ^{13}C NMR

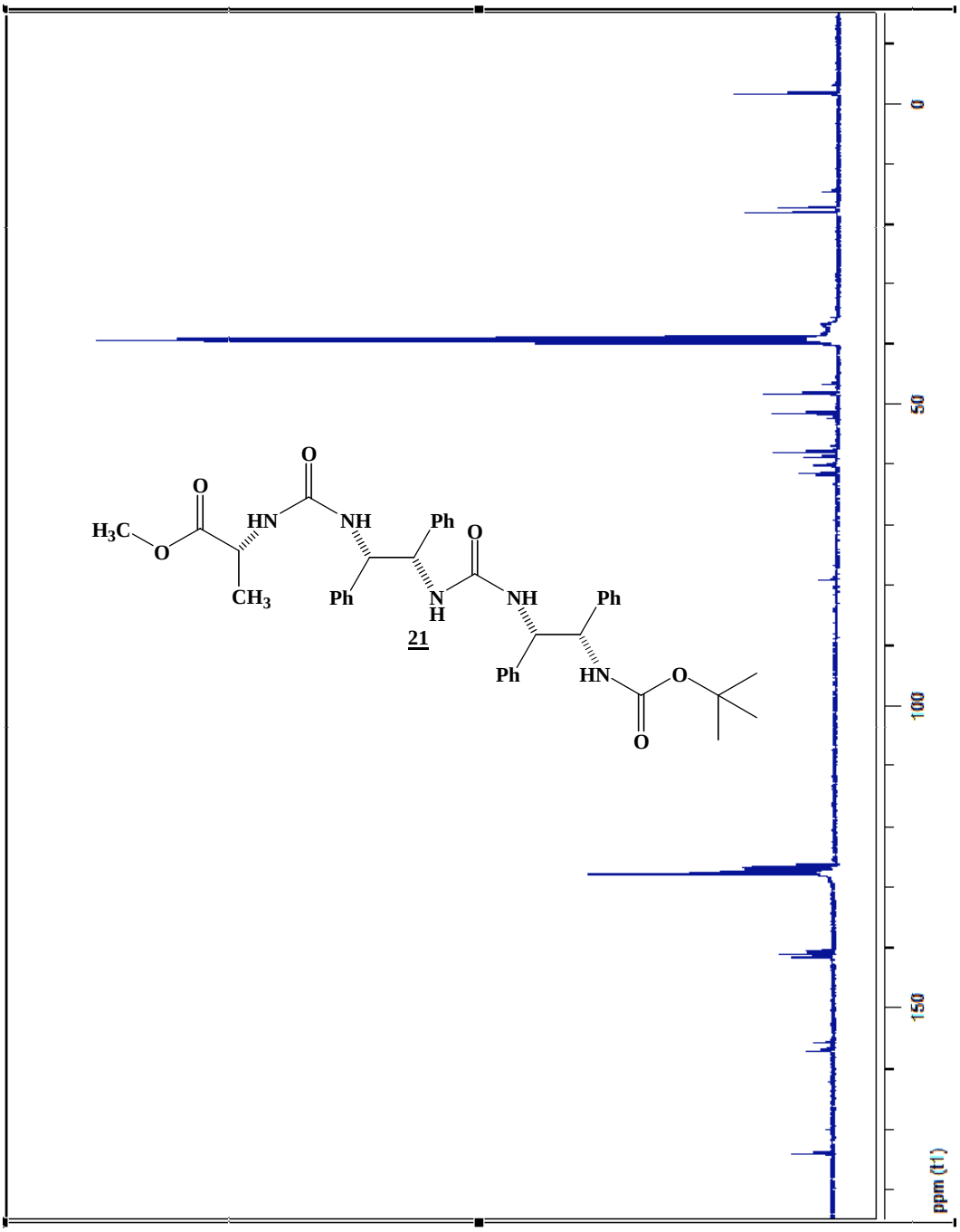

A. 17 *S*,*S*–Teoc–Ala–Trimer, <u>21</u>, MALDI–TOF–MS

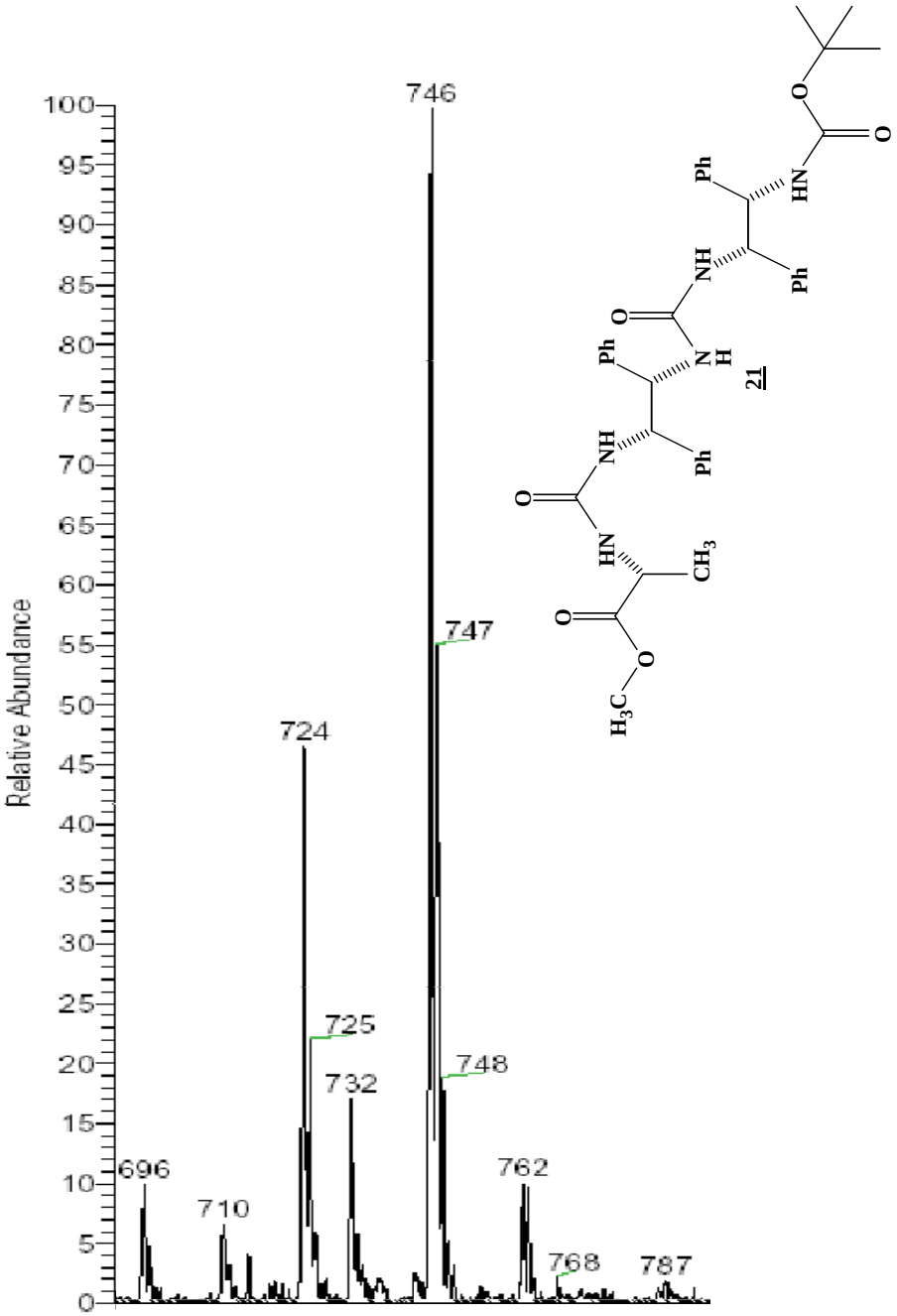

A. 18 *S*,*S*–Teoc–Ala–Trimer Acid, 22, MALDI–TOF–MS

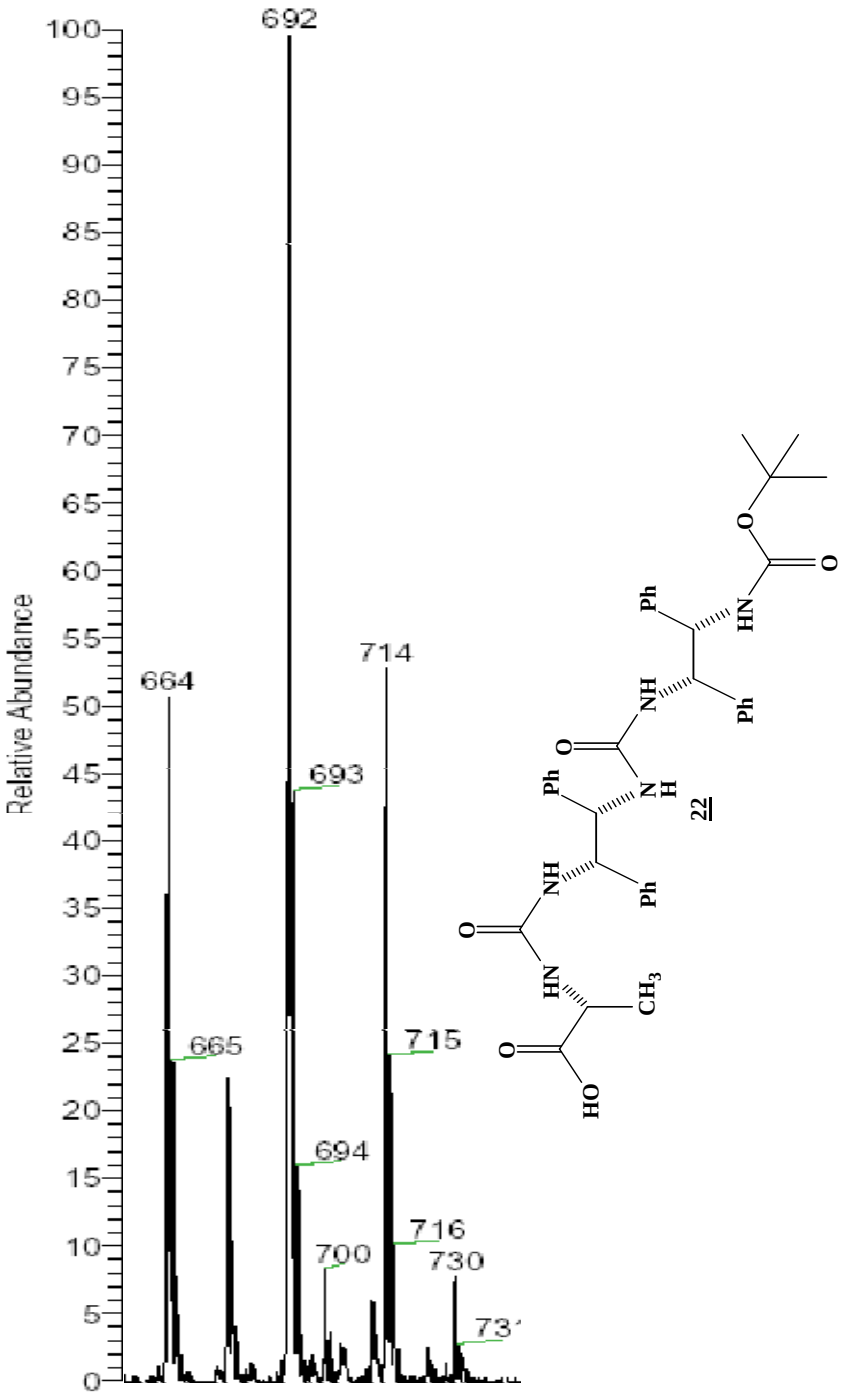

A. 19 Picture of Protected Knorr Resin Beads

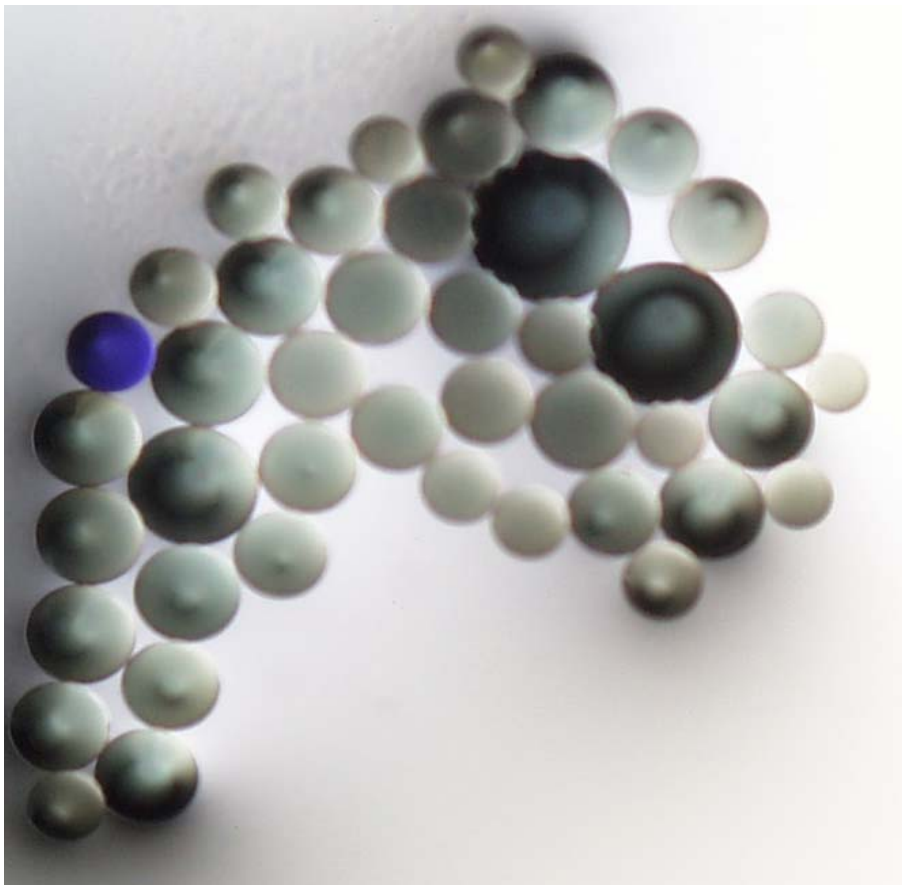

A. 20 Picture of deprotected Knorr Resin Beads after Kaiser Test

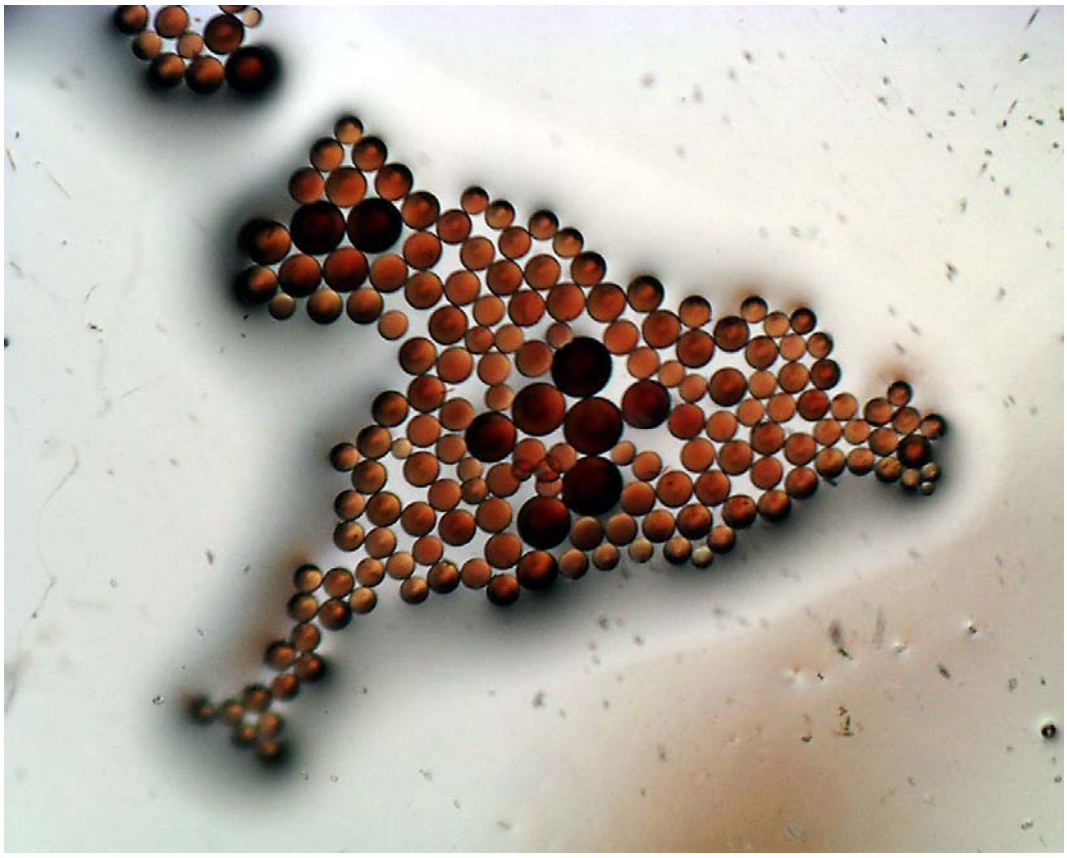

References

(1) Latham, P. W. *Nat. Biotechnol* **1999**, *17*, 755-757.

(2) Spom, M. B.; Roberts, A. B. *J. Clin. Invest.* **1986**, *78*, 329-332.

(3) Fletcher, M. D.; Campbell, M. M. *Chem. Rev.* **1998**, *98*, 763-795.

(4) Halverson, K.; Fraser, P. E.; Kirschner, D. A.; Lansbury, P. T. *Biochemistry* **1990**, 2639-2644.

(5) Patch, J. A.; Barron, A. E. *Curr. Opin. Chem. Biol.* **2002**, *6*, 872-877.

(6) Alimonti, J. B.; Ball, T. B.; Fowke, K. R. *J. Gen. Virol.* **2003**, *84*, 1649-1661.

(7) Force, T.; Pombo, C. M.; Avruch, J. A.; Bonventre, J. V.; Kyriakis, J. M. *Circulation Res.* **1996**, *78*, 947-953.

(8) Gellman, S. H. *Acc. Chem. Res.* **1998**, *31*, 173-180.

(9) Simon, R. J.; Kania, R. S.; Zuckermann, R. N.; Huebner, V. D.; Jewell, D. A. *Proc. Natl. Acad. Sci. U.S.A.* **1992**, *89*, 9367-9371.

(10) Hanessian, S.; Luo, X. H.; Schaum, R.; Michnick, S. *J. Am. Chem. Soc.* **1998**, *120*, 8569-8570.

(11) Wilson, M. E.; Nowick, J. S. *Tetrahedron Lett.* **1998**, *39*, 6613-6616.

(12) Lokey, R. S.; Iverson, B. L. *Nature* **1995**, *375*, 303-306.

(13) Kübel, C.; Mio, M. J.; Moore, J. S.; Martin, D. C. *J. Am. Chem. Soc.* **2002**, *124*, 8605-8610.

(14) Licini, G.; Prins, L. J.; Scrimin, P. *Eur. J. Org. Chem.* **2005**, *2005*, 969-977.

(15) Dill, K. A. *Protein Sci.* **1999**, *8*, 1166-1180.

(16) Kirshenbaum, K.; Zuckerman, R. N.; Dill, K. A. *Curr. Opin. Chem. Biol.* **1999**, *9*, 530-535.

(17) Ramagonal, U. A.; Ramakumar, S.; Mathur, P.; Joshi, R.; Chauthan, V. S. *Protein Eng.* **2002**, *15*, 331-335.

(18) Pauling, L., and R. B. Corey *Proc. Natl. Acad. Sci. U.S.A.* **1951**, *37*, 241-50.

(19) Saunders, M.; Houk, K. N.; Wu, Y.-D.; Still, W. C.; Lipton, M.; Chang, G.; Guida, W. C. *J. Am. Chem. Soc.* **1990**, *112*, 1419-1427.

(20) Metropolis, N. R.; W., R. A.; Rosenbluth, M. N.; Teller, A. H.; Teller, E. *J. Chem. Phys.* **1953**, *21*, 1087-1092.

(21) Howard, A. E.; Kollman, P. A. *J. Med. Chem.* **1988**, *31*, 1669-1675.

(22) McDonald, D. Q.; Still, W. C. *Tetrahedron Lett.* **1992**, *33*, 7743.

(23) Still, W. C.; Tempczyk, A.; Hawley, R. C.; Hendrickson, T. *J. Am. Chem. Soc.* **1990**, *112*, 6127-6129.

(24) Amidon, G. L.; Yalkowsky, S. H.; Anik, S. T.; Valvani, S. C. *J. Phys. Chem.* **1975**, *72*, 2239-2246.

(25) Hermann, R. B. *J. Phys. Chem.* **1972**, *76*, 2754-2759.

(26) Long, S.; Hoben, J.; Cammers, A. *Personal Communication* **2002**.

(27) Luque, F. J.; Zhang, Y.; Aleman, C.; Bachs, M.; Gao, J.; Orozco, M. *J. Phys. Chem.* **1996**, *100*, 4269-4276.

(28) Merrifield, R. B. *J. Am. Chem. Soc.* **1963**, *85*, 2149-2154.

(29) Marshall, G. R. *J. Peptide Sci.* **2003**, *9*.

(30) Vaino, A. R.; Janda, K. D. *J. Comb. Chem.* **2000**, *2*, 579-596.

(31) Gordon, K.; Balasubramanian, S. *J. Chem. Technol. Biotechnol.* **1999**, *74*, 835-851.

(32) Backes, B. J.; Virgilio, A. A.; Ellman, J. A. *J. Am. Chem. Soc.* **1996**, *118*, 3055-3056.

(33) Krafft, G. A.; Sutton, W. R.; Cummings, R. T. *J. Am. Chem. Soc.* **1988**, *110*, 301-303.

(34) LLoyd-Willams, P.; Albericio, F.; Giralt, E. *Tetrahedron* **1993**, *49*, 11065-11133.

(35) Boman, H. G. Cell 1991, 68, 205-207.

(36) Oren, Z.; Shai, Y. Eur. J. Biochem. 1996, 237, 303 - 310.

(37) Cruciani, R. A.; Barker, J. L.; Durell, S. R.; Raghunathan, G.; Guy, H. R.; Zasloff, M.; Stanley, E. F. Eur. J. Pharmacol. 1992, 226, 287-296.

(38) Anderson, R. C.; Wilkinson, B.; Yu, P. Australian Journal of Agricultural Research 2004, 55, 69 - 75.

(39) Oren, Z.; Shai, Y. Biopolymers 1999, 47, 451-463.

(40) Pouny, Y.; Rapaport, D.; Mor, A.; Nicolas, P.; Shai, Y. Biochemistry 1992, 12416-12423.

(41) Hancock, R. E. W.; Chapple, D. S. Antimicrob. Agents Chemother. 1999, 1317-1323.

(42) Perez-Paya, E.; Houghten, R. A.; Blondelle, S. E. *Biochem J.* **1994**, *299*, 587-591.

(43) Delatorre, P.; Olivieri, J. R.; Ruggiero Neto, J.; Lorenzi, C. C. B.; Canduri, F.; Fadel, V.; Konno, K.; Palma, M. S.; Yamane, T.; de Azevedo, W. F. *Biochemica et Biophysical Acta* **2001**, *1545*, 372 - 376.

(44) Konno, K.; Miki, H.; Naoki, H.; Itagaki, Y.; Kawai, N.; Miwa, A.; Yasuhara, T.; Morimoto, Y.; Nakata, Y. *Toxicon* **2000**, *38*, 1505 - 1515.

(45) Jouirou, B.; Mosbah, A.; Visan, V.; Grissmer, S.; M'Barek, S.; Fajloun, Z.; van Rietschoten, J.; Devaux, C.; Rochat, H.; Lippens, G.; El Ayeb, M.; De Waard, M.; Sabateir, J.-M. *Biochem J.* **2004**, *377*, 37-49.

(46) van't Hof, W.; Veerman, E. C. I.; Helmerhorst, E. J.; Amerongen, A. V. N. *Biol. Chem.* **2001**, *382*, 597-619.

(47) Eisenberg, D.; Weiss, R. M.; Terwilliger, T. C. *Proc. Natl. Acad. Sci. USA* **1984**, *81*, 140 - 144.

(48) Selsted, M. E.; Novotny, M. J.; Morris, W. L.; Tang, Y. Q.; Smith, W.; Cullen, J. S. *J. Biol. Chem.* **1992**, *267*, 4292-4295.

(49) Falla, T. J.; Karunaratne, D. N.; Hancock, R. E. W. *J. Biol. Chem.* **1996**, *271*, 19298-19303.

(50) Ladokhin, A. S.; Selsted, M. E.; White, S. H. *Biochemistry* **1999**, *38*, 12313-12319.

(51) Subbalakshmi, C.; Krishnakumari, V.; Nagaraj, R.; Sitaram, N. *FEBS Lett.* **1996**, *395*, 48-52.

(52) Phadke, S. M.; Deslouches, B.; Hileman, S. E.; Montelaro, R. C.; Wiesenfeld, H. C.; Mietzner, T. A. *J. Nutr.* **2005**, *35*, 1289-1293.

(53) Bulet, P.; Hetru, C.; Dimarcq, J.-L.; Hoffmann, D. *Dev. Comp. Immunol.* **1999**, *23*, 329 - 344.

(54) Lawyer, C.; Pai, S.; Watabe, M.; Borgia, P.; Mashimo, T.; Eagleton, L.; Watabe, K. *FEBS Lett.* **1996**, *390*, 95 - 98.

(55) Romeo, D.; Skerlavaj, M.; Gennaro, R. *J. Biol. Chem.* **1988**, *263*, 9573-9757.

(56) Wu, M.; Hancock, R. E. W. *Antimicrob. Agents Chemother.* **1999**, 1274 - 1276.

(57) Morikawa, N.; Hagiwara, K.; Nakajima, T. *Biochem. Biophys. Res. Commun.* **1992**, *189*, 184 - 190.

(58) Fehlbaum, P.; Bulet, P.; Chernysh, S.; Briand, J.-P.; Roussel, J.-P.; Letellier, L.; Hetru, C.; Hoffmann, J. A. *Proc. Natl. Acad. Sci. USA* **1996**, *93*, 1221 - 1225.

(59) Silva, P. I.; Daffre, S.; Bulet, P. *J. Biol. Chem.* **2000**, *275*, 33464 - 33470.

(60) Dathe, M.; Wieprecht, T. *Biochim. Biophys. Acta* **1999**, *1462*, 71-87.

(61) Matsuzaki, K.; Sugishita, K.; Miyajima, K.; McIntosh, T. J.; Holloway, P. W. *FEBS Lett.* **1999**, *4492*, 221-224.

(62) Rana, F. R.; Macias, E. A.; Sultany, C. M.; Modzrakowski, M. C.; Blazyk, J. *Biochemistry* **1991**, *30*, 5858-5866.

(63) Ludtke, S. J.; He, K.; Heller, W. T.; Harroun, T. A.; Yang, L.; Huang, H. W. *Biochemistry* **1996**, *35*, 13723-13728.

(64) Yang, L.; Harroun, T. A.; Weiss, T. M.; Ding, L.; Huang, H. W. *Biophys. J.* **2001**, *81*, 1475-1485.

(65) Hara, T.; al, e. *J. Biochem* **2001**, *130*, 749-755.

(66) Yang, L.; Weiss, T. M.; Lehrer, R. I.; Huang, H. W. *Biophys J.* **2000**, *79*, 2002-2009.

(67) Uematsu, N.; Matsuzaki, K. *Biophys. J.* **2000**, *79*, 2075-2083.

(68) Guo, L.; Lim, K. B.; Poduje, C. M.; Daniel, M.; Gunn, J. S.; Hackett, M.; Miller, S. I. *Cell* **1998**, *95*, 189-198.

(69) Ganz, T.; Lehrer, R. I. *Pharmacol. Ther.* **1995**, *66*, 191-205.

(70) Friedrich, C.; Scott, M. G.; Karunaratne, N.; Yan, H.; Hancock, R. E. *Antimicrob. Agents Chemother.* **1999**, *43*, 1542-1548.

(71) Yeaman, M. R.; Soldan, S. S.; Ghannoum, M. A.; Edwards, J. E.; Filler, S. G.; Bayer, A. S. Infection and Immunity **1996**, *64*, 1379 - 1384.

(72) Guina, T.; Yi, E. C.; Wang, H.; Hackett, M.; Miller, S. I. *J. Bacteriol* **2000**, *179*, 7040-7045.

(73) Groisman, E. A. *J. Bacteriol* **2001**, *183*, 1835-1842.

(74) Groisman, E. A.; Kayser, J.; Soncini, F. C. *J. Bacteriol* **1997**, *179*, 7040-7045.

(75) Ernst, R. K.; Guina, T.; Miller, S. I. *J. Infect. Dis.* **1999**, *286*, S326-330.

(76) Dorrer, E.; Teuber, M. *Arch. Microbial.* **1997**, *114*, 87- 89.

(77) del Castillo, F. J.; del Castillo, I.; Moreno, F. *J. Bacteriol* **2001**, *183*, 2137-2140.

(78) Corey, E. J.; Imwinkelried, R.; Pikul, S.; Xiang, Y. *J. Am. Chem. Soc.* **1989**, *111*, 5493-5495.

(79) Corey, E. J.; Decicco, C. P.; Newbold, R. C. *Tetrahedron Lett.* **1991**, *32*, 5287-5290.

(80) Zhang, W.; Jacobsen, E. N. *J. Org. Chem.* **1991**, *56*, 2296-2298.

(81) Mangeney, P.; Tejero, T.; Alexakis, A.; Grojean, F.; Normant, J. F. *Synthesis* **1988**, 255-259.

(82) Wang, Z.; Kakiuchi, K.; Sharpless, K. B. *J. Org. Chem.* **1994**, *59*, 6895-6897.

(83) Mistryukov, E. A. *Russ. Chem. Bull.* **2002**, *51*, 2308-2309.

(84) Pikul, S.; Corey, E. J. *Org. Synth.* **1992**, *71*, 22-32.

(85) Weiss, M. *J. Am. Chem. Soc.* **1952**, *74*, 200-202.

(86) Xu, D.; Prasad, K.; Repic, O.; Blacklock, T. J. *Tetrahedron Lett.* **1995**, *36*, 7357-7360.

(87) Lowe, C. *Eur. J. Biochem.* **1977**, *73*, 265-274.

(88) Eckert, H.; Forster, B. *Angew. Chem., Int. Ed. Engl.* **1987**, *26*, 894-895.

(89) Majer, P.; Randad, R. S. *J. Org. Chem.* **1994**, *59*, 1937-1938.

(90) Batey, R. A. ;.Yoshina-Ishii V. S., C and Taylor, S. D. *Tetrahedron Lett.* **1998**, *39*, 6267.

(91) Yang, L.; Berk, S. *Proc. Natl. Acad. Sci. USA* **1998**, *95*, 10836–10841.

(92) Heras, M.; Font, D.; Linden, A.; Villalgordo, J. M. *Helv. Chim. Acta* **2003**, *86*, 3204-3214.

(93) Gagnon, P.; Huang, X.; Therrien, E.; Keillor, J. W. *Tetrahedron Lett.* **2002**, *43*, 7717-7719.

(94) Rosowsky, A.; Wright, J. E. *J. Org. Chem.* **1983**, *48*, 1539-1541.

(95) LLoyd-Willams, P.; Albericio, F.; Giralt, E. *Tetrahedron* **1993**, *49*, 11065-11133.

(96) Vaino, A. R.; Janda, K. D. *J. Comb. Chem.* **2000**, *2*, 579-596.

(97) Kaiser, E.; Colescott, R. L.; Bossinger, C. D.; Cook, P. I. *Anal. Biochem.* **1970**, *34*, 595-598.

(98) Humphrey, J. M.; Chamberlin, A. R. *Chem. Rev.* **1997**, *97*, 2243-2266.

Vita

Marlon D. Jones was born on the 21st of November, 1970 in Hawthorne, California, USA. He received his high school diploma from Centennial High School in Compton, CA in 1988. Marlon received a B.S. degree from the University of Nevada, Las Vegas, in Las Vegas, Nevada in May 1995. While attending UNLV, he worked as a laboratory research assistant testing various routes to the desulfurization of organosulfur compounds, as well as mechanistic studies into the mechanism in thiocyanate-isothiocyanate rearrangements. In August of 1995 Marlon joined the chemistry department at the University of Kentucky. In addition to this, he received a NIH grant in 2000 and has been a participant in the National Science Foundation - IGERT program, since 2002.